FACULDADE DE CIÊNCIAS E TECNOLOGIA
UNIVERSIDADE NOVA DE LISBOA

Departamento de Engenharia Electrotécnica e Computadores

Integrating Wind Generation in the Distribution Network

Marco Filipe Matos da Fonseca

Dissertação apresentada na Faculdade de Ciências e Tecnologia da Universidade Nova de Lisboa para obtenção do Grau de Mestre em Energias Renováveis – Conversão Eléctrica e Utilização Sustentáveis

Orientador: João Murta Pina

Março 2012

FACULDADE DE CIÊNCIAS E TECNOLOGIA
UNIVERSIDADE NOVA DE LISBOA

Departamento de Engenharia Electrotécnica e Computadores

Integrating Wind Generation in the Distribution Network

Marco Filipe Matos da Fonseca

Dissertação apresentada na Faculdade de Ciências e Tecnologia da Universidade Nova de Lisboa para obtenção do Grau de Mestre em Energias Renováveis – Conversão Eléctrica e Utilização Sustentáveis

Orientador: João Murta Pina

Março 2012

Título da Dissertação de Mestrado: Integrating Wind Generation in the Distribution Network, “Copyright” Marco Filipe Matos da Fonseca, Faculdade de Ciências e Tecnologia, Universidade Nova de Lisboa.

À minha família

À memória da minha avó

To my family

To the memory of my grandmother

Agradecimentos

Este último ano houve bastantes desafios, não só o facto de estar longe do meu país e família mas também a adaptação a uma cultura e país differentes. Eu quero agradecer ao meu irmão por todo o apoio ao longo do primeiro ano e por me ter ajudado a focar no caminho mais objectivo e concreto para a realização da tese e para não subestimar as minhas capacidades perante pessoas muito mais experientes.
Quero agradecer à minha família pela coragem e força transmitida.

This last year was full of challenges, not only the fact of being far from my country and family but also due to the adaptation to a different country and culture. I want to say thank you to my brother for all the support he gave me throughout this year, for helping me focus on the most objective and wise path for the conclusion of this thesis and to not underestimate my abilities among more experienced people.
I want to thank my family for the courage and strength transmitted.

Resumo

Um dos desafios actuais da rede eléctrica é a ligação futura de geração à rede sem a necessidade de a reforçar. Esta dissertação vai estudar o uso de índices dinâmicos nas linhas aéreas de forma a aumentar a sua capacidade e consequentemente adiar grandes investimentos no reforço de infra-estrutura.

A quantidade de corrente que uma linha aérea consegue suportar num dado momento é definida pela distância ao solo que é proporcional à temperatura do condutor e é dado por um índice estático através da norma P27 – "Current Rating Guide for High Voltage Overhead Lines Operating in the UK Distribution System". Este índice estático varia de estação para estação e depende de valores específicos para temperatura ambiente, velocidade, direcção do vento e da probabilidade num ano da temperatura do condutor exceder a temperatura para qual foi desenhado. Esta norma é vista como sendo muito restricta e um factor limitante na capacidade das linhas aéreas quer para futuras ligações de geração quer para carga.

A velocidade e direcção do vento são importantes para o arrefecimento das linhas aéreas e na ocorrência de ventos fortes, o condutor arrefece, permitindo que exista um maior fluxo de corrente para a mesma temperatura de funcionamento. Ao usar dados meteorológicos em tempo real, é possível calcular a corrente máxima que pode fluir na linha para uma dada temperatura de funcionamento e posteriormente avaliar a quantidade extra de corrente que pode fluir, dada pela diferença entre o índice estático e o índice dinâmico.

Um ponto de vista mais objectivo da quantidade extra de energia produzida, bem como a redução de emissões de CO_2 e lucro vão ser apresentadas.

Termos chave: índice dinâmico, índice de corrente num condutor, índice térmico, linhas de transmissão, reforço de linhas aéreas

Abstract

One of the current challenges the electricity grid has is to actively connect future generation to its network without the need to fully reinforce it. This dissertation will study the use of dynamic ratings on overhead lines to increase its capacity and thus defer major investment on infrastructure reinforcement.

The amount of current an overhead line can withstand in a given time is defined by the distance towards the ground, which is proportional to the conductor´s temperature, which is given by a static rating stated in the P27 standard – "Current Rating Guide for High Voltage Overhead Lines Operating in the UK Distribution System". This rating changes from season to season and depends on specific values for ambient temperature, wind speed, wind direction and the probability that in a year the conductor exceeds its design temperature. This standard is seen as being very restrictive and a limiting factor on overhead line capacity for both future generation connections and demand.

Wind speed and direction are extremely important on the cooling of overhead lines and in times of strong winds the conductor cools down, allowing extra amount of current to flow through it. By using real time weather data, it´s possible to obtain the maximum current that can flow in an overhead line for a specific operating temperature and assess the amount of headroom possible given by the difference between the static ratings and the new dynamic ratings is assessed.

A view on the extra amount of energy produced, as well as CO_2 emission savings and profit will also be presented, giving a practical result by applying dynamic ratings.

Keywords: dynamic line rating; DLR; thermal rating; current rating; transmission lines; overhead lines reinforcement;

Simbology

A'	Projected area of conductor per unit length	$\frac{m^2}{m}$
C	Solar azimuth constant	degrees
D	Conductor diameter	mm
H_c	Degrees of solar altitude	degrees
H_e	Elevation of conductor above sea level	m
I	Conductor current	A
K_{angle}	Wind direction factor	---
K_{solar}	Solar altitude correction factor	---
k_f	Thermal conductivity of air	$\frac{W}{m \times ℃}$
$Latitude$	Degrees of latitude	degrees
N	Day of the year	---
q_n	Natural convection	W/m
q_{clow}	Forced convection for low wind speeds per unit length	W/m
q_{chigh}	Forced convection for high wind speeds per unit length	W/m
q_r	Radiated heat loss per unit length	W/m
q_s	Heat gain rate per unit length	W/m
Q_s	Total heat flux received by a surface at sea level	$\frac{W}{m^2}$
Q_{se}	Q_s with elevation correction factor	$\frac{W}{m^2}$
$R(T_c)$	DC Resistance of conductor at operating temperature T_c per unit length	$\frac{\Omega}{m}$
T_a	Ambient temperature	℃
T_c	Conductor operating temperature	℃
T_m	Average temperature between T_a and T_c	℃
V_w	Wind speed at conductor	$\frac{m}{s}$

Z_c	Azimuth of the sun	degrees
Z_l	Azimuth of the line	degrees
α	Solar absorptivity	---
δ	Solar declination	degrees
ε	Emissivity	---
ϕ	Angle between wind and the axis of the conductor	degrees
β	Angle between wind and perpendicular to the conductor´s axis	degrees
ρ_f	Air density	$\frac{\text{kg}}{\text{m}^3}$
θ	Effective angle of incidence of the sun´s rays	degrees
μ_f	Dynamic viscosity of air	Pa-s
ω	Hour angle	degrees
χ	Solar azimuth variable	---

Notation

ABSD	Air Breaker Switch Disconnector
ACCC	Aluminum Conductor Composite Core
ACSR	Aluminum Conductor Steel Reinforced
Al	Aluminum
ANM	Active Network Management
CB	Circuit Breaker
CERL	Central Electricity Research Laboratory
CI	Customer Interruptions
CML	Customer Minutes Lost
CT	Current Transformer
Cu	Copper
DECC	Department of Energy and Climate Change
DEFRA	Department for Environment, Food and Rural Affairs
DG	Distributed Generation
DLR	Dynamic Line Rating
DNO	Distribution Network Operator
DPCR	Distribution Price Control Review
EDF	Electricité de France
EHV	Extra High Voltage (132 kV)
EPN	Eastern Power Networks
FCL	Fault Current Limiter
FPP	Flexible Plug and Play
GSP	Grid Supply Point
HTLS	High Temperature Low Sag
HV	High Voltage (>11 kV)
IEEE	Institute of Electrical and Electronics Engineers
IFI	Innovation Funding Initiative
LCL	Low Carbon London
LCNF	Low Carbon Network Fund
LDC	Line Drop Compensation
LPN	London Power Networks
LV	Low Voltage (400/260 V)
NG	National Grid
NOP	Normally Open Point
OF	Oil Filled
OFGEM	Office of Gas and Electricity Markets
OHL	Overhead Line
POC	Point of Connection
RIIO	Revenue = Incentives + Innovation + Outputs
SC	Single Core
SCADA	Supervisory Control and Data Acquisition
SCP	Single Core Poly
St	Steel

UG	Underground
UKPN	UK Power Networks

Material Index

Figure Index

Table Index

1 Introduction

1.1 Motivation

A new way of thinking is out of reach. Global warming has been in the spotlight for several years now, dividing the skepticisms and the believers into affirming slightly different views on the same subject. For the latter, the chance to research and study novel ways and technologies to reduce our CO_2 emissions presents itself. For the former, the urgency of the issue is underestimated and every resolution towards resolving it may be seen as futile. A resolution can be achieved not only by the use of modern technology, but by changing the way people see the world and how every action performed has a consequence to their surroundings. People have to think as a whole and not individually and the pursuit of this conviction will be difficult, but possible. With the present economic downturn, saving costs is a primary focus which will introduce a degree of challenge to global investments.

The UK low carbon transition plan has an ambitious strategy which aims to reduce UK emissions by 34 % by 2020 and at least 80 % by 2050 through investment in energy efficiency and clean energy technologies such as renewable, nuclear and carbon capture and storage. Around 30 % of electricity is expected to come from renewable generation by 2020 with a correspondent increase in distributed generation (DG). Advances in the electrification of heat and transport will help to decrease the emissions as well.

The connection and operation of DG uncovers a number of network planning and operation challenges, with potential issues such as power flow management, voltage control and fault levels. However, it also presents opportunities that can lead to the research and implementation of low carbon technologies and facilitate access to DG, maximizing the present power network and thus help achieving several goals:

- Avoid or defer major network reinforcement costs and allow increasing DG connected to the network through the use of smart grid solutions;
- Resolve network constraints arising from increasing DG connections;
- Power flow understanding and management;
- Improve the global efficiency of distribution networks and reduce the number of customer interruptions (CI) and customer minutes lost (CML).

Will power networks withstand the increase in generation connection enquiries without major reinforcement to the grid? With budget constraints, that reinforcement may be too expensive and consequently renewable generation may never be built. At the moment there are several ways to facilitate that same connection that present significant savings when compared to classical reinforcement. One of those technologies is dynamic line ratings [17], [18], [19], [20], [21].

1.2 Scope of Work

This thesis takes hold of a theory application of calculations related to overhead line capacity and bonds it with real time data for real results, although based in assumptions related directly with the use of the ever inconstant weather characteristics. The main objective of this thesis is to give a result of the gain obtained by using dynamic ratings on overhead lines. That gain can be understood as the extra amount of generation that can be connected to the circuit group being studied or the extra current it can withstand. As dynamic ratings depend on the occurrence of wind, its application is usually seen in areas close to wind farms.

Two circuits were chosen for this assessment and a series of studies were performed in order to reach the final milestone: the amount of headroom that can be gained by applying dynamic line ratings.

1.3 Work Flow Summary

Adopting dynamic ratings to existing overhead lines to increase its capacity is an approach that is still in a testing phase, with only a few implementations across UK and throughout the world. Moving from a business as usual method to a new, modern technique presents certain difficulties. The thesis adopts the following steps:

- **Research**
    - Information on dynamic ratings. Familiarizing with the assumptions and the limitations of applying dynamic ratings on an overhead line. IEEE 738 standard on ampacity calculation was examined and all relevant factors were indentified;

    - Study of network limitations and focusing on specific circuits of the network grid in which to adopt dynamic ratings. Data on circuit components – type of conductor, existing restrictions and the current rating components. Grid and primary substations and present wind generation were also assembled;

    - Weather Data – In order to apply dynamic ratings, weather data. Various weather stations near the circuits being analyzed were indentified but proved to be unreliable and were therefore rejected. After coming into terms with a wind farm developer, data on wind speed, wind direction and ambient temperature were provided. Due to the sensitivity of it, this information will not be provided.

- **Simulations**
    - Several simulations under Digsilent modeling software [(1)] were carried out to analyze the present condition of circuits being studied. The amount of static headroom was determined and evaluated, serving as a base value for future simulations;

[(1)] Digsilent-PowerFactory is a power system analysis software for applications in generation, transmission, distribution and industrial systems. http://www.digsilent.de/

- With information on the amount of current present in both circuits, an assessment using dynamic line ratings followed. Four scenarios are studied, each using different network arrangements and bearing slightly different results. For each half hour, the dynamic rating is obtained and the headroom is determined.

- **Results/Conclusions**
  - After determining the headroom, the extra volume of generation that can be connected to those circuits is assessed and the additional energy produced, CO_2 emission savings and profit is calculated.

1.4 Thesis Structure

This thesis will begin with a brief description of the electricity supply system and the way it evolved over time. Context on all different distribution network operators (DNO) will be presented as well, with focus on UK Power Networks (UKPN). A brief description of the low carbon London objectives with future reference to specific projects that will help implement innovative technologies will be presented. The subject itself will be divided into different sections:

- Definition and explanation of the core mechanics – what is dynamic line rating and how does it work. What are the major assumptions, restrictions and theoretical components that are inputs to all mathematical calculations;

- Theoretical analysis for a specific conductor under static conditions, i.e. static steps in wind speed, five different wind angles and solar irradiance over three different seasons;

- Definition and explanation of four simulation scenarios. The present headroom available for each scenario is assessed by means of a modeling tool;

- Route profile assessment carried with circuits being split into different sections. Values for wind roughness were then chosen for future use in ampacity calculation;

- Ampacity was obtained for each 30min during 2010 and the amount of headroom was assessed.

The conclusion of this thesis will present several advantages of applying dynamic ratings, through the gains in profit and emission savings. Future improvements to be made in the continuity of this subject will be presented.

2 Context

2.1 Electricity Supply System

In the beginning of the electricity supply systems, all generators were close to the loads, thus, distribution networks were not very complex and the power flew from large generating plants downstream to the distribution network and costumers, also known as the “waterfall” system.

In the 1930s, National Grid (NG) came into operation with the highest transmission voltage of 132 kV. Later in the 1950s and 1960s a new voltage system was built that came to be the transmission system currently being used, operating at 400 kV.

In the 1990s building large power stations was seen as a viable option, benefiting from the economies of scale, i.e., decreasing costs due to expansion. Most stations were located near its source of fuel and thus generators started to move away from the residential areas, both geographically and electrically. A typical traditional power system with no distributed generation is present in the following Figure 2.1 [7].

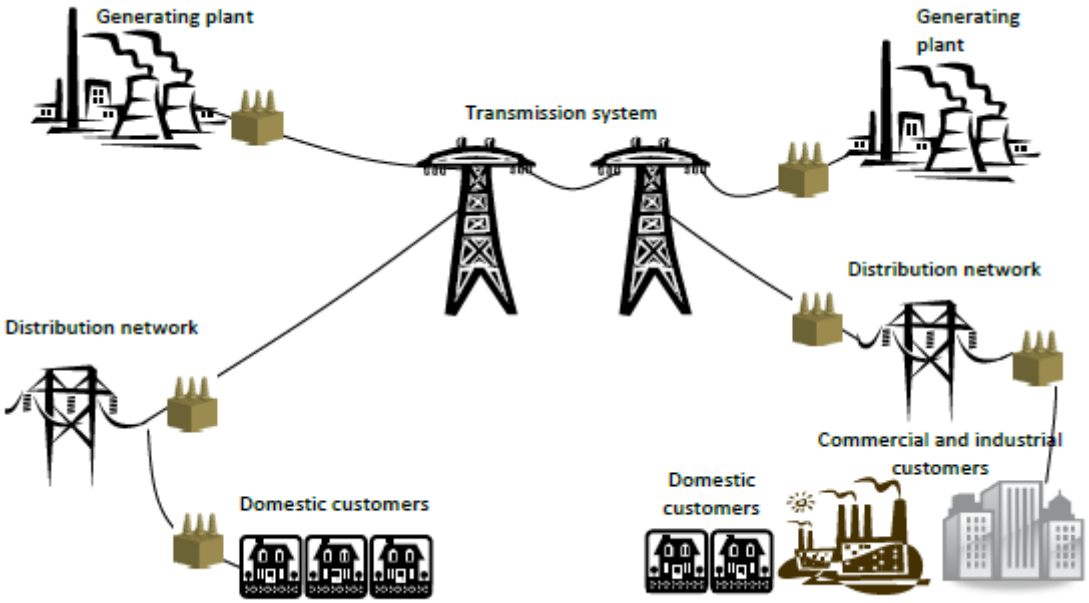

Figure 2.1- Traditional Power System [7].

The power grid sector in the UK has been changing, particularly since the early 80s due to the privatization of industry and soon after a new trend of environmental awareness was born. With this new green mentality, a new wave of technology and movements began to arise, changing the complexity of the network. New smaller generators started to be built and connected to the distribution network instead of the transmission network (Distributed Generation). The power started to flow upstream to the transmission grid and local loads began to be fed by these smaller generators. The “waterfall” system ceased to exist and the traditional power system evolved as seen in Figure 2.2 [6] [7].

For all major load connections customers are offered a point of connection strategy based on its capacity, security requirements and local network topography. That strategy is based on network analysis studies carried out to assess several important factors. The impact on system load flows, voltage levels, fault levels and general stability.

A new set of challenges started to arise due to the growth in Distributed Generation: Primarily the management of power flows, voltage level control and system fault level.

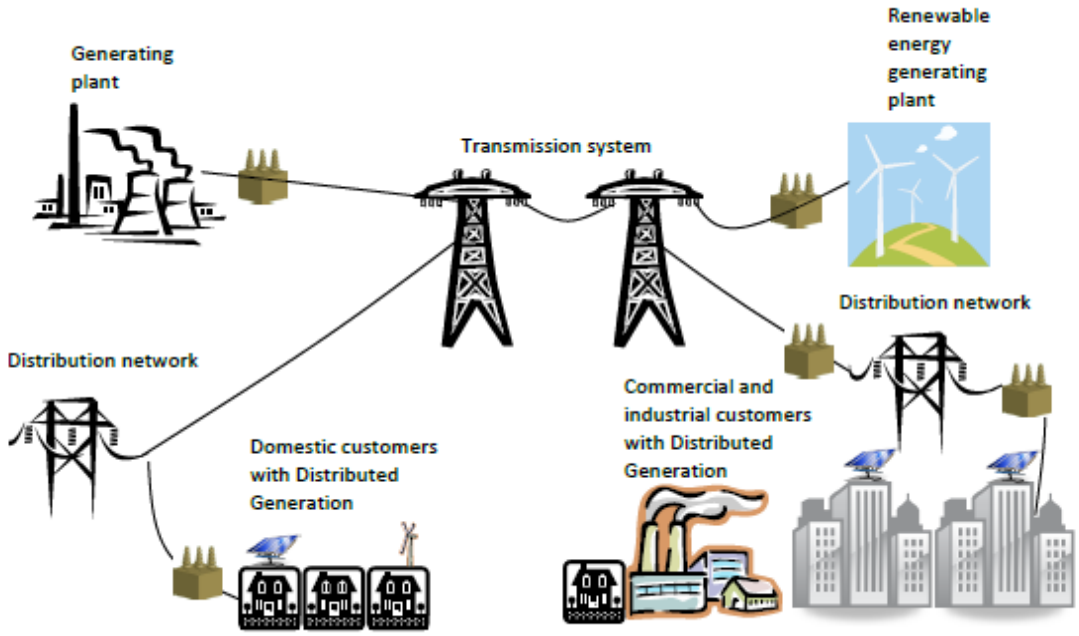

Figure 2.2 - Evolved Traditional Power System [7].

2.2 UK Power Networks

UK Power Networks owns, operates and manages three of the fourteen distribution networks in the United Kingdom. It manages several areas – London, South East and East of England, covering an approximate area of thirty thousand kilometers, being the largest distribution network operator in the UK with over 8 million customers. Figure 2.3 shows the geographical boundaries of each DNO operating in the UK. UKPN is a distribution company and not an energy supplier as it carries electricity taken from National Grid´s transmission network operating at 400 kV and 275 kV to the end user. The distribution follows a succession of networks from 132 kV, 66 kV (in LPN), 33 kV, 22 kV (in LPN), 11 kV, 6.6 kV and down to 400/230 V.

All DNO´s are regulated by the Office of Gas and Electricity Markets known as OFGEM which controls prices and identifies more efficient ways to provide an adequate network capacity, security, reliability and quality of service. Each DNO submits a five year plan to OFGEM as part of the distribution price control review (DPCR).

The current price control, DPCR5[(1)], will run from the first of April 2010 until 31 March 2015 and determines the amount of money a DNO has to run its network, as well as any investment. This process agrees the money we can raise from customers to pay for the network to operate, from stationery and salaries, transformers, etc. also defining the standards of service UKPN has to meet. Each DNO is either penalized or rewarded for its performance and ability to reach the goals previously defined. In October 2010, OFGEM introduced a new approach to network regulation entitled RIIO (revenue = incentives + innovation + outputs). It aims to promote smarter gas and electricity networks for a low carbon future, aiming for a more sustainable future and will run for eight years from April 2015 onwards [1].

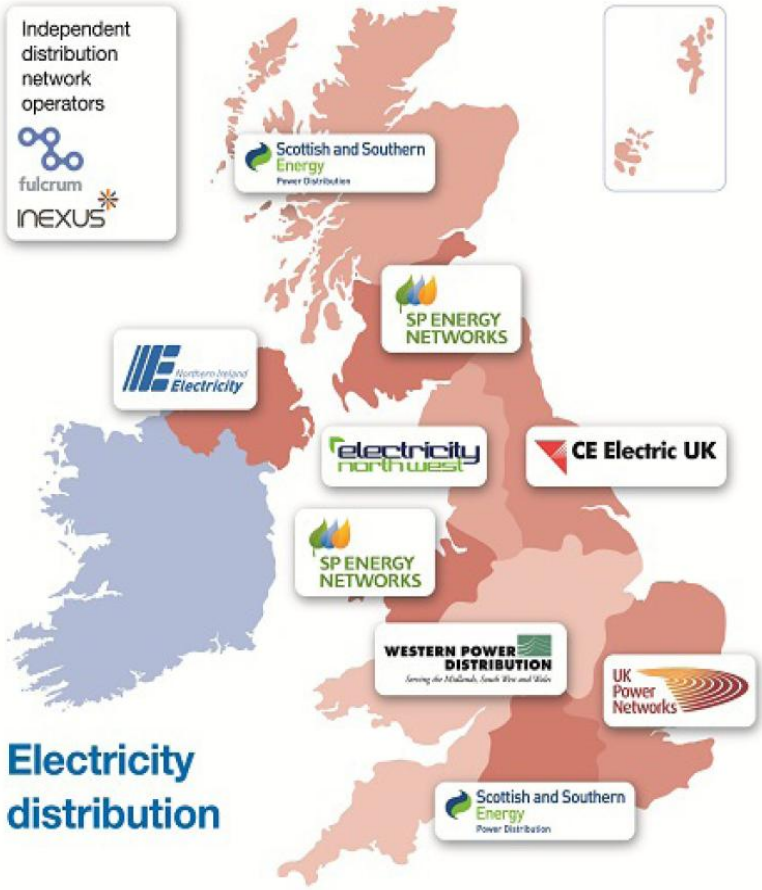

Figure 2.3 - Electricity Distribution UK map [1].

Focusing now on the Eastern Power Network of UKPN, it supplies electricity over an area of more than 20 thousand square kilometers with approximately three and a half million consumers connected to it. The network is designed and operated in order to ensure that safety, security of supply, quality and reliability meet the highest standards. To achieve that in an organized way, a plan of action is issued entitled long term development plan. It provides detailed data on the network to developers to carry out assessments of project feasibility. That data covers various fields from transformer and circuit data, load information, schematics, etc.

(1) It is called DPCR5 because it is the fifth DPCR since privatisation of UKPN

2.3 Low Carbon Initiative

Low Carbon London is an initiative funded by OFGEM's Low Carbon Networks Fund which focuses on developing a network comprised of more modern and smarter technology. It is a collaborative initiative between UK Power Networks and other partners including Siemens, National Grid, Logica, Smarter Grid Solutions, EDF Energy, EnerNOC and Flexicitry.

The UK Low Carbon Transition Plan's main target is a cut of 34 % in carbon emissions on 1990 levels by 2020 and further reduction of 60 % on 1990 levels by 2025 with 25 % of heat and power generated by distributed generation. It's an ambitious goal that will bring an increase in distributed and micro-generation, use of electrical vehicles, combined heating and heat pumps.

Renewable energy is the main focus of the UK Low Carbon Transition plan. In its strategy, the DECC (Department of Energy and Climate Change) set a target of 30 % of UK´s electricity to be produced by renewable sources by 2030. In order to achieve this objective, electricity distribution networks will need to analyze its grid and increase the amount of renewable generation, such as wind farms and reinforce the power network accordingly [8].

UK Power Networks has been regarded as a pursuer of technology innovation, being one of the DNO´s to use OFGEM´s innovation funding incentive (IFI) to study and implement technology innovation schemes. Some innovation areas are presented next:

- Active distributed generation
    - Dynamic restriction (curtailment) of wind farm generation when its export exceeds the network capacity.

- Active voltage control
    - By connecting generators to the network, there is a voltage rise at the point of connection (POC). In 33 kV and 11 kV primary substations, line drop compensation (LDC) is used as part of the automatic voltage control. Its objective is to give a voltage boost at the 11 kV bus-bar to compensate the voltage drop along the 11 kV feeders. By connecting generation at the end of an 11 kV feeder, there is a risk of achieving voltage levels that are higher than the statutory values. The active voltage control system optimizes the voltage according to the amount of generation export and the load on 11 kV feeders.

- Active dynamic rating [12], [17]
    - Dynamic line ratings, or dynamic thermal ratings, help to postpone major reinforcement projects by allowing an increase of circuit capacity using real time weather information, real time conductor temperature monitoring systems or other.

- Superconducting Fault Current Limiters [16]
    - Allows for more demand and generation to be connected as it limits fault levels. In normal operation the superconducting FCL operates with low impedance, and are seen as "invisible" components within the electrical system. In the event of a fault, the FCL develops impedance which in turn limits the fault current.

3 Distribution Networks – Technical Data

3.1 Network Configuration

3.1.1 Grid Supply Point, Grid and Primary Substations

The UK electricity network is composed of a transmission and distribution networks. The former has a maximum operating voltage of 400 kV, owned by National Grid and the latter a maximum of 132 kV and in between these two networks there are grid supply points (GSP). The network from 132 kV and below is fed by these exit points and their location is dependent on the transmission circuit and several network circumstances. In heavily dense areas, 33 kV networks can be interconnected to more than one exit point in order to supply the higher demand. These arrangements provide a transfer capability and an increased level of security to major loads centers in the event of a loss of an exit point. UK Power Networks is constituted by both rural and urban areas.

The naming of substations varies:

- Exit Point or Grid Supply Point (EPN), Bulk Supply Point (LPN) – A substation where the DNO takes bulk power supply infeed to its network from NG transmission system;
- Grid Substation – Substations in which the voltage is stepped down from 132 kV or 66 kV to 33 kV or 11 kV;
- Primary Substation – Substations in which the voltage is stepped down from 33 kV to 11 kV or 6.6 kV;
- Secondary Substation – Substations in which the voltage is stepped down from 11 kV or 6.6 kV to LV;

Eastern Power Network is mainly rural (Norfolk, Suffolk and Chilterns) while London Power Network is the most densely populated region of the United Kingdom. Southern Power Network is growing with new towns like Crawley and Ashford.

EPN network is composed of Grid and Primary substations and there are 22 interfaces with the NG and six transfer points with other DNO´s. It is generally based on double circuit transmission lines in a radial arrangement to grid substations and interconnecting the grid supply points. A standard 400/132 kV GSP is usually composed of 4 super grid transformers, while a grid substation has two grid transformers with 175 mm^2 or 300 mm^2 conductor incoming circuits. At the grid substation, the 33 kV bus-bars are interconnected to the extent that it can be achieved within the fault rating of the switchgear.

A primary station has two transformers and between six to twelve feeders at 11 kV, which generally interconnect to other primary sites. Figure 3.1 shows a typical EPN grid and primary network [13]. The 11 kV networks are configured on an open-ring basis with overhead radial spurs in more rural areas and cabled open interconnection between primaries in urban areas [13].

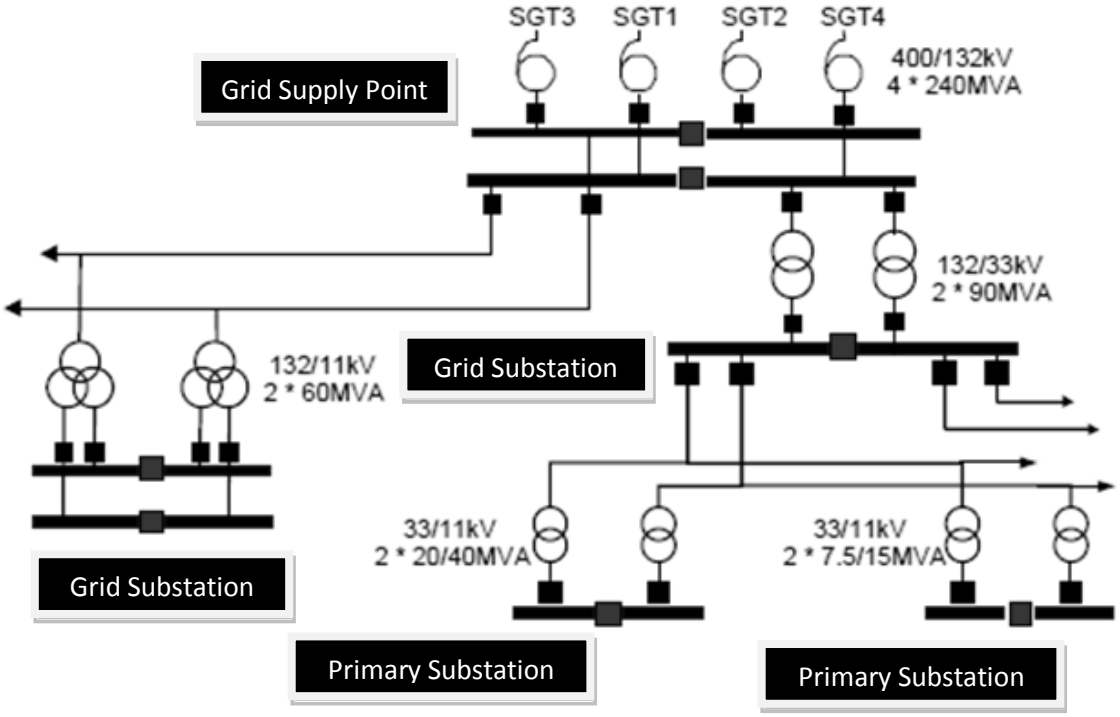

Figure 3.1 - EPN Network Configuration [13].

In LPN, the majority of 132 kV circuits are radial transformer feeders with limited interconnection at this voltage. The EHV circuits are configured as transformer feeders to a main substation equipped with two, three or four two-winding transformers, as seen in Figure 3.2. Three winding transformers are also used with dual secondary windings with each transformer secondary winding connecting to a separate high voltage bus-bar section [13].

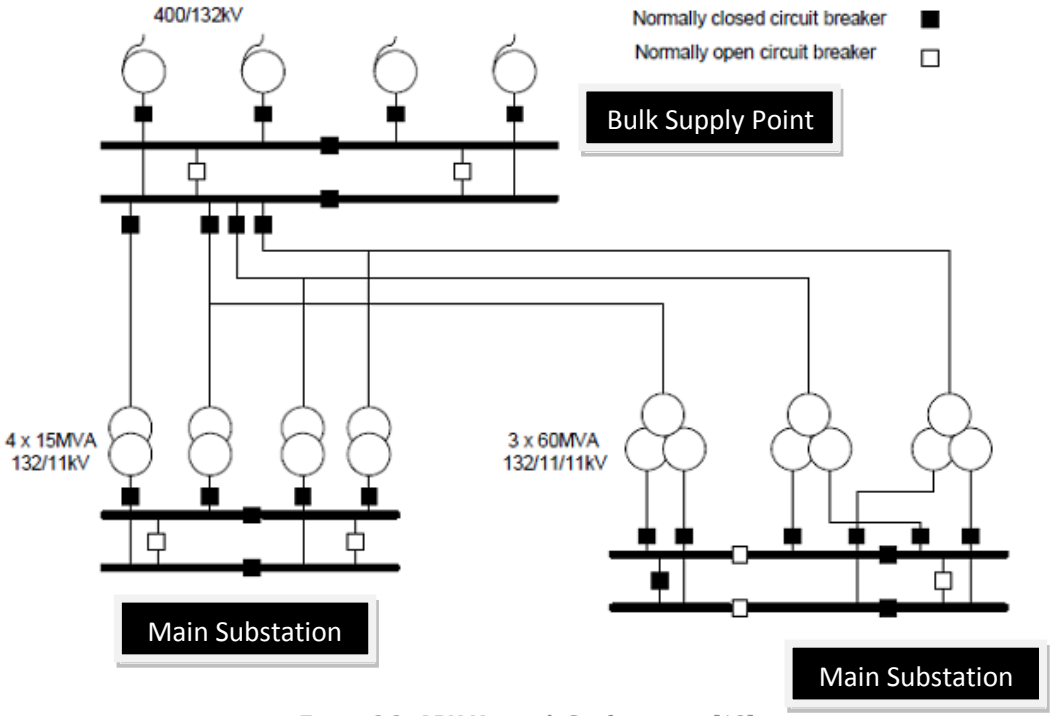

Figure 3.2 - LPN Network Configuration [13].

In SPN, there are 13 interfaces with the NG transmission system and a few with LPN. The 132 kV circuits are generally overhead lines. Most primary substations are fed by two or more 33 kV circuits and transformers, usually from one grid substation. In more rural areas, open ring single circuit 33 kV systems are used with source supplies that may emanate from different grid substations and in some cases, from grids served from different BSP sites. There are several secondary substations that only have one transformer. These substations rely on the 11 kV interconnection to provide security of supply [13].

3.1.2 Overhead Lines Component

The maximum power transfer capability of an overhead line system is limited by the conductor´s maximum current capacity. It is restricted by the conductor´s properties, design, environmental and operational conditions and the structures of the overhead line system itself that restrain the use of heavier conductors. All these properties have an impact on the plastic, elastic and thermal elongation, which are dependent on conductor tension, weight and current flow respectively. Elongation is due to permanent mechanical forces during its life time with its maximum mechanical loading occurring when ice is covering the conductor or in the presence of strong winds. Thermal elongation happens in times of high electrical loading. During these occurrences, the conductor can reach the limit of its ground clearance minimum heights, which prevents further increases in current flow. Overhead lines have a maximum operating temperature to prevent clearance violations and overheating which can cause the annealing of the conductor, i.e. loss of tensile strength that can potentially cause the conductor to break. To avoid these conditions, thermal ratings are applied that limit the amount of current that flows through the conductor. Those ratings are seen as static and they apply to two seasons, winter and summer, and another for autumn and spring. An explanation on static ratings is presented in Chapter 6. By increasing the operating temperature of the conductor its tension decreases, resulting in a higher fall of the conductor towards the ground as seen in Figure 3.3. The fall height is called sag and it is of utmost importance to maintain all safety clearances towards the ground and all objects that can pass below the line. Sag is also affected by the conductor´s properties, namely its elasticity, thermal expansion and strength, as well as specific overhead line system properties, particularly the strength of its structure, span distance, height, and others.

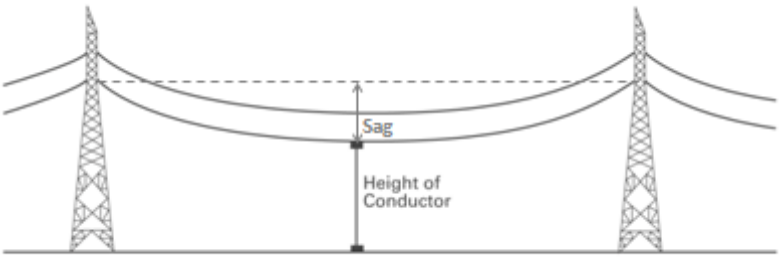

Figure 3.3 - Conductor Sag.

3.1.3 Single Circuit and Double Circuit Arrangements

Lines can be arranged into two different types: single circuit or double circuit. For a single circuit arrangement, and for a three-phase system, each tower supports three conductors, one for each phase. For a double circuit arrangement, there are six conductors in total. Figure 3. shows a typical

33 kV transmission line for single and double circuit arrangements. The structure and foundations change according to the terrain and the size of the conductors to be installed, ranging from simple wood poles to more complex steel lattice tower structures. Overhead lines are subject to extreme weather and loading conditions and the maximum amount of current that can flow through them is limited by a specific conductor based rating. The P27 standard defines the most common overhead lines ratings based on a static and conservative approach in which each season has a specific rating based on fixed conditions. These ratings were calculated by the Central Electricity Research Laboratory (CERL) with measurements of a 400 mm^2 Zebra conductor over a 2-year period at Leatherhead in the 1970´s. This location had specific weather and environmental conditions typical of that region and it was situated at sea-level in southern England. After determining the ratings, they were then extrapolated to all other conductors, but since the first conductor was located in a specific region in England, those ratings are more appropriate to conductors under those conditions. Therefore, the P27 ratings are an element of the location from which the original ratings were gathered rather than the conductor used to determine the data-set. The P27 ratings are based on the exceedence, which is the probability that throughout the year, the conductor temperature will exceed its design temperature. For double circuit arrangements, the current is shared between two circuits, thus, each one carries half of the total current. In this case, the exceedence is stated at 3 %, which means that the circuit is expected to be above its design temperature for 3 % of the year. For single circuit arrangements, as the current is only flowing through a single circuit, that circuit is not expected to be above its design temperature and has an exceedence is 0.001 % [2].

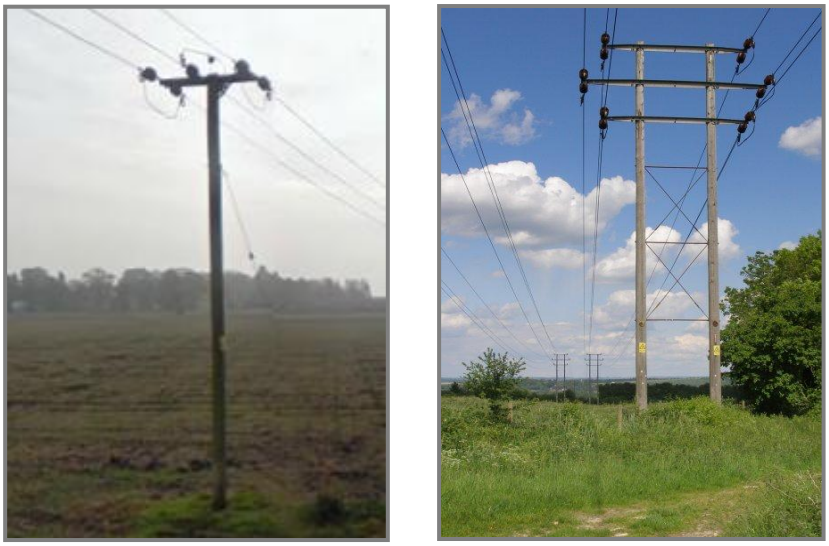

Figure 3.4 - Single (image on the left) and double (image on the right) circuit arrangements.

There are several types of conductors and each with different configurations. The most common in the UK for 33 kV circuits are Aluminum Conductors Steel Reinforced (ACSR) and are usually referred to their nominal aluminium area. An ACSR conductor with a specification of 30 + 7/2.79 mm (or 30/7/2.79) means that it has 30 aluminium strands surrounding 7 steel strands and all strands of diameter 2.79 mm. Both strands can have different diameters as seen for a 100 mm^2 ACSR 6/4.72Al + 7/1.57St. One other type of conductor worth mentioning is the new aluminum conductor composite core (ACCC). This conductor has a carbon composite core with a much lower thermal expansion coefficient compared to steel, aluminum or other core materials and thus can withstand higher temperatures while keeping its sag to minimum values. They are usually referred as high temperature, low sag (HTLS) conductors [22]. The next set of images show the most used ACSR conductors for 33 kV circuit arrangements.

Figure 3.5 - (a) 100 mm² DOG (b) 150 mm² DINGO (c) 175 mm² LYNX (d) 400 mm² ZEBRA.

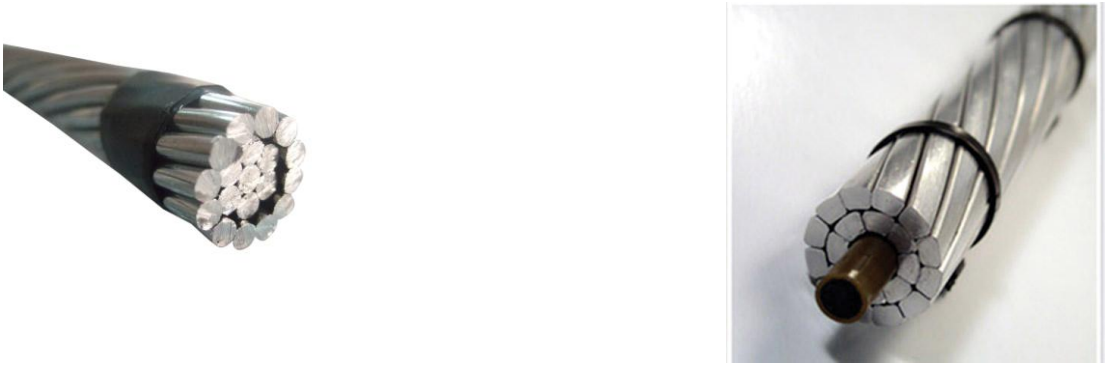

Figure 3.6 - ACSR on the left and ACCC conductor on the right.

3.2 Protection

The goal of this chapter is to give a brief insight on some protection schemes that are used on 132 kV networks and below. It is not intended to be a thoroughly explanation on network protection.
The protection design of a network is divided into zones. These zones affect the entire network giving different layers of isolation to limit the extent of the power system that is disconnected when a fault occurs, see Figure 3.7.

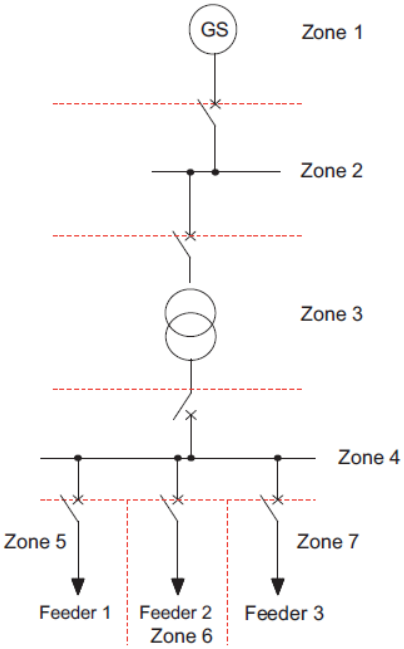

Figure 3.7 - Protection zones [10].

A unit protection scheme includes all protection oriented equipment – current transformers (CT´s), circuit breakers (CB´s), relays, etc. Relays can be located remotely from each other. They communicate between themselves and are instructed to perform certain actions like tripping, i.e. a controlled isolation of a circuit breaker. By tripping a circuit breaker, a protection signal is sent to both ends of a faulted circuit. That signal is acknowledged by the remaining relays on that circuit causing them to trip as well. Since they only act after receiving the signal, the process is called intertripping. The overall fault clearance time is the sum of the time the protection signal takes to reach the relay, the operating times of the relay, trip relay and circuit breaker. The fault can only exist during a certain interval of time defined by the resilience of the network equipment and the faster the protection works, less damage occurs on the network. Various types of carriers exist for protection signaling, ranging from telephone cables to radio channels and the most modern optical

fibers. If the current or voltage in the network is too high to connect relays, transformers are used to lower those values, namely voltage and current transformers [10].

3.3 Directional Overcurrent Protection

The impedance of a line is proportional to its length and changes in the event of a fault. A distance relay measures the impedance of a line up to a specific point, also known as the reach point and compares it with the impedance at the relay location. The reach [(1)] impedance measured at the reach point is calculated by dividing the voltage with the current at that point and then compares it with the measured impedance at the relay location. If the reach impedance is bigger than the measured impedance it is assumed that a fault exists between the relay and the reach point.

Take this example for instance: In the event of a fault on the 132 kV network, the grid substation circuit breaker will detect the fault current and make them trip by the directional over current protection. It will then send a signal to all transformers circuit breakers connected to it intertripping them. The fault will then be isolated and thus preventing any damage. If the protection does not work for a specific transformer circuit breaker, the fault current which is proportional to the impedance of the network flows through it.

Every transformer has a maximum setting that is always lower to its firm capacity called DOC protection, also known as directional over current protection. Even if there isn´t any fault, the DOC protection of transformers can be activated due to generation output. In the worst scenario of all generation being in its maximum output and low load conditions, most export flows backwards to the substation transformers. That back flow is called reverse power flow and if it exceeds the threshold value of the DOC protection, the transformer trips. Essentially the DOC can be activated in two scenarios; a fault or high generation output (under certain circumstances). When studying generation connections to the power network, one of the focal points is reverse power flows issues. If the minimum load of the connected primary and grid substations is below the maximum export of the generation site, there is a probability that there will be reverse power flows equal to the difference between that same export and the minimum load.

In the event of reverse power flows exceeding the threshold value of the transformer DOC protection the wind farms generating that extra amount of output must be restricted to avoid the transformer tripping out. Good communication between the distribution network and wind farms control is important in order to act quickly in case the export starts to reach its higher reverse power flow limit, thus, megawatt monitoring is fundamental as well. One of the ways to solve this issue would be to implement double intertripping systems instead of single. This way the transformers would be allowed to operate at their firm capacity as there would be two protection layers and the probability of both DOC protections failing is very low. As downside, the double intertripping system needs reliable communication and different pilots going different routes to each substation.

British Telecommunication is currently replacing all telephone cables with Ethernet cables. One of the differences is the delay time. It is not possible to determine the delay of the signal by using an Ethernet network since the route the signal takes is not fixed but dynamic and thus its travelling time is not predictable. With telephone cables and fiber optics is possible to know exactly the delay time of the signal. UKPN is in the process of implementing a fiber optic system named BT21 which will allow more advanced protection schemes like the duplication of intertripping systems.

[(1)] Name given to facilitate explanation and is not technically known.

4 Flexible Plug and Play Project

4.1 Introduction to Flexible Plug and Play

One of Future Networks projects, entitled Flexible Plug and Play (FPP), won £6.7 m funding award from Ofgem late 2011 and will play an important role in achieving the low carbon vision. Its scope of work will center on an area in North Cambridgeshire, between March and Peterborough where there is already a substantial amount of generation connected to its 33 kV network and a significant amount is planned to be installed as well. Its main scope is to produce a strategy implementing smart grid technologies to reduce or postpone major reinforcement costs, decreasing generation connection costs on this area. FPP project´s ambition is to study several approaches and devise a tool that enables to dynamically choose the most cost effective technology to provide enough capacity to several levels of generation. The effectiveness of different communication systems will be studied under the FPP project that may enable smart grid solutions to be implemented. Several technologies will be studied, for example:

- Dynamic line ratings using real time weather measurements of wind speed, wind direction and ambient temperature;

- Dynamic line ratings using fiber for direct conductor temperature analysis;

- Active Network Management (ANM) which brings a dynamic and automatic management to the power network, enabling control of output of generation sites according to circuit capacity and automatically move open points.

The scope of this thesis is to study the advantages that dynamic line ratings can bring to the power network, enhancing the capacity on overhead lines by increasing its thermal ratings, thus delaying network capital investment and increase network utilization.

4.2 Background and Context

The area chosen for this study is located between Peterborough and March with an area of 5000km^2. It is mainly rural with clusters of population around small towns, thus not being high on demand. The present infrastructure consists of a few 132 kV grid supply points and a 33 kV network connected to it that supplies small 33/11 kV primary substations. The landscape is very flat and open, making it ideal for the installation of wind turbines. Ten wind generation sites are already in operation, with a maximum combined output of 100MW and a further 7 sites with a capacity of 57 MW are already consented. There is insufficient capacity on the existing power network, and the protection, communications and SCADA infrastructure in the area has limited ability to support additional connections, being entirely based on classical reinforcement approaches. This specific area is currently experiencing issues due to a high amount of generation and no single project is able to withstand the infrastructure investment that is required to solve them. Some of the issues currently existing within the network are presented:

- Thermal constraints: Thermal ratings are reached at times of strong winds when the output of a wind farm is at its maximum, forcing it to decrease its export, also known as curtailment. Circuits are already in its full capacity with no or little headroom for future generation connections with thermal issues arising on both overhead lines and underground sections;

- The use of an active management of thermal constraints may be implemented by the use of dynamic ratings or conductor operating temperature real time analysis.

- Reverse power flows: Existence of power flows towards the lowest source impedance is another issue, resulting in unbalanced flows and thermal overload at various points in the grid while others have spare capacity. Transformer reverse power flow limits are also reached;

    - Reconfiguring the normally open points (NOP) may reduce the amount of reverse power flow within a specific circuit. The use of phase-shifting transformers or quadrature boosters may also be beneficial in order to manipulate the flow of power and be directed along less utilized paths within the power network.

- Voltage constraints: With the increase penetration of generation, voltage levels may reach or even exceed statutory limits under normal operating conditions. The ability to maintain an optimum voltage within statutory limits may be difficult even with existing voltage compensation components, transformers tap changers;

    - Active management of voltage levels within the power network will be implemented. It will modify reactive power flows accordingly and maximize real power flow exports.

The best way would be to develop a long term strategic plan that would focus in solving the above issues and by not using piecemeal investment for each project.

4.3 Network Configuration

This dissertation will mainly focus in two circuits between two primary substations and one grid substation.
Several wind farms are already connected to the 33 kV network as well as smaller ones on the 11 kV network. They are mainly consisted of wind turbines ranging from 1.6 MW to 2 MW. Table 4.1 gives information of the current wind farms connected to the 33 kV network being studied. Their output along the year varies greatly as seen in the next graphics and only reaches full capacity few times in a year. Bear in mind that the output of a wind farm doesn´t show details on how many wind turbines are operating at a given time.

Table 4.1 - Grid/primary substations and wind farms.

Primary Substations		Grid Substation
Bry Primary	**Frct Primary**	**Ptr Central Grid**
7.5/15 MVA	10/14.5/17 MVA	60 MVA
(2 Transformers)	(2 Transformers)	(2 Transformers)

Wind Farms				
Site	**Nº Turbines**	**Capacity [MW]**	**Capacity [A]**	**Connection**
RdT 1	5	10	175	Ptr Central Grid
RdT 2	7	14	265	
Glssmoor	8	16	280	

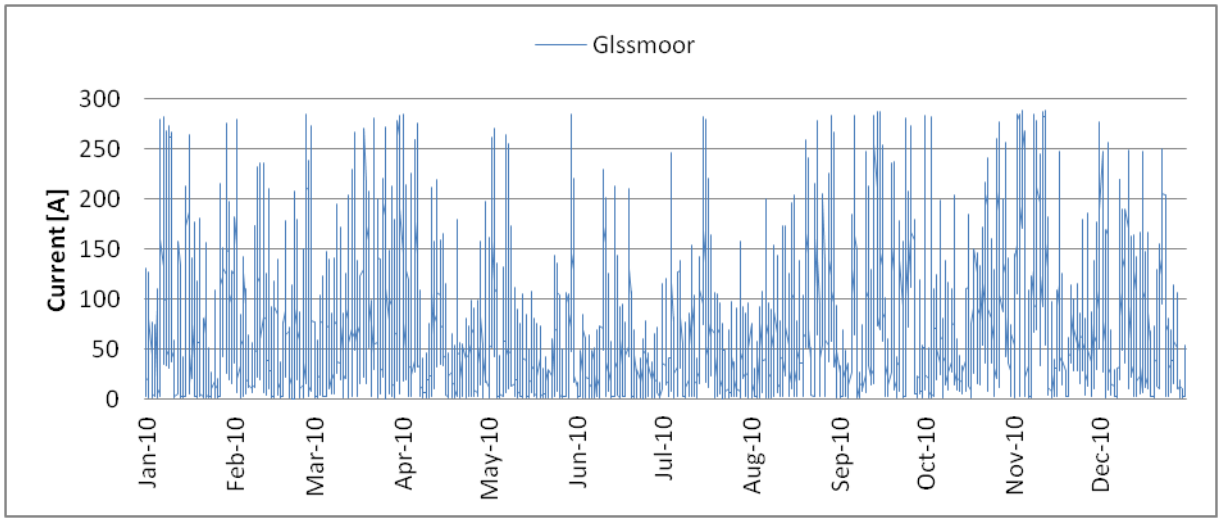

Figure 4.1 - Glssmoor wind farm generation profile.

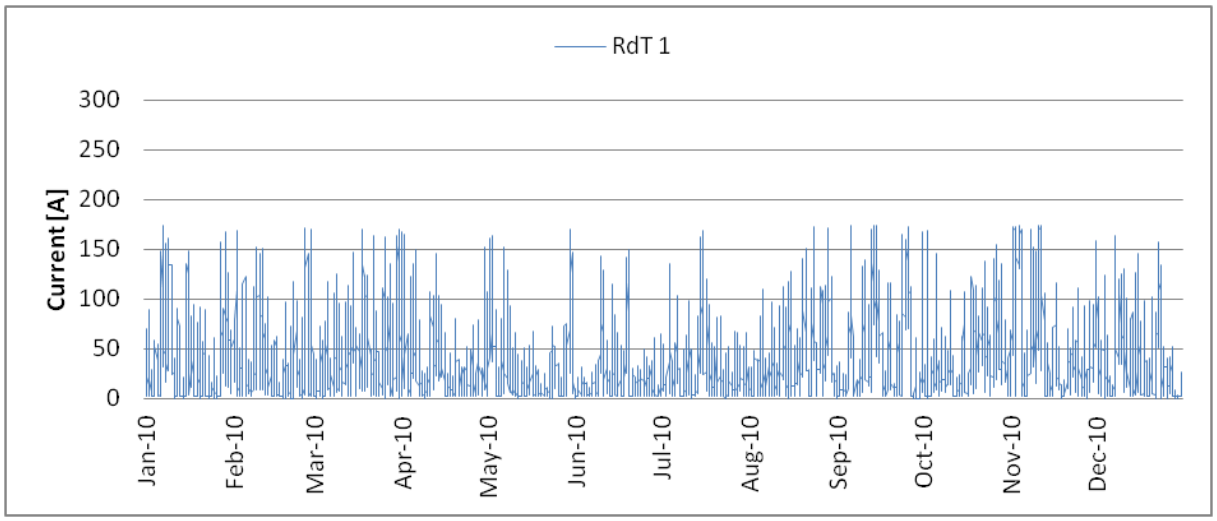

Figure 4.2 - RdT 1 wind farm generation profile.

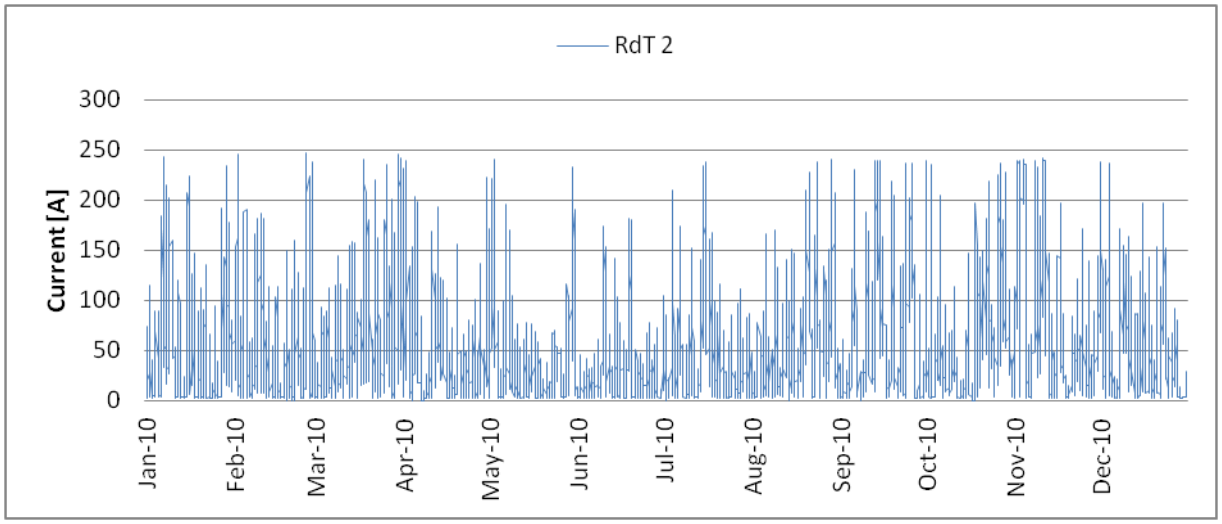

Figure 4.3 - RdT 2 wind farm generation profile.

The generation profile of all three wind farms is very erratic, not proving to be a stable source of electricity production. These three sites are relatively close to each other, and in times of high wind speeds they approach full export, reaching to as much as 26 MW flowing on a single overhead line from Glssmoor and RdT 1 wind farms.
Figure 4.4 shows the estimates of the amount of MWh produced as well as CO_2 emission savings and profit for each wind farm.

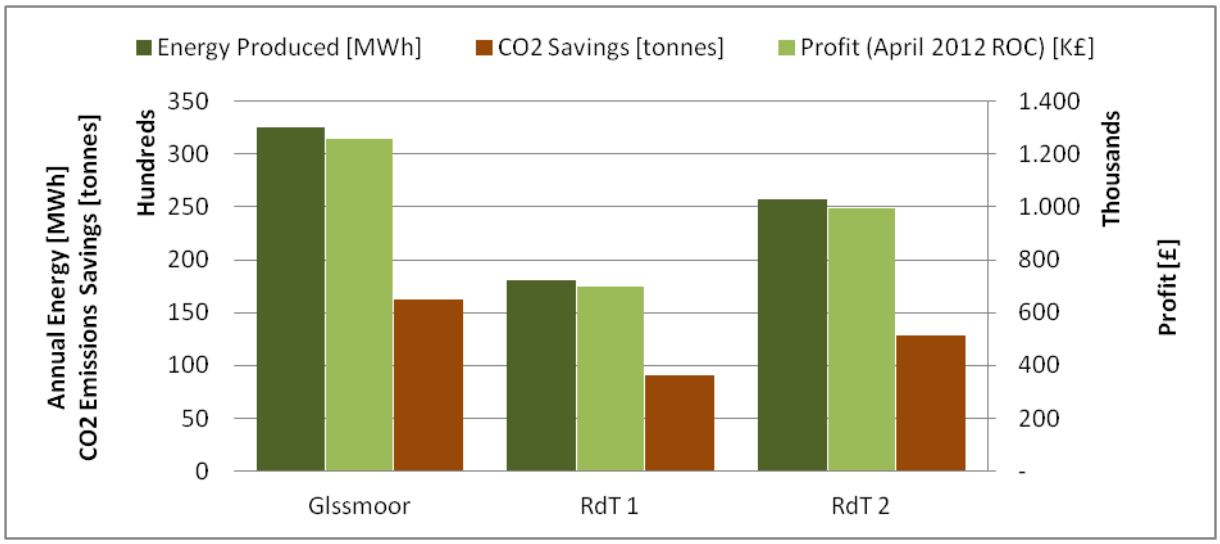

Figure 4.4 - Estimates of annual energy, CO_2 emissions savings and profit.

5 Overhead Line Reinforcement

There are several ways of increasing power delivered by an overhead line and are grouped into two categories: conductor methods and real time monitoring.

5.1 Conductor Methods – Conductor Retention, Increased Operating Temperature, Conductor Change

These methods range from no reinforcement or a very slight change to the conductor to a completely new conductor and the complexity, cost and capacity increases proportionally.

Conductor retention is a method in which the conductor is re-tensioned. The ground clearances are increased due to lower fall of the conductor towards the ground. There are no changes to the route or right-of-way of the overhead line, making it a first option when assessing increases in overhead line capacity. An increase in the conductor´s operating temperature gives a proportional increase in its rating. A survey of the overhead line is needed to detect sections where the increase in operating temperature might not be possible due to reduced clearances. Changes to the structure may be needed to allow the extra sag and the cost of those changes is dependent on the type of poles and foundations. Table 5.1 shows the increase in thermal ratings in amperes for four different overhead lines in the summer season and the increase in percentage relative to the operating temperature of 50 °C.

Table 5.1 - Overhead Lines Single Circuit Rating in amperes for 50 °C, 65 °C and 75 °C [4].

Conductor	Operating Temperature		
	50 °C	65 °C	75 °C
100 mm^2 DOG ACSR	253	302 (+19 %)	330 (+30 %)
150 mm^2 DINGO ACSR	338	408 (+21 %)	447 (32 %)
175 mm^2 LYNX ACSR	382	462 (+21 %)	507 (+33 %)
200 mm^2 JAGUAR ACSR	408	493 (+21 %)	541 (+33 %)

The gain in increasing the operating temperature of the conductor is significant, with a 20 % rating boost for a 30 % temperature rise. Despite the interesting advantages of conductor retention, physical work is probably needed to grant the extra temperature by raising structures and removing obstructions that may violate ground clearance like vegetation. Another issue is the continued monitoring of the overhead line route to see if they are still within ground clearance levels. If an area of the network is experiencing high load growth and/or increased embedded generation connections, conductor retention may only be a very short time solution to solve overhead line capacity issues. In these scenarios a different approach is needed and conductor change is the preferred solution albeit not so easy to implement. First of all, by changing to a different conductor, the foundations and poles have to withstand the extra weight; otherwise the cost increases as the need for new stronger structures arise. The largest conductor that can be installed on a 33 kV overhead line is 200 ACSR and although there are stronger conductors like 300 ACSR, its foundations and structures are bigger which may be difficult to setup due to permission from landowners and

public acceptance as well. The use of ACCC conductors, also known as high temperature low sag conductors are a good alternative to the ACSR conductors as they allow bigger operating temperatures with decreased sag. As they have similar weight to the 175 mm^2 LYNX ACSR conductor, there is no need to strengthen the foundations and structures, and only a re-tension of the conductor is needed [22].

5.2 Real Time Monitoring

The conductor tension and temperature can be analyzed in real time with the use of certain devices that capture that information. Data on tension and conductor temperature is gathered and used to optimize the ampacity of the existing overhead line while keeping ground clearances within statutory limits, thermal limits or the annealing properties of the conductor. For the flow of information to be successful, the communication system has to be reliable, secured and compatible with the systems in use. The data has to be sent securely to a core center in real time and then analyzed to achieve the new capacity of the transmission line. When introducing real time readings and consequently real time ratings, it is important to evaluate if other components on the circuit are able to withstand the new conditions. Information on circuit breakers, current transformers, joints and clamps is desired to examine the maximum thermal rating possible in that part of the network.

5.2.1 Tension Measurement

The temperature of the conductor is dependent on the weather conditions and the specification of the conductor itself. For example, during winter the existence of ice on the lines increases its weight, increasing its sag as well. It is possible to evaluate the sag as well as operating temperature of the conductor by measuring the tension of the conductor at the end of each section bearing in mind that its sag-tension relationship also takes into account permanent elongation, creep, overloads and more. Figure 5.1 shows a typical tension measurement equipment.

Figure 5.1 - Tension measurement [www.nexans.de].

5.2.2 Conductor Temperature Measurement

The conductor temperature can be obtained using several methods, ranging from the use of specific optical fibers in contact with the conductor or systems like the one shown on Figure 5.2 . This system is called power donut and it provides the conductor temperature. One of the issues is that the conductor temperature varies along its length and it is important to assess possible hot spots along the line route.

Figure 5.2 - Power donut [14].

5.2.3 Real Time Weather Data

Weather data like wind speed, wind direction, solar irradiance and ambient temperature can be measured by weather stations (Figure 5.3). By having all this information in real time, it is possible to calculate the ampacity of the overhead line for each time step of data, i.e. the current that can flow for a specific conductor´s temperature. Essentially, the temperature is set to a fixed value in which it obeys ground clearances and the maximum operating temperature of the conductor and the current for that weather conditions is calculated. This means that the sag will not increase and any issues that occur with high temperatures like the annealing of the conductor.

Figure 5.3 - Weather station [14].

5.2.4 Day/Night Time Ratings

By using day/night ratings, an increase of ratings during the day and a decrease at night would be possible. Day time for summer and winter is assumed to be from 7 am to 6 pm and from 8 am to 4 pm respectively. Night time for summer and winter is assumed to be from 6 pm to 7 am and from 4 pm to 8 am respectively. Figure 5.4 shows the average hourly demand of transformer 1 from Frct Primary Substation (Frct T1) of 2010. Low demand occurs at night, between 11 pm and 6 am, with an increase starting around 6:30 am onwards until it peaks around 6 pm. The overhead line chosen is a 150 ACSR with a summer single circuit rating of 382 A and a winter single circuit rating of 472 A. The reason to choose this overhead line is discussed in sub-chapter 6.6. The data behind the figures is taken from SCADA and for a specific hour, for example 5 pm, the demand at that hour of Frct T1 for each day of the year is averaged and split into summer and winter seasons. According to the Engineering Recommendation P27 “Current Rating Guide for High Voltage Overhead Lines Operating in the UK Distribution System”, summer season rating is between the 1st of May and the 30st of August, while winter season rating is between the 1st of December and the 28th of February. The same approach is used for both winter and summer generation export with SCADA data of Glssmoor and RdT 1 wind farms with the hourly averaged results shown in Figure 5.5.

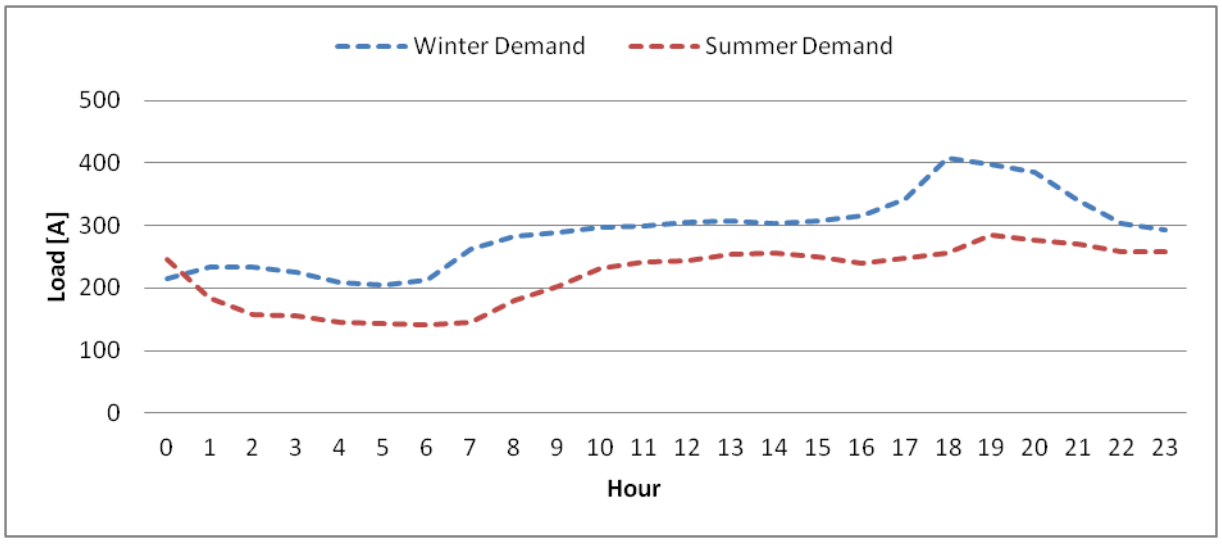

Figure 5.4 - Frct T1 Average Daily Demand.

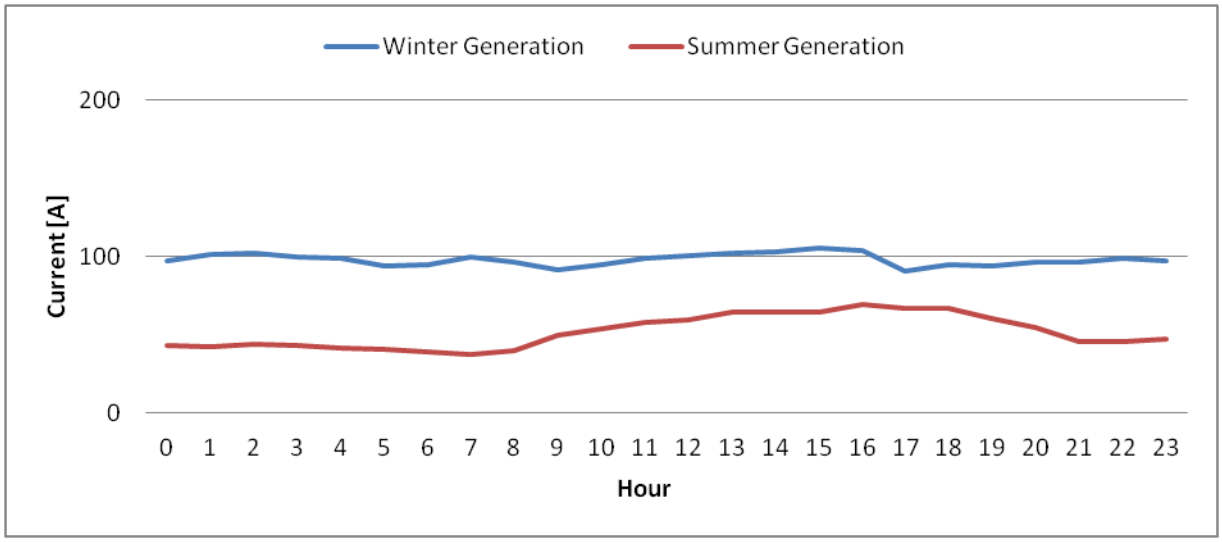

Figure 5.5 - Average Daily Generation.

In Figure 5.6 the resulting available capacity is plotted for winter and summer seasons. It was obtained by subtracting the static rating of the corresponding season with the difference between Frct demand and generation export:

$$Capacity = Static\ Rating - (Frct_{T1\ demand} - Generation)$$

For example, at 6 pm during winter there is around 95 A of generation export and a Frct demand of approximately 210 A. The current flowing in the line is approximately 115 A, therefore, the overhead line capacity at 6 pm during winter is:

$$Capacity_{6\ pm,winter} = 472 - 115 = 357\ A$$

There is an evident gain in applying a higher rating during the day as there would be an immediate increase in overhead line capacity. To follow this approach to a specific area, a detailed assessment and route profile would be necessary with relevant information on the existing load and generation to determine the risk in increasing the rating during the day and decrease it at night as there are consequences to both conductor´s overall condition and overhead line clearances.

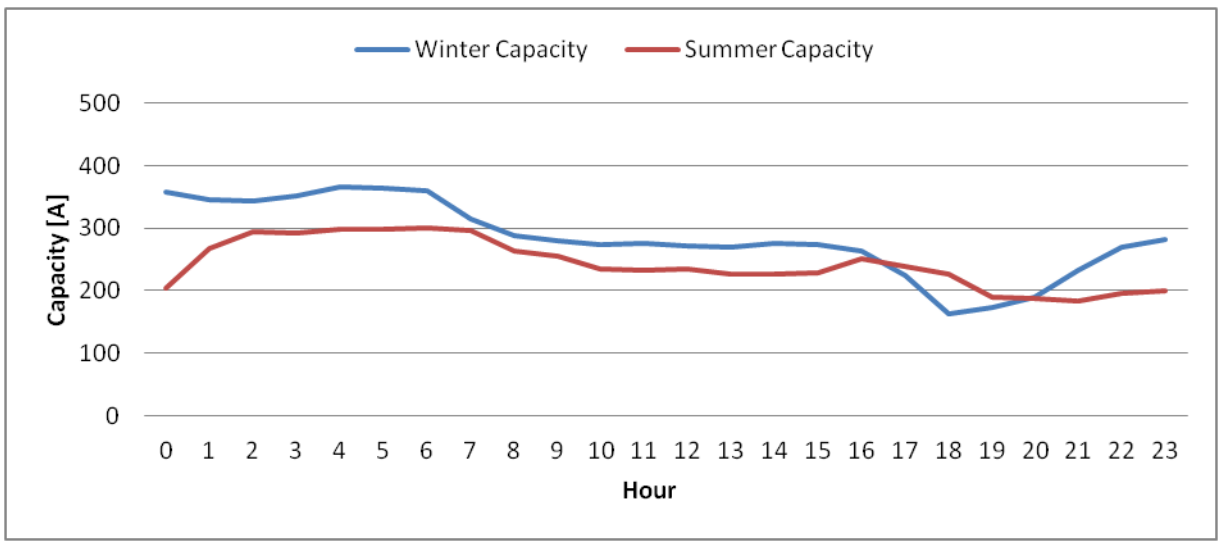

Figure 5.6 - Average Daily Available Capacity.

6 Dynamic Line Rating

6.1 Description

One of the challenges that exist at the moment is the viability of wind energy integration and other generation sources as well. The time it takes to install a wind farm is far less than reinforcing the network and that same reinforcement may never happen since it is very expensive for only one project to fund it. In most cases it is easier to decrease the power of a wind farm by installing less wind turbines or limit their power export, i.e. curtailment. The application of dynamic line rating may address this issue by allowing more current through the overhead lines at a lesser cost than classical reinforcement schemes.

Wind farms are normally at the outer limits of the distribution system and the lack of loads to feed on those specific sites results in most energy output to be exported to other places. The original lines were not designed to support the increase in distributed generation that is occurring, and with that, other problems arise like reverse power flows, increased fault levels, increased voltage levels and overhead lines ratings can be exceeded. Instead of applying static ratings for each season, a more dynamic approach on overhead line ratings can be followed, and with it enhancements on line ratings can be achieved, reducing the need for network reinforcement.

When a wind farm is generating power it means that there is favorable wind condition. That same wind also has a cooling effect on the overhead lines surrounding that site, thus, it would allow an increase of its thermal ratings. The wind speed and direction can change along that same conductor, resulting in different wind speeds and directions and consequently different temperatures along the line as seen in Figure 6.1 and Figure 6.2. In the presence of this situation, the rating of the overhead line would be restricted by the less cooled line section. The existence of buildings or high vegetation is very important to assess the cooling efficiency and the identification of possible hot spots along the line is essential. This decrease in cooling efficiency due to the properties of the terrain is called roughness and is explained in Chapter 7.

The direction of wind is an important parameter on the cooling effect of the overhead line. The best case scenario is when it is perpendicular to the conductor and the worst case being parallel to it. The line will not be hit by the same wind vector in all its length and consequently it will give different heat losses across it. Consequently, the dynamic thermal rating applied will need to be constrained in value to the less cooled section of the conductor or an underground section that is limiting the circuit upstream.

There are two distinct ways to determine the steady-state thermal rating, either by following the IEEE standard or the CIGRE. Both standards produce reliable results, and choosing one over the other is down to the complexity needed, which in most cases is not necessary. The difference between the two for the most usual weather conditions is less than 1 % but in some cases it can be up to 8.5 % with IEEE giving lower steady state ratings for higher wind speeds and with wind parallel to the line [9]. When it comes to solar radiation and the effect of ambient temperature, IEEE allows for a slightly higher ampacity. Please refer to “Appendix – IEEE & CIGRE Standards” for more information.

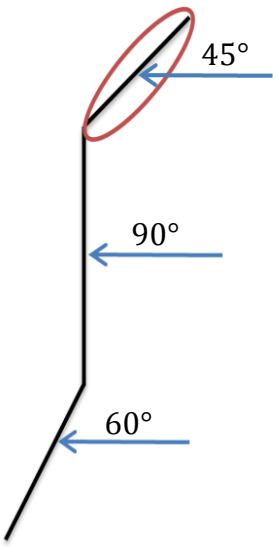

Figure 6.1 - Angle between wind and axis of conductor.

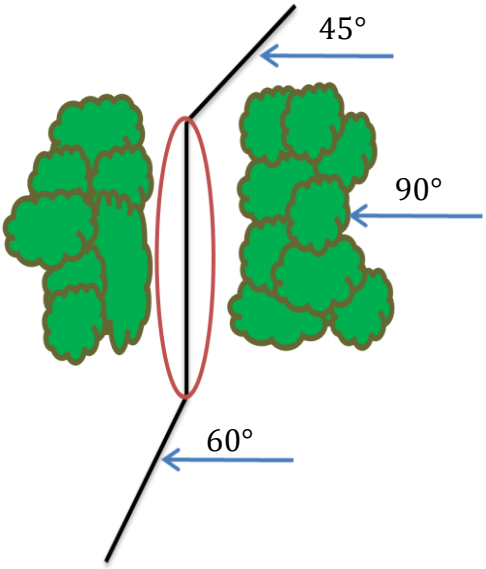

Figure 6.2 - Hot spots.

In order to avoid equipment degradation, critical temperatures and corresponding exposure times are specified by the manufacturer, ANSI Standard or by the utility design engineer. These critical temperatures and exposure times are used in conjunction with conservative values of thermal heat losses and historical electrical loading assumptions to calculate "thermal ratings", also referred to as ampacity. This rating represents the maximum current that a circuit can carry without exceeding its sag temperature or the annealing onset temperature of the conductor [5, 6]. The sag temperature corresponds to the value in which the ordained height of the conductor is met and if it exceeds that temperature, the height clearance can be compromised. These ratings are considered safe since they assume the worst case scenario of heat loss and are expressed in "MVA" or amperes [3]. There are essentially two different types of ratings, steady-state thermal rating and transient thermal rating. The first one represents the constant electrical current that would give the maximum allowable conductor temperature for specified weather conditions and conductor characteristics granting that the conductor is in thermal equilibrium. The second one is the highest current that gives the maximum allowable conductor temperature in a specified time and is considered to be an emergency thermal rating [2]. The calculation of the static rating for high voltage overhead lines operating in the UK distribution system is determined by a set of weather conditions; wind speed, ambient temperature of all seasons and solar radiation. The static ratings currently being applied are designed around a wind speed of 0.5 m/s and 12.5° direction, ambient temperatures of 2 °C, 9 °C and 20 °C for winter, spring/autumn and summer respectively and also does not assume any solar radiation.

6.2 Heat Balance Equation

A conductor is subject to seven energies as seen in Figure 6.3. As heating energy, there is the Joule heat effect yield by the flow of current, the solar radiation, the magnetic and corona heating. As cooling energy there is convective cooling (q_c), radiative cooling (q_r) and the cooling provided by the evaporation of water in contact with the conductor (q_w) [5].

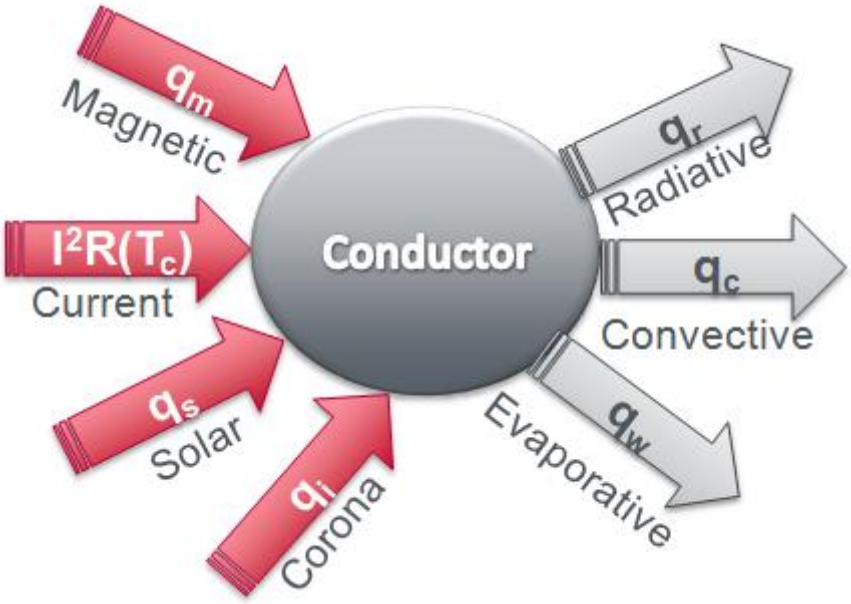

Figure 6.3 - Heat balance.

$$I^2R - Joule\ Heating;\ q_s - Solar\ Heating;\ q_w - Evaporative\ Cooling$$

$$q_m - Magnetic\ Heating;\ q_i - Corona\ Heating;$$

$$q_c - Convective\ Cooling;\ q_r - Radiated\ Cooling;$$

The general concept for calculating the rating of a line is based on the law of conservation of energy, as seen in equation 6.1.

$$I^2R(T_c) + q_s + q_m + q_i = q_c + q_r + q_w \tag{6.1}$$

The joule heating $(I^2R(T_c))$ results from the resistive losses due to current flow that heat the conductor during line operation. The solar heating (q_s) is the amount of irradiance that directly hits the conductor. It depends on several factors like the orientation of the overhead line, latitude, characteristics of the conductor and time of day. The magnetic heating (q_m) is due to a magnetic flux that is originated from AC operation which may induce eddy currents in the ferromagnetic core. In ACSR conductors, the aluminum wires are twisted around the steel core in opposite directions resulting in a cyclic magnetic flux and the magnetic fields cancel each other. The corona heating (q_i) originates from ionization of the air that is close to the conductor. Free air in the atmosphere has an electrostatic voltage gradient also known as sky voltage which can have a different voltage potential relative to the surface of the planet or the conductor itself. That gradient depends on atmospheric conditions like rain. The evaporative cooling (q_w) also depends on the amount of precipitation, thus both corona heating and the cooling from water evaporation are usually neglected as they largely cancel out. Convective cooling (q_c) takes into account the speed and direction of wind, and is the component that most contributes to lessen the conductor´s operating temperature. The radiative cooling (q_r) is given by the difference between ambient and the conductor´s operating temperatures. After neglecting the Corona, Magnetic heating, as well as the evaporative cooling, equation 6.1 becomes:

$$I^2R(T_c) + q_s + \cancel{q_m} + \cancel{q_i} = q_c + q_r + \cancel{q_w} \quad (6.2)$$

The ampacity of the conductor is thus given by:

$$I = \sqrt{\frac{q_c + q_r - q_s}{R(T_c)}} \quad (6.3)$$

The theoretical analysis of a conductor ampacity takes into account various parameters: the diameter of the conductor, air viscosity, air density, thermal conductivity of air, the difference between the conductor and ambient temperatures, wind speed and the effective angle of wind, i.e. the angle between the conductor axis and the wind. Although solar irradiance also affects the temperature of the conductor especially in summer with low wind speed conditions, the most important factor on the cooling of overhead lines is wind and its components – speed and direction.

There are two forms of convection: natural and forced. Natural convection is always present and depends on the conductor temperature, ambient temperature, overall diameter of the conductor and the air density. Forced convection is the cooling provided by wind. There are two types of forced convection, one for low wind speeds and another for high wind speeds and having as reference the IEEE standard, the biggest value of the natural and the two forced convection components is used. For more information on IEEE standard calculations please refer to Appendix – IEEE Standard for Calculating the Current-Temperature of Bare Overhead Conductors or reference [2].

6.3 General Theoretical Analysis

A theoretical approach was made to assess the advantages of dynamic line ratings on four different overhead lines used on 33 kV networks: 100 ACSR, 150 ACSR, 175 ACSR and 200 ACSR. To perform these studies, data on all lines is needed to obtain the dynamic rating of the overhead line. The resistance of the line at 50 °C was interpolated from the DC resistance at 25 °C and 75 °C. The next two tables include the gathered data for all lines: resistance at 20 °C and 75 °C, temperature coefficient, overall diameter, emissivity and solar absorption.

Table 6.1 - Conductor data [11].

Overhead Lines	Resistance @ 20°C [Ω/km]	Temp. Coeff. [1/K]	Overall Diameter [mm]	Emissivity	Solar Absorption	Resistance @ 75°C [Ω/km]
DOG 100 ASCR	0,2733	0,00403	14,15	0,7	0,9	0,329
DINGO 150 ASCR	0,1828		16,75			0,220
LYNX 175 ASCR	0,1576		19,53			0,190
JAGUAR 200 ASCR	0,1362		19,3			0,164

Table 6.2 - Overhead line single and multi circuit ratings [2].

Overhead Lines	Single & Multi Circuit Ratings [A]					
	Single Circuit			Multi Circuit		
	Summer	Spring Autumn	Winter	Summer	Spring Autumn	Winter
DOG 100 ASCR	253	290	311	284	327	351
DINGO 150 ASCR	338	391	421	382	443	476
LYNX 175 ASCR	382	442	476	433	501	539
JAGUAR 200 ASCR	408	472	508	462	534	575

6.4 Weather Conditions

Weather data, specifically the speed and direction of wind was fixed with steps of 0.5 m/s for wind speed and five different angles for wind direction: 90°, 45°, 30°, 15° and 0°. The angle is relative to the overhead line, so a wind direction of 90 and 0 degrees means that it is perpendicular and parallel to the line respectively.
Solar irradiance also affects the temperature of the conductor but to a much lesser degree when compared to wind. The graphic that follows shows the global irradiation in kWh/m^2 for a year in Europe. Global clear sky irradiance values were gathered for one day of each month and the highest value was chosen for each specific month. The information was then averaged for each season: summer, spring/autumn and winter.
The ratings obtained with these weather conditions are then compared to the static ratings of each overhead line for three different seasons: summer, spring/autumn and winter.

Table 6.3 - Global clear-sky irradiance [source: PVGIS estimates of average daily profiles taken from the Joint Research Centre].

Month	Global Clear-sky Irradiance on a Fixed Plane 0° [W/m^2]	Total Heat Flux (Q_s) for each Season Averaged [W/m^2]
January	257	
February	395	Summer
March	569	812
April	754	
May	832	
June	866	Spring/Autumn
July	824	584
August	746	
September	609	
October	448	Winter
November	293	287
December	210	

6.5 Calculations

The current flowing in a conductor is given by equation 6.1 and depends on the wind speed, wind direction, radiated cooling, solar heating and the conductor data as seen in Table 6.1. In this Chapter, the solar heating and radiated cooling is constant in each season.

6.5.1 Problem Statement

All equations are in Appendix – but will be shown here as well for convenience. All equations and tables taken from this Appendix will not have any reference to it to avoid continuous repetitions.
Thermal rating or current for a JAGUAR 200 mm^2 ACSR conductor, under the following conditions:

1. Wind speed of 1 m/s perpendicular to the conductor: $V_w = 1\ m/s$
2. Emissivity: $\varepsilon = 0.7$
3. Solar absorptivity: $\alpha = 0.9$

4. Ambient air temperature: $T_a = 20$ ℃
5. Conductor operating temperature: $T_c = 50$ ℃
6. Overall Diameter: $D = 19.3\ mm$
7. Conductor DC resistance is:

   $R(20\ ℃) = 0.1362\ \Omega/km$

   $R(75\ ℃) = 0.164\ \Omega/km$
8. Average conductor elevation: $H_e = 10\ m$

Air viscosity (μ_f), air density (ρ_f) and air thermal conductivity (k_f) are shown in Table 6.4. They are obtained through equations I.2, I.4 and I.5.

Table 6.4 - Air viscosity, air density and air thermal conductivity for summer, spring/autumn and winter.

	Air Viscosity [Pa]	*Air Density [kg/m³]*	*Air Thermal Conductivity [W/m°C]*
Summer	1,884E-05	1,144E+00	2,685E-02
Spring/Autumn	1,858E-05	1,165E+00	2,644E-02
Winter	1,841E-05	1,179E+00	2,618E-02

To simplify the calculations, the radiated cooling, total heat flux and consequently the solar heating is fixed for each season, therefore, data on the azimuth of the overhead line, latitude, solar altitude are not needed.

6.5.1.1 Convection Heat Loss (q_{cn})

Natural convection depends entirely on the ambient and conductor´s temperature and is given by means of equation 6.4.

$$q_{cn} = 0.0205{\rho_f}^{0.5} D^{0.75} (T_c - T_a)^{1.25} \quad (6.4)$$

$$q_{cn} = 0.0205\ \times (1.144\ )^{0.5} \times (19.3)^{0.75} \times (50 - 20)^{1.25} = 14\ W/m$$

Since the wind speed is greater than zero, the forced convection heat loss for perpendicular wind is obtained according to equation 6.5 and 6.6.

$$q_{clow} = \left[1.01 + 0.0372 \left(\frac{D\rho_f V_w}{\mu_f}\right)^{0.52}\right] k_f K_{angle} (T_c - T_a) \quad (6.5)$$

$$q_{chigh} = \left[0.0119 \left(\frac{D\rho_f V_w}{\mu_f}\right)^{0.6}\right] k_f K_{angle} (T_c - T_a) \quad (6.6)$$

Equation 6.5 gives the forced convection loss for low wind speeds, while equation 6.6 the forced convection for high wind speeds. The largest of the heat losses due to both natural and the two forced convections is used to calculate the thermal rating.
K_{angle} is the wind direction factor, where Ø is the angle between the wind direction and the conductor axis and is given by equation 6.7.

$$K_{angle} = 1.194 - \cos(\emptyset) + 0.194\cos(2\emptyset) + 0.368\sin(2\emptyset) \quad (6.7)$$

Replacing Ø with 90 °:

$$K_{angle} = 1$$

Forced convection for low wind speeds is given by:

$$q_{clow} = \left[1.01 + 0.0372 \times \left(\frac{19.3 \times 1.144 \times 1}{1.884 \times 10^{-5}}\right)^{0.52}\right] \times 2.685 \times 10^{-2} \times 1 \times (50 - 20)$$
$$= 43.73\ W/m$$

Forced convection for high wind speeds is given by:

$$q_{chigh} = \left[0.0119 \times \left(\frac{19.3 \times 1.144 \times 1}{1.884 \times 10^{-5}}\right)^{0.6}\right] \times 2.685 \times 10^{-2} \times 1 \times (50 - 20) = 41.99\ W/m$$

The largest of these three heat losses, q_{cn}, q_{clow} and q_{chigh} is chosen for the thermal rating calculation.

6.5.1.2 Radiated Heat Loss (q_r)

Radiated heat loss is calculated with equation 6.8.

$$q_r = 0.0178D\varepsilon\left[\left(\frac{T_c+273}{100}\right)^4 - \left(\frac{T_a+273}{100}\right)^4\right] \quad (6.8)$$

$$q_r = 0.0178 \times 19.3 \times 0.7 \times \left[\left(\frac{50+273}{100}\right)^4 - \left(\frac{20+273}{100}\right)^4\right] = 8.45\ W/m$$

6.5.1.3 Solar Heat Gain (q_s)

Solar heat gain is given by equation 6.9.

$$q_s = \alpha Q_s sin(\theta) A' \quad (6.9)$$

Where

$$Q_s = 812\ W/m^2$$

$$A' = \frac{D}{1000} = \frac{19.3}{1000} = 0.0193\ m$$

$$\theta = \arccos[\cos(H_c)\cos(Z_c - Z_1)]$$

With H_c being the altitude of the sun, Z_c the azimuth of the overhead line and Z_1 is either 90° or 270° depending on the value of Z_c as the subtraction has to be above zero. $\theta = 1$ to facilitate calculations in this Chapter.

$$q_s = 0.9 \times 812 \times 1 \times 0.0193 = 14.10\ W/m$$

6.5.1.4 Thermal Rating (I)

The thermal rating is given by equation 6.10.

$$I = \sqrt{\frac{q_c + q_r - q_s}{R(T_c)}} \tag{6.10}$$

Where $R(T_c)$ is the resistance of the conductor at the operating temperature chosen, i.e. at 50 °C. The resistance of the conductor at that operating temperature can be interpolated using known values, i.e. having the temperature for 20 °C and 75 °C it is possible to obtain the resistance at 50 °C.

$$R(T_c) = \left[\frac{R(T_{high} - R(T_{low})}{T_{high} - T_{low}}\right](T_c - T_{low}) + R(T_{low})$$

$$R(50) = \left[\frac{R(75) - R(20)}{75 - 20}\right](50 - 20) + R(20)$$

$$R(50) = \left[\frac{0.164 - 0.1362}{75 - 20}\right] \times (50 - 20) + 0.1362 = 0.0001514\ \Omega/m$$

Using Equation 6.10 the thermal rating is calculated using the largest convection heat loss, the radiated heat loss, the solar heating and the resistance of the conductor at an operating temperature of 50 °C.

$$I = \sqrt{\frac{43.73 + 8.45 - 14.10}{0.0001514}} = 501.5\ A$$

This procedure is repeated for wind speeds ranging from 0 m/s to 18 m/s in steps of 0.5 m/s for wind directions of 90°, 45 °, 30 °, 15 °, 0 ° and for three different seasons. The difference in thermal rating due to wind direction is the wind direction factor K_{angle} that decreases the cooling effect of forced convection on the overhead line.
For each specific wind direction, the wind direction factor is given by:

$K_{angle}(90\ °) = 1$
$K_{angle}(45\ °) = 0.85$
$K_{angle}(30\ °) = 0.74$
$K_{angle}(15\ °) = 0.58$
$K_{angle}(0\ °) = 0.39$

As seen in the forced convection calculations, the wind direction factor gives a decrease in that same cooling effect. For the same wind speed, wind hitting the conductor with a direction of 30 ° has 26 % less cooling effect on it.

For very low wind speeds there is a slight delay in the thermal rating increase as seen in Figure 6.6, Figure 6.7 and Figure 6.8. This happens due to the natural convection heat loss being higher that both forced convection heat losses for those wind speeds. Bearing in mind that this natural convection depends on the conductor overall diameter, ambient temperature, conductor temperature and air viscosity, and those three components are fixed in this Chapter for each season, it means that the natural convection heat loss is the same value for each season.

$$q_{cn}\,(summer) = 0.0205\ \times (1.144\ )^{0.5} \times (19.3)^{0.75} \times (50-20)^{1.25} = 14.2\ W/m$$

$$q_{cn}\,(spring\ and\ autumn) = 0.0205\ \times (1.165\ )^{0.5} \times (19.3)^{0.75} \times (50-9)^{1.25} = 21.1\ W/m$$

$$q_{cn}\,(winter) = 0.0205\ \times (1.179\ )^{0.5} \times (19.3)^{0.75} \times (50-2)^{1.25} = 25.9\ W/m$$

The thermal rating for these three natural convection heat losses and for each specific season with the corresponding solar heating and radiated heat losses components:

$$I_{summer} = \sqrt{\frac{14.2 + 8.45 - 14.10}{0.0001514}} = 237.3\ A$$

$$I_{spring\ and\ autumn} = \sqrt{\frac{21.1 + 10.97 - 10.15}{0.0001514}} = 380.8\ A$$

$$I_{winter} = \sqrt{\frac{25.9 + 12.42 - 4.99}{0.0001514}} = 469.1\ A$$

These thermal ratings are represented as constant lines for very low wind speeds because the natural convection heat loss is larger than the two forced convection heat losses for that range of wind speeds.

6.5.2 Contribution of Convection, Radiated Heat Loss and Solar Heat Gain

Figure 6.4 represents the contribution of each component (convection, radiated heat loss and solar heat gain) compared to the rating of a 200 ACSR conductor during day and night times for winter and summer seasons. The chosen days were the 22nd of January 2010 and 6th of June 2010 with day times from 8 am to 4 pm and 7 am to 6 pm for winter and summer respectively. The procedure was to initially choose a time of day that would represent a good base case for both radiated heat loss and solar heat gain, i.e. for summer a day and night temperatures of 25 °C and 12 °C respectively taken from the 6th of June were chosen. For winter, a day and night temperatures of -2 °C and -7 °C respectively taken from the 22nd of January were chosen. The radiated heat loss and solar heat gain contributions were calculated as static values for day and night. Wind cooling was then plotted for each wind speed step change, ranging from 0 m/s to 15 m/s, thus giving a better idea of wind convection overall contribution to the overhead line cooling.

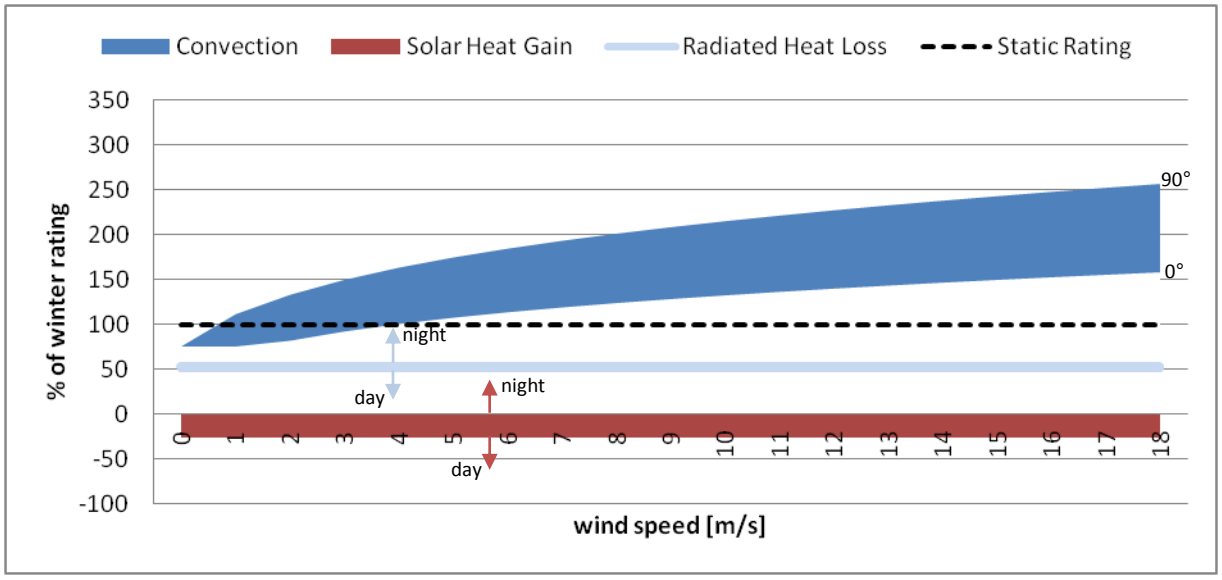

Figure 6.4 - % Increase in rating for winter day/night.

The cooling effect of wind, represented in dark blue, is very important in the overall temperature of the conductor, and is responsible for an increase up to 156 % of the winter rating. The upper limit is for a wind incidence perpendicular to the conductor axis, while the lower limit is for a wind parallel to the line. In winter, the radiated heat loss, in light blue, ranges from 51 % to 53 % for day and night times respectively. This happens mostly because the temperature difference between day and night is small. The solar heating, in red, ranges from -27 % (it is negative because it decreases the rating) to 0 % for day and night times respectively, being canceled by the radiated heat loss. By including only the convective cooling energy and neglecting solar heating and radiative cooling, it is possible to determine the ampacity of the overhead line that results solely from the convective cooling for each step in wind speed. Bear in mind that this approach is only to demonstrate the contribution of all energies involved and compare it with the static rating.

As an example, for a wind speed of 6 m/s perpendicular to the conductor at an operating temperature of 50 °C and using the same approach given in sub-chapter 6.4.1, there is the following increase in rating for winter season:

$$I = \sqrt{\frac{q_{c6m/s\perp}}{R(T_c)}} = \sqrt{\frac{170}{0.0001514}} = 1059\ A \xrightarrow{\%\ rating} \% = \frac{1059 \times 100}{575} = 184\ \%$$

For a wind speed of 6 m/s parallel to the conductor we have the following:

$$I = \sqrt{\frac{q_{c6m/s\parallel}}{R(T_c)}} = \sqrt{\frac{66}{0.0001514}} = 662\ A \xrightarrow{\%\ rating} \% = \frac{662 \times 100}{575} = 115\ \%$$

Radiative cooling for day and night times slightly changes:

$$I = \sqrt{\frac{q_{r(day)}}{R(T_c)}} = \sqrt{\frac{13}{0.0001514}} = 293\ A \xrightarrow{\%\ rating} \% = \frac{293 \times 100}{575} = 51\ \%$$

$$I = \sqrt{\frac{q_{r(night)}}{R(T_c)}} = \sqrt{\frac{14}{0.0001514}} = 304\ A \xrightarrow{\%\ rating} \% = \frac{304 \times 100}{575} = 53\ \%$$

Solar heating only occurs during the day:

$$I = \sqrt{\frac{q_{s(day)}}{R(T_c)}} = \sqrt{\frac{4}{0.0001514}} = 162\ A \xrightarrow{\%\ rating} \% = \frac{162}{575} = -28\ \%$$

If we then sum all the individual contributions we find the thermal rating of the conductor during the day and for winter:

$$I_{6\ m/s\ \perp} = 1059 + 293 - 162 = 1190\ A \xrightarrow{\%\ rating} \% = \frac{1190 \times 100}{575} - 100 = 107\ \%$$

$$I_{6\ m/s\ \parallel} = 662 + 293 - 162 = 793\ A \xrightarrow{\%\ rating} \% = \frac{793 \times 100}{575} - 100 = 38\ \%$$

For wind speeds near zero, the natural convection is above the forced convection.

$$I_{0\ m/s} = \sqrt{\frac{MAX(q_{cn}; q_{clow}; q_{chigh})}{R(T_c)}} = \sqrt{\frac{MAX(28.7; 1.4; 0)}{0.0001514}} = 435\ A \xrightarrow{\%\ rating} \% = 76\ \%$$

For a wind speed of 0 m/s, the current is 24 % below the static rating of 575. For a wind speed of 6 m/s, the thermal rating of the conductor varies from a 38 % increase to 107 %, which shows a high dependency on wind direction. For a summer day and night as seen in Figure 6.5, the convection percentage rating band is the same while there are significant changes to both radiated heat loss and solar heat gains. Due to a rise in day and night temperatures, solar heat gain is higher during the day while the radiated heat loss is lower throughout the day and night. In summer, the solar heat gain plays a bigger part in the heat balance equation and the overall increase in conductor´s temperature.

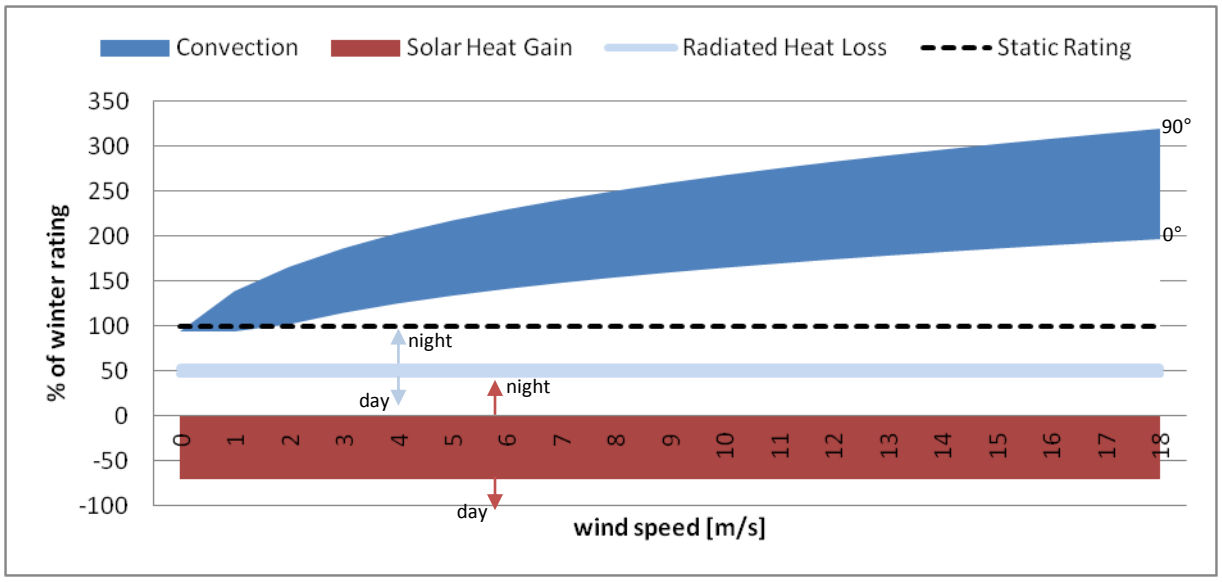

Figure 6.5 - % Increase in rating for summer day/night.

Radiative cooling for day and night times slightly changes:

$$I = \sqrt{\frac{q_{r(day)}}{R(T_c)}} = \sqrt{\frac{7}{0.0001514}} = 215\ A \xrightarrow{\%\ rating} \% = \frac{215 \times 100}{462} = 47\ \%$$

$$I = \sqrt{\frac{q_{r(night)}}{R(T_c)}} = \sqrt{\frac{10}{0.0001514}} = 257\ A \xrightarrow{\%\ rating} \% = \frac{257 \times 100}{462} = 56\ \%$$

Solar heating only occurs during the day:

$$I = \sqrt{\frac{q_{s(day)}}{R(T_c)}} = \sqrt{\frac{16}{0.0001514}} = 325\ A \xrightarrow{\%\ rating} \% = \frac{325 \times 100}{462} = -70\%$$

If we then sum all the individual contributions we find the thermal rating of the conductor during the day and for summer:

$$I_{6\ m/s\ \perp} = 1059 + 215 - 325 = 949\ A \xrightarrow{\%\ rating} \% = \frac{949 \times 100}{462} - 100 = 105\ \%$$

$$I_{6\ m/s\ \parallel} = 662 + 215 - 325 = 552\ A \xrightarrow{\%\ rating} \% = \frac{552 \times 100}{575} - 100 = 19\ \%$$

The increase in rating especially when wind is parallel to the conductor is lower during summer than winter as the solar heating is much higher during summer.

6.6 Results

In this sub-chapter the static ratings of each season are plotted against dynamic thermal ratings using the previous method presented in sub-chapter 6.4.1 for different speeds and directions of wind. There are other upstream components that prevent the full gain of dynamic ratings, for example, air breaker switch disconnectors have their continuous rated current at 600 A.
Figure 6.6, Figure 6.7 and Figure 6.8 represent the gain by using dynamic line ratings for a 200 mm^2 ASCR overhead line when compared to multi circuit static ratings.

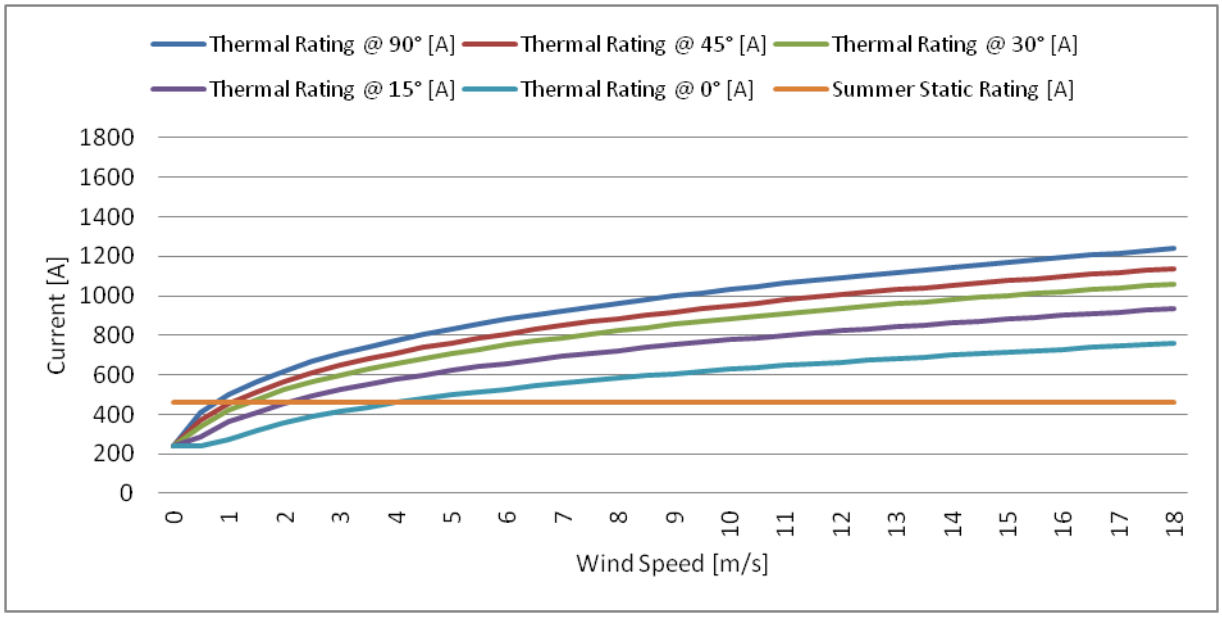

Figure 6.6 - Dynamic ratings vs. static ratings 200 mm^2 ASCR conductor (summer).

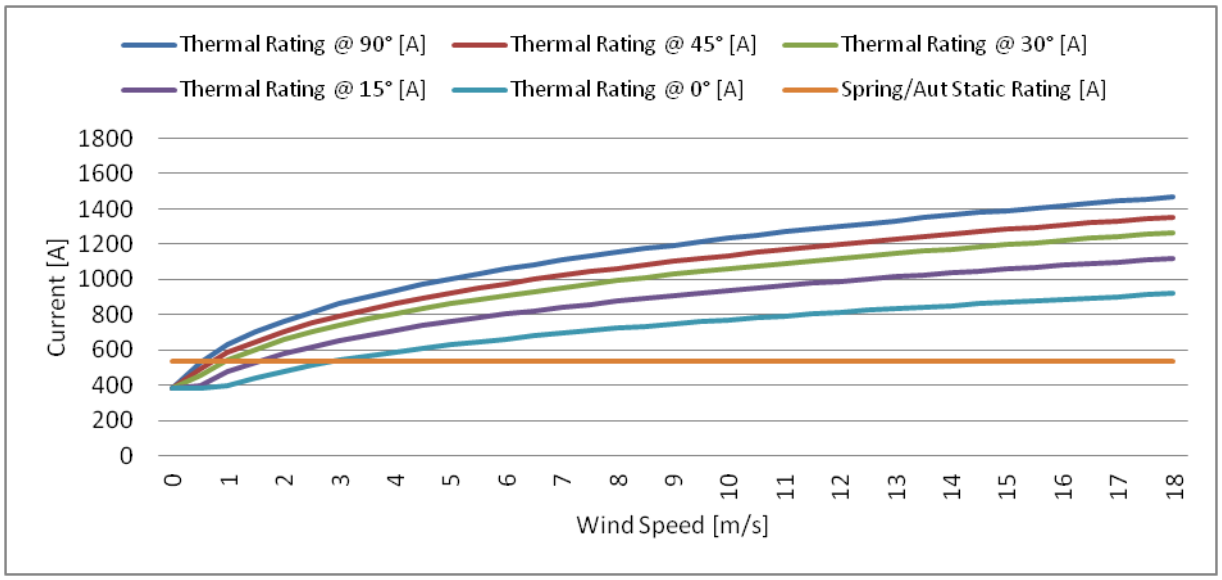

Figure 6.7 - Dynamic ratings vs. static ratings 200 mm² ASCR conductor (spring/autumn).

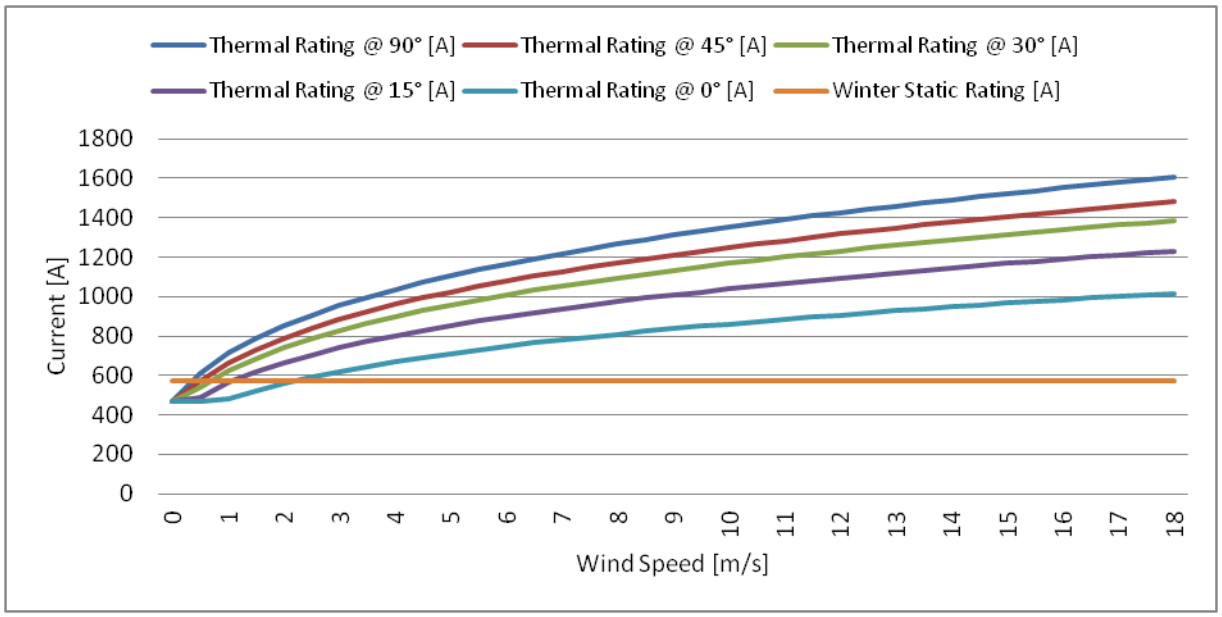

Figure 6.8 - Dynamic ratings vs. static ratings 200 mm² ASCR conductor (winter).

6.7 Case Study Theoretical Analysis

6.7.1 Approach

Initially the approach was to focus on parts of the network that are experiencing heavy increase in embedded generation connected to the 33 kV network.

After identifying those sections, a desktop route profile study was carried using aerial photography to analyze possible obstructions along the line. Wind speed, direction of wind and ambient temperature were taken from Glssmoor wind farm mast at a height of 60 meters and all studies were carried with the following assumptions:

1) The wind speed and wind direction taken at the height of 60 meters at Glssmoor wind farm is the same in the area;

2) The maximum theoretical value is obtained using the power curve of the wind turbine used, thus producing an ideal theoretical export, i.e. losses were not accounted;

3) For the line route itself, certain values on wind roughness were assumed that indicate a decrease in wind speed according to different levels of obstructions, i.e. vegetation, buildings, etc.

4) Results do not account for losses along overhead lines and cables and assumes a constant voltage of 33 kV, except for Frct T1 that varies from 48.53 % in volts when there is no generation to 62.5 % when the generation is at its present maximum (26 MW).

To determine the amount of solar irradiance per half hour, information on the day of the year and latitude is needed. It affects the number of solar hours per day and consequently the solar irradiance that exists.

A series of studies were carried to analyze the amount of headroom available by applying dynamic line ratings. With the export of wind farms around the area being studied, it is possible to determine the headroom in those circuits and assess the possible increase in generation capacity. The calculation of dynamic ratings is based on the "IEEE Standard for Calculating the Current-Temperature of Bare Overhead Conductors"; therefore those ratings will be theoretical. Two comparisons will be made; one will be between the theoretical generation export taken from the wind turbines power curve and the theoretical dynamic ratings. The other between the wind farm real generation export, taken from SCADA, and the theoretical dynamic ratings. The theoretical maximum export was obtained using the power curve of the turbines installed at the wind farms (see Figure 7.1). For each 0.1 m/s of wind speed step, the export (in Ampere and kW) was obtained and then multiplied by the number of existing turbines. This method gives an approximate value of the ideal export with all wind turbines operating at the same time.

The assessment will be split into two circuit arrangements, as the flow of current is different in both. Circuit 1 is between the tee point at Glssmoor wind farm and Frct Primary Substation. Circuit 2 is between Frct Primary Substation tee and Ptr Central Grid Substation. These circuits were chosen because they are near their maximum capacity. During normal operating conditions, both RdT 1 and Glssmoor wind farms will have their export flowing to Frct Primary and Ptr Central Grid as Bry Primary is supplied from a different Grid source.

On circuit 1, all generation is flowing through that single overhead line. It is considered to be the first study case and is highlighted in Figure 6.9. According to the network arrangement, most generation is flowing to Frct Primary T1. Only when there is an outage on Frct T1 or when the export is higher than Frct T1 load there is current flowing to Ptr Central Grid. Under normal operating conditions, Bry

Primary is fed by a different Grid Substation, while Frct Primary T1 is fed by Ptr Central Grid Substation. In certain circumstances, the normal open point at Bry Primary T1 closes and the bus bar opens. Consequently, Bry T1 is supplied by Ptr Central Grid Substation with the load being defined by the 11 kV feeders.

On circuit 2, under normal arrangement, the current is given by the difference between Frct T1 load and the generation. When Bry T1 is supplied by Ptr Central Grid, the current on circuit 2 is the difference between the sum of Frct T1 and Bry T1 loads with the generation.

Several scenarios arise due to the arrangement of this network:

1) Normal operating conditions: Frct Primary T1 supplied by Ptr Central Grid while Bry T1 is supplied by a different Grid Substation. Frct Primary T2 operational (see Figure 6.10);

$$I_{C1} = I_{Glss} + I_{RdT\ 1} \qquad I_{C2} = I_{C1} - I_{Frct\ T1} \tag{6.11}$$

2) N-1 normal operating conditions: Frct Primary T1 supplied by Ptr Central Grid while Bry T1 is supplied by a different Grid Substation. Outage on Frct Primary T2 (see Figure 6.11);

$$I_{C1} = I_{Glss} + I_{RdT\ 1} \qquad I_{C2} = I_{C2} - I_{Frct\ T1\&T2} \tag{6.12}$$

3) Bry Primary T1 and Frct Primary T1 both supplied by Ptr Central Grid and Frct Primary T2 operational (see Figure 6.12);

$$I_{C1} = I_{Glss} + I_{RdT\ 1} - I_{Bry\ T1} \qquad I_{C2} = I_{C1} - I_{Frct\ T1} \tag{6.13}$$

4) N-1: Bry Primary T1 and Frct Primary T1 both supplied by Ptr Central Grid and an outage on Frct Primary T2 (see Figure 6.13).

$$I_{C1} = I_{Glss} + I_{RdT\ 1} - I_{Bry\ T1} \qquad I_{C2} = I_{C1} - I_{Frct\ T1\&T2} \tag{6.14}$$

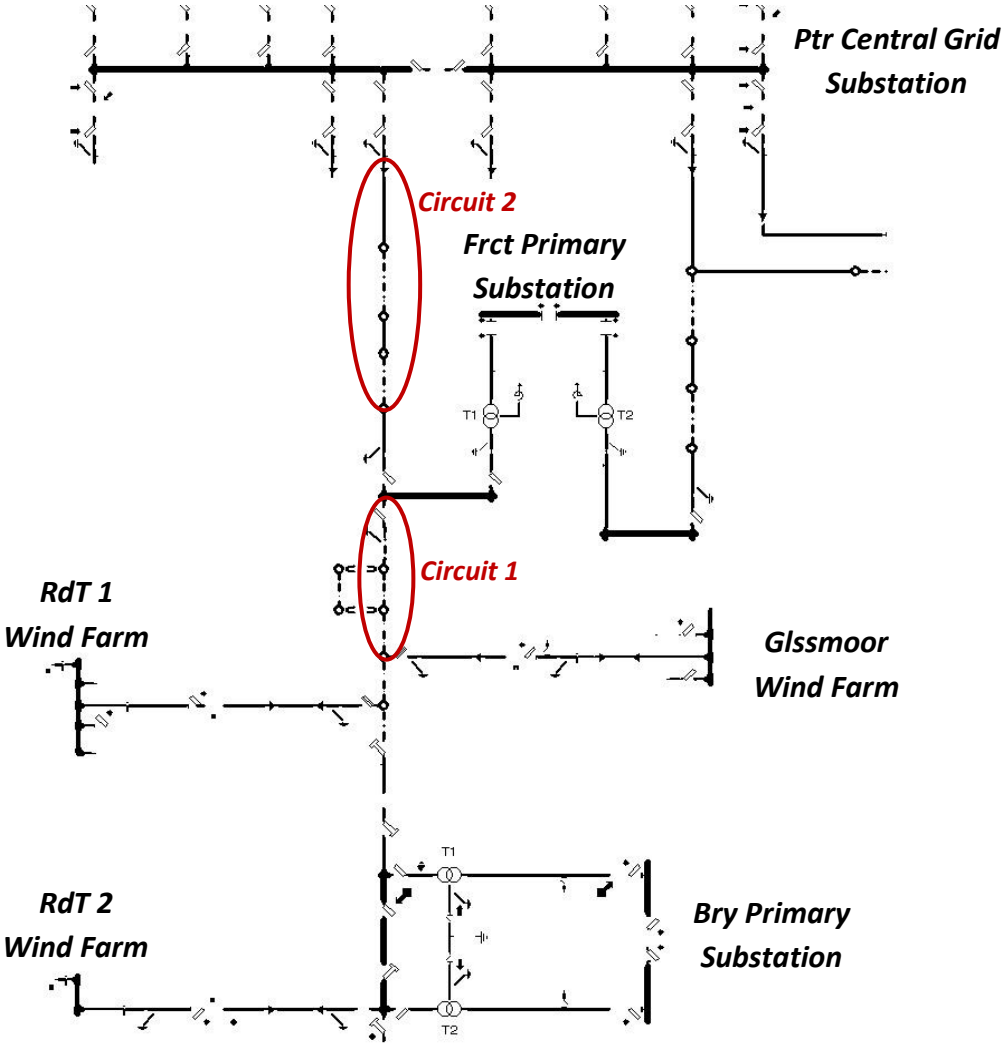

Figure 6.9 - Circuit 1 and 2
Ptr Central grid substation, Frct Primary substation, Bry Primary substation
RdT 1, RdT 2 and Glssmoor wind farms.

Later on Chapter 7, only scenario 1 and 3 will be considered as they represent normal operating conditions.
The currents showing in Figure 6.10, Figure 6.11, Figure 6.12 and Figure 6.13 are positive, i.e. current flowing to Ptr Central Grid Substation is positive (export), while current flowing from it is negative.

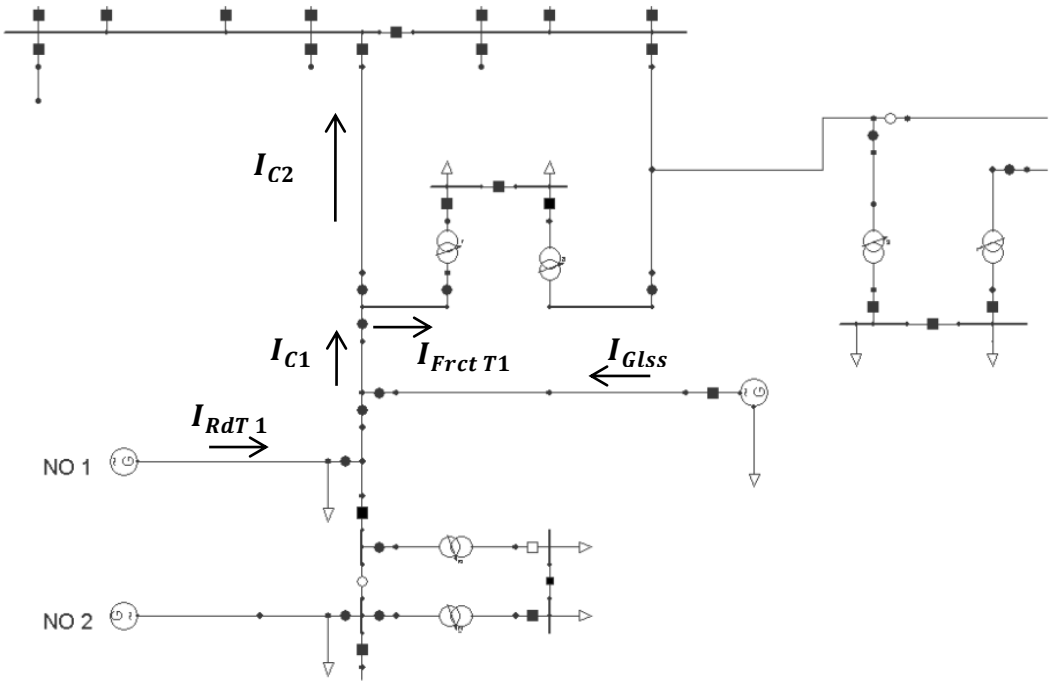

Figure 6.10 - Circuit under scenario 1.

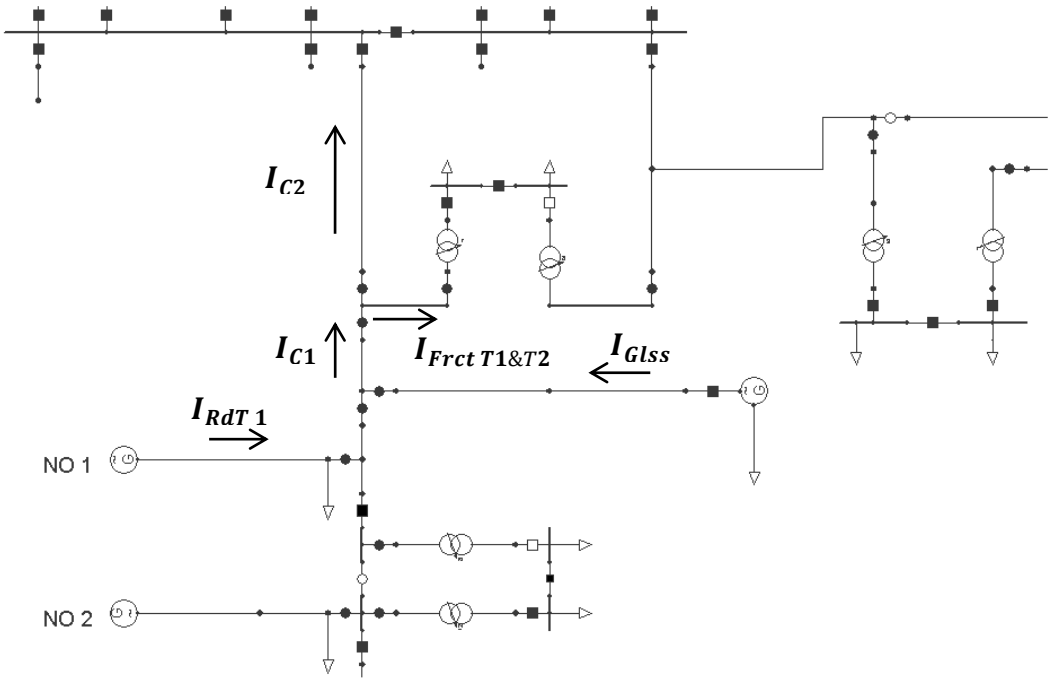

Figure 6.11 - Circuit under scenario 2.

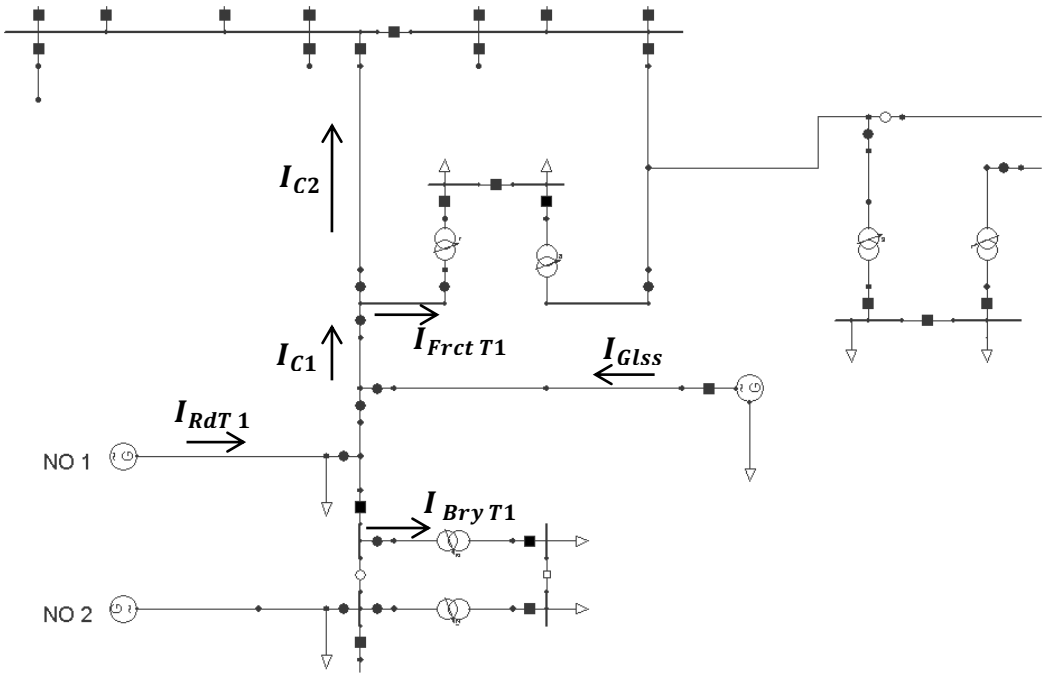

Figure 6.12 - Circuit under scenario 3.

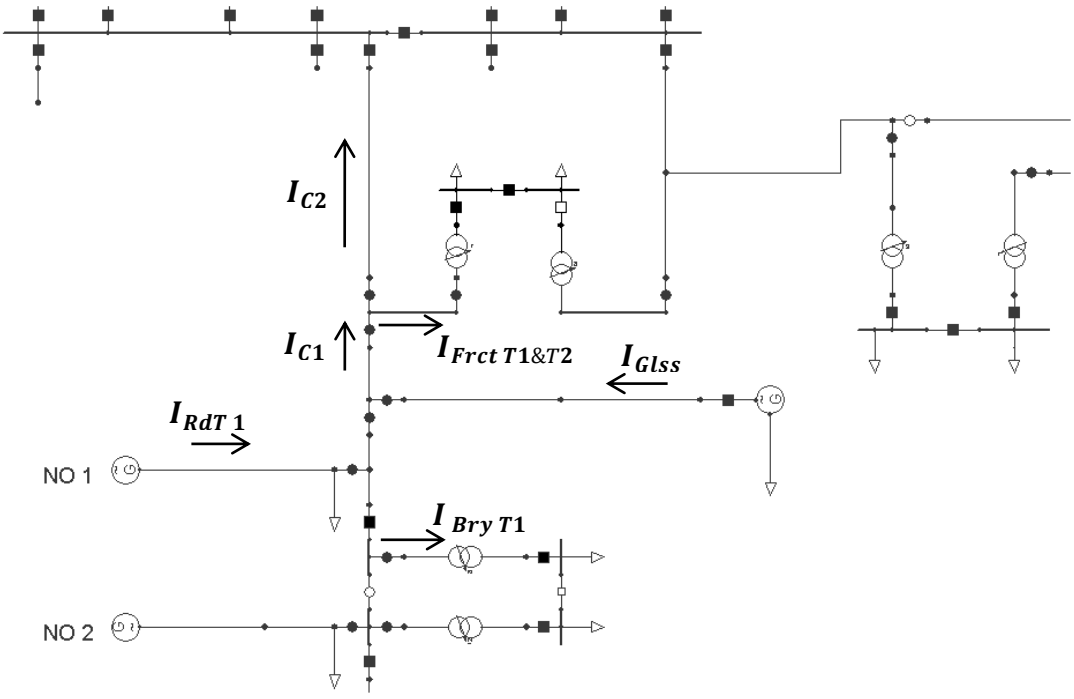

Figure 6.13 - Circuit under scenario 4.

By presenting other normal running arrangements, the N-1 outage scenarios alter. Scenario 3 represents a new running arrangement and scenario 4 its N-1 worst case outage. Circuit 1 comprises of 10km of 200 ACSR overhead line while circuit 2 has several types of underground cables and overhead lines as seen in Table 6.5. The main restriction on the second circuit is the 150 ACSR

overhead line section and several underground sections comprising of 0.45 Al single core and 300 Al with a total of 20 m and 142 m respectively. The largest conductor that can be practically installed on 33 kV network is 200 ACSR, since it´s difficult to get permission from landowners to erect a 300 ACAR conductor due to the size of its structures and foundations. Therefore, the only way to reinforce the circuit in a classical way would be to install a new overhead line.

Table 6.5 has both circuits stripped down into sections, each with its respective distribution rating for all year seasons.

Table 6.5 - Circuit 1 and circuit 2 data.

	Type	Length [m]	Distribution Ratings [A]		
			Summer	Spring/Autumn	Winter
Circuit 1	200 ACSR	10170	462	534	575
Circuit 2	0.45 AL SC (UG)	10	461	485	504
	0.45 OF AL (UG)	35	521	549	570
	400 CU DT (UG)	120	729	-	767
	0.45 OF AL (UG)	1689	521	549	570
	300 AL (UG)	142	470	495	515
	0.45 OF AL (UG)	68	521	549	570
	0.45 AL SC (UG)	10	461	485	504
	150 ACSR	382	382	443	476
	200 ACSR	1220	462	534	575
	630 AL DT (UG)	140	782	803	824

6.7.2 Overhead Line Route Study

The route map of both circuits are analyzed to evaluate the direction of the line and possible obstructions like forestation or high buildings, which would mean a higher roughness and consequently a lower wind speed in contact with the overhead line. Information on wind speed and direction is taken from Glssmoor wind farm.

Figure 6.14 shows the predominant winds on that area for 2010 under a wind rose vector graph. Figure 6.15 shows the route map of circuit 1, from Frct Primary to Glssmoor tee. It is comprised of only one type of conductor, 200 ACSR.

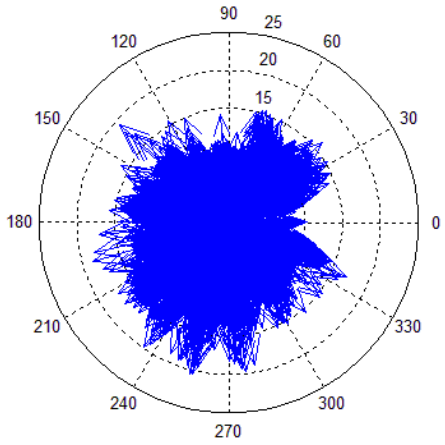

Figure 6.14 - Glssmoor wind rose.

6.7.2.1 Circuit 1

Figure 6.15 is an overview of the route map for circuit 1. This 200 ACSR overhead line is split into several sections, each one with a specific angle relative to the north direction. All angles are measured relative to the north, i.e. an overhead line that is oriented to the north has an angle of 0°. If a line is west or east bound its angle is 90°.

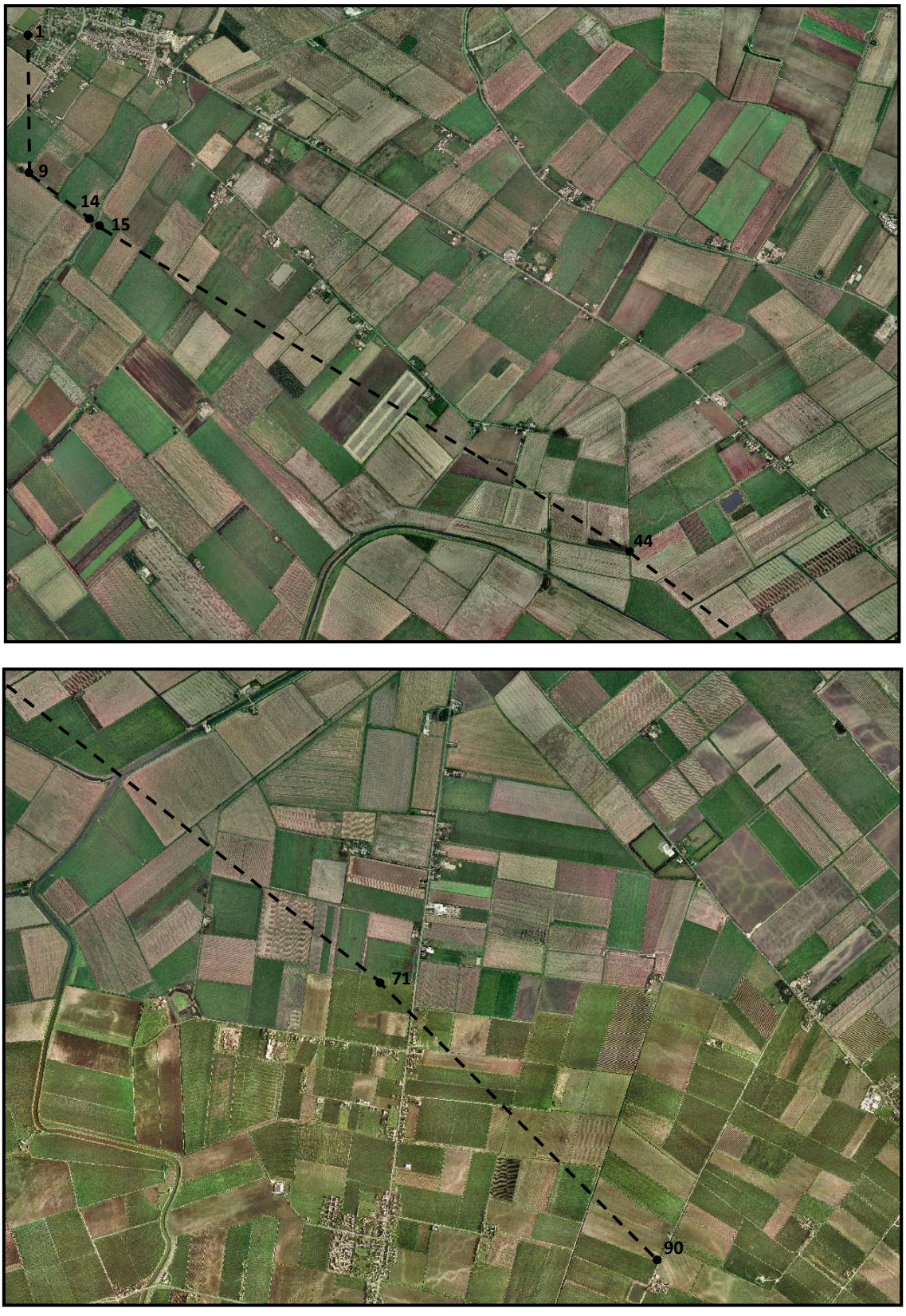

Figure 6.15 - Circuit 1 assessment Frct Primary – Glssmoor Tee [Source: Netmap].

The approximate angle, latitude and type of each section are presented in Table 6.6.

Table 6.6 - Circuit 1 assessment data.

From	To	Angle [°]	Latitude [°	Type
1	9	10	52.84	200 ACSR
9	14	40		
14	15	50		
15	44	45		
44	71	40		
71	90	45		

6.7.2.2 Circuit 2

As seen in Figure 6.16, the circuit is split into several sections. There is some vegetation between pole 23 and 15 which may decrease the wind affecting the overhead lines. The orange sections represent the 150 ACSR line, the black the 200 ACSR line and the blue line the 650 Al underground cable.

Figure 6.16 - Circuit 2 assessment Ptr Central Grid Substation - Frct Primary Substation [Source: Google maps].

Information on angle, latitude and type for each section is specified on Table 6.7. The assessment of dynamic ratings will be only for the 150 ACSR overhead line, therefore, the angle for this section is

not needed. Between pole 17 and 16 there is a highway crossing using an underground cable, which won´t enter in the dynamic ratings calculation as well as it is not affected by wind.

Table 6.7 - Circuit 2 assessment data.

From	To	Angle [°]	Latitude [°]	Type
25	23	350	53	150 ACSR
23	21	310		
21	18	350		
18	17	30		
17	16	X		630Al UG
16	4	X		200 ACSR
4	1	360		150 ACSR

Appendix – Route Map Circuit 1“ and “Appendix – Route Map Circuit 2” contains all graphics of the assessment of the route and will give a better understanding of all obstructions and roughness of the surface along the way.
Circuit 1 route does not present any particular challenges regarding obstructions and hot spots along the 200 ACSR OHL. In circuit 2, there is a possibility for decreased overhead line cooling from wind due to the existence of medium sized vegetation.

6.8 Results Analysis – Digsilent Simulations Scenario 1, 2, 3 and 4

Initially, several arrangements were studied using Digsilent. For each scenario, three conditions were assessed:

1. Generation = 0 & Load = Max
2. Generation = Max & Load = Min
3. Generation = Max & Load = Max

A load flow for each scenario was performed for both summer and winter seasons giving valuable information on the behavior of the network and the amount of current flowing in all sections of the circuits. The static headroom was then determined, given by the difference between the static rating of the overhead line and the current flowing through.

As seen in the following figures, scenarios 2 and 4 represent N-1 conditions and are shown in light blue and light green respectively. Scenarios 1 and 3 correspond to normal operating arrangements (see equations 6.11 to 6.14) and are shown in blue and green respectively. During summer, the P27 static ratings are low and the headroom available is much smaller when compared to winter. By comparing scenarios 1 and 3, both being normal operating arrangements, there are advantages by having Bry T1 being fed by Ptr Central Grid when generation is at its maximum, regardless of the load, with a maximum increase of 83 A and 106 A of headroom for circuit 1 and 2 respectively as seen in Figure 6.17 and Figure 6.18. This could present a good opportunity to change the normal arrangement of the network and with it increase the circuit capacity. The headroom available in circuit 2 as seen in Figure 6.18 is smaller for scenario 1 when compared to circuit 1. For scenario 3, the headroom on circuit 2 is bigger than in circuit 1 because most generation export is feeding Frct T1 load, freeing capacity on circuit 2.

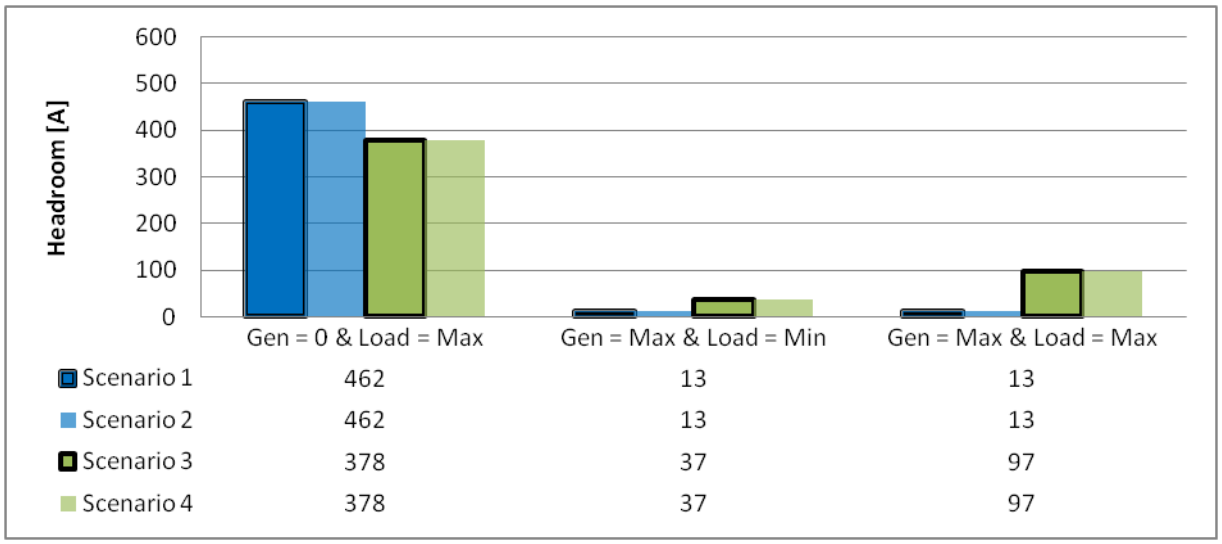

Figure 6.17 - Present static headroom circuit 1 during summer.

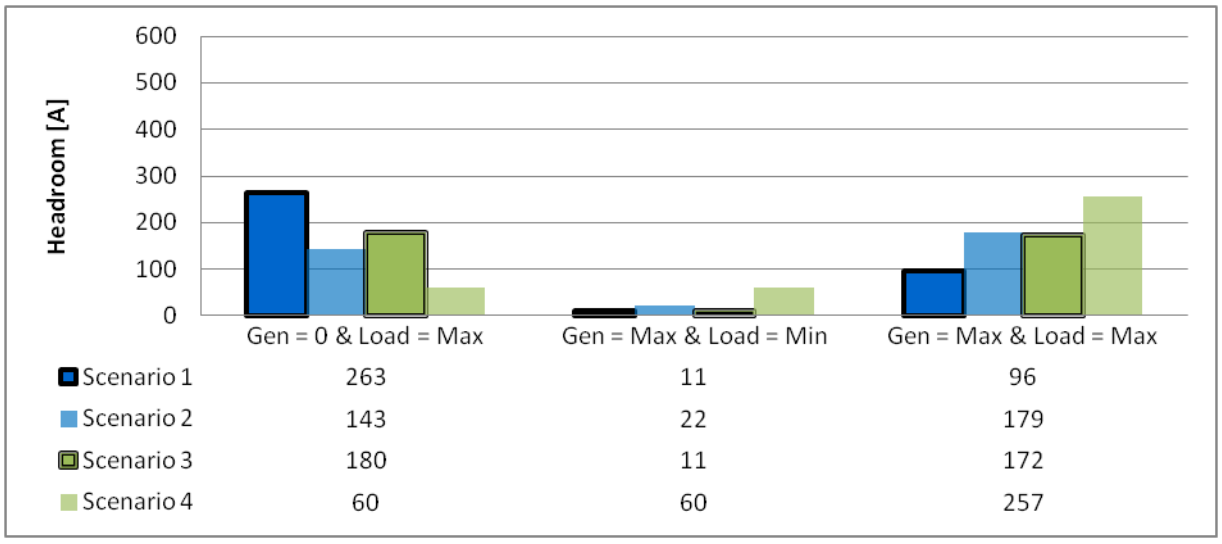

Figure 6.18 - Present static headroom circuit 2 during summer.

During winter, the headroom increases even with the higher winter demand. The reason for it is the winter static ratings which are superior to the summer ratings. The radiative cooling is higher during winter due to lower ambient temperatures and there are historically higher winds. On circuit 2, the headroom, when compared to circuit 1, is lower when there is no generation and higher when both load and generation is at its maximum. By increasing the load at Frct T1, the generation export flowing to Ptr Central Grid will continuously decrease, until a threshold point is reached. When Frct T1 is fully supplied by the wind farms, generation will start to flow to Ptr Central Grid given by the difference between the current at Frct T1 and the sum of all generation.

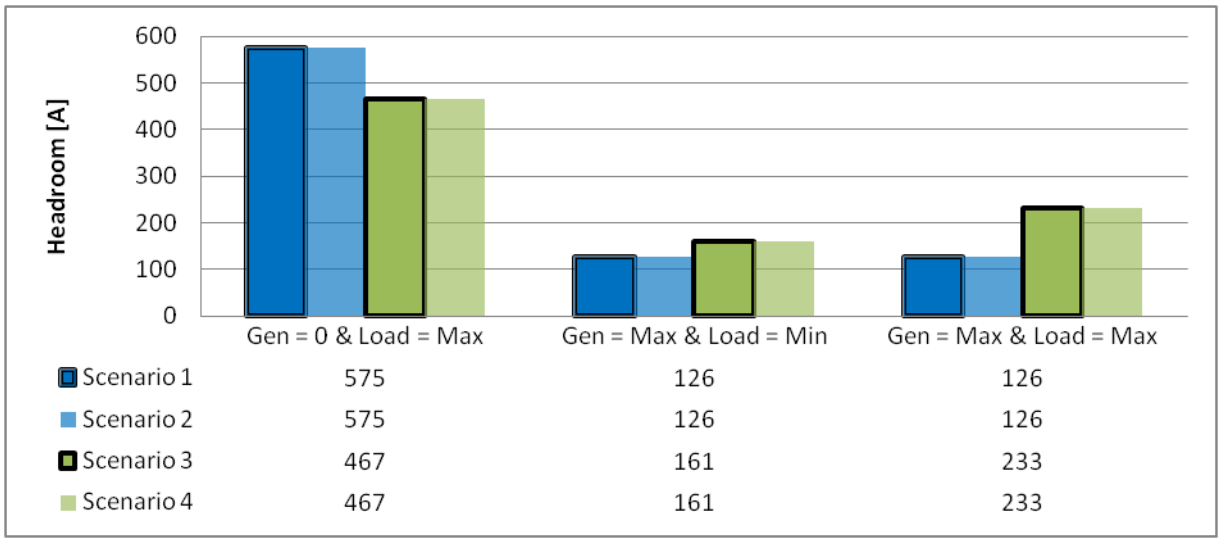

Figure 6.19 - Present static headroom circuit 1 during winter.

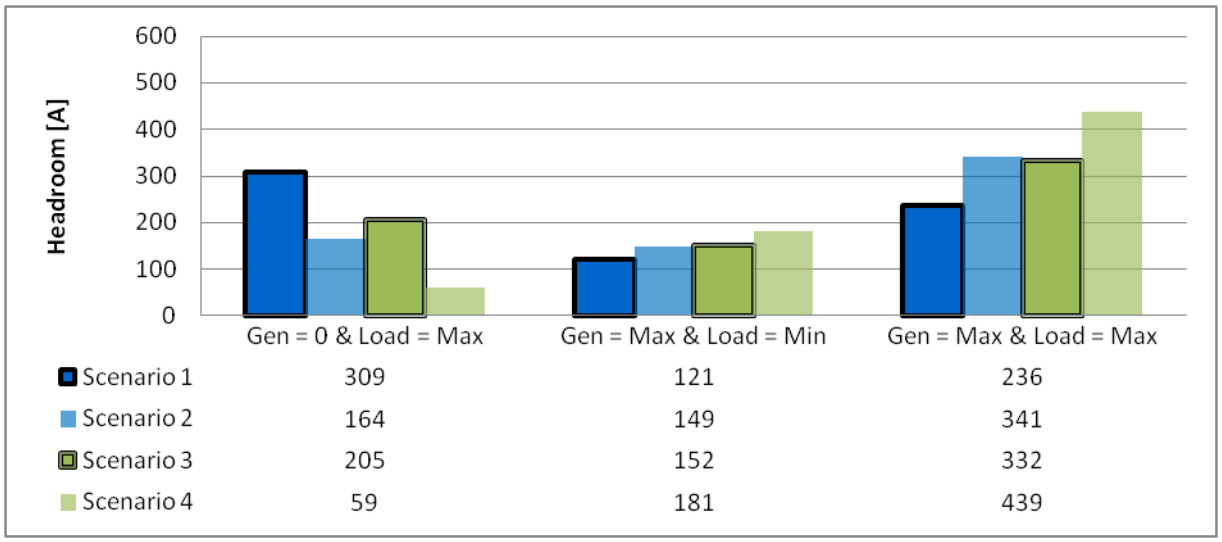

Figure 6.20 - Present static headroom circuit 2 during winter.

7 Theoretical Approach – Scenarios 1 and 3

This approach will use theoretical values for the generation export. By having the installed wind turbines power curve, it´s possible to obtain the electrical power for each step change in wind speed. The following Figure 7.1 shows the power curve for a Repower MM82 2 MW wind turbine with cut-in and cut-out wind speeds of approximately 3.5 m/s and 25 m/s respectively. It is assumed that all wind turbines are always operating.

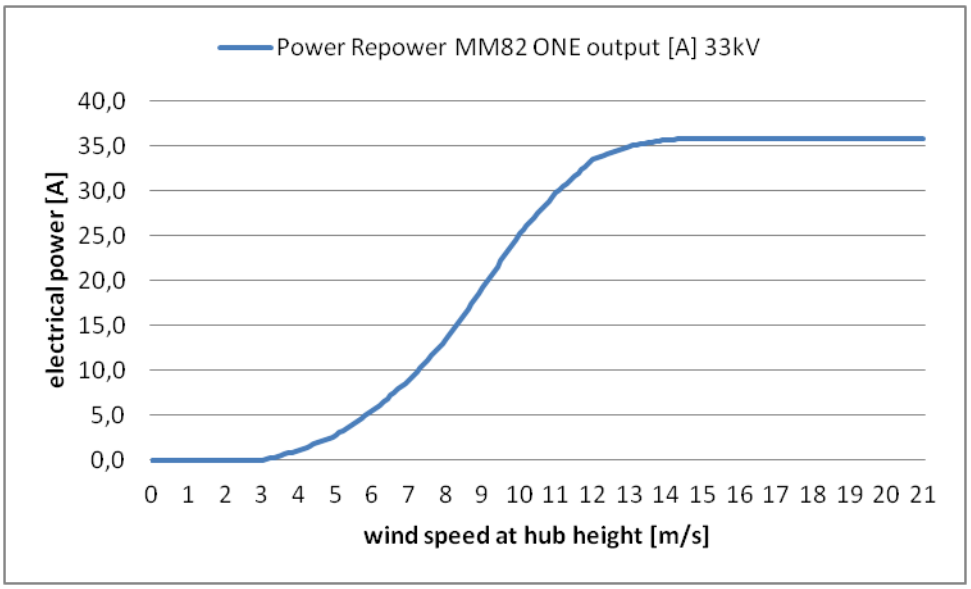

Figure 7.1 - Repower MM82 power curve [Source: www.repower.de].

When there is a high amount of generation, it means that there is at least 12m/s wind speed, the speed at which wind turbines are reaching their maximum output. The existence of strong winds does not necessarily means that the cooling of the overhead lines will be high as well. Wind direction is a very important factor. The cooling of an overhead line for a wind speed of 12 m/s might be worse than for a wind speed of 9 m/s if the former is parallel and the latter perpendicular to the line. The assessment of dynamic ratings is not straightforward to acquire as there is a need to account for several factors.

CIRCUIT 1

The first circuit being assessed is between the connection point of RdT 1 and the tee point with Frct Primary, with the current flowing through a 200 ACSR overhead line. The increase given by DLR are decreased due to the existence of other limiting components such as the air breaker switch disconnector, with its continuous rated current at 600 A, which is below the maximum rating achieved by dynamic ratings. Multi circuit ratings were used for this assessment.

CIRCUIT 2

The assessment of circuit number two is less simple as there is load at Frct Primary transformer 1. By increasing the generation at RdT 1 and Glssmoor wind farms, the voltage at transformer 1 will go up. The voltage increase rate is not perfectly linear; nevertheless, by using the amount of generation and the load at T1, it is possible to approximate the voltage increase as seen in Figure 7.2.

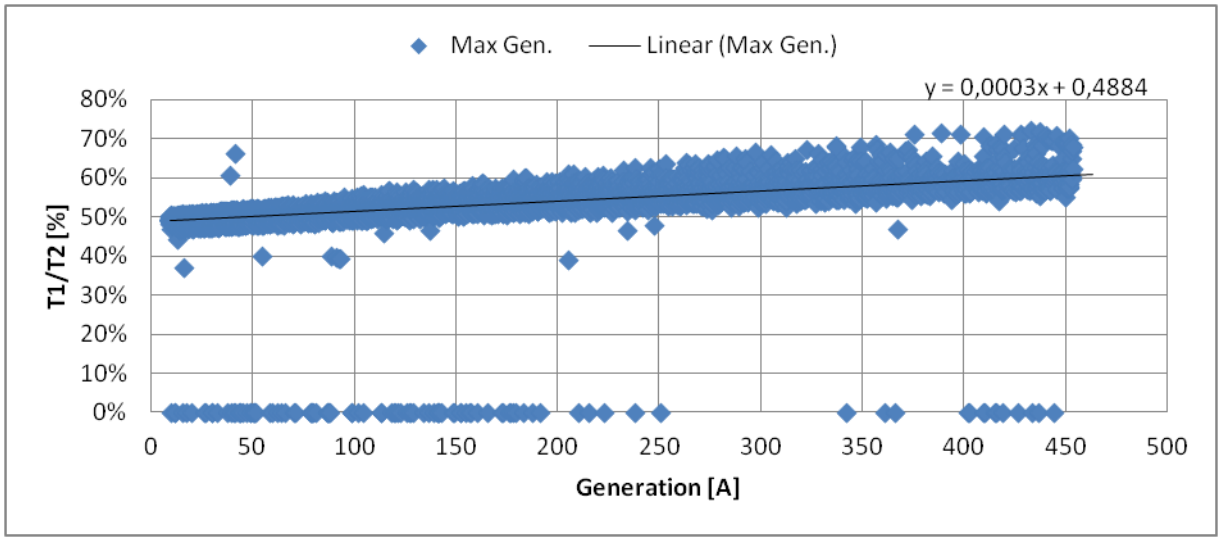

Figure 7.2 - Load balancing at Frct.

With increased generation comes a decrease of export flowing through circuit 2 as most will be flowing into Frct transformer 1. For example, in times of low generation, Frct T1 load is being fed by Ptr Central Grid along circuit 2. In times of high generation and high load, most export goes directly to Frct transformer 1, never flowing to Ptr Central Grid; therefore, there is high headroom in that circuit. For an increase in generation there is an increase in headroom as well, until a threshold limit is reached when Frct T1 load is being totally fed by the generation export. After that point, generation starts to flow to Ptr Central Grid. The headroom for circuit 1 and 2 changes according to the restrictions being applied. For the first circuit only one restriction is used (ABSD), therefore, headroom will be split into three bands: Static headroom, i.e. the present headroom using P27 static ratings; Dynamic headroom which represents the headroom achieved by dynamic ratings without any restrictions and finally the headroom given by the dynamic ratings but restricted by the ABSD. For circuit 2, there are 4 total headrooms. The first one is the static headroom, the second is the dynamic headroom with no restrictions, the third is applying the present restriction of the 0.45 AL SC cable and the final is by reinforcing the present cable with a 0.45 OF SC cable.

7.1 Example - 2nd January 2010 12:00 Thermal Rating Calculation

This example aims to explain the process of calculating the thermal rating in a given time. It is slightly different than the one explained in Chapter 6, as it now no longer uses fixed values for solar heating, radiated heat loss, dynamic viscosity of air, air density and thermal conductivity of air. The natural

and both forced convection heat losses are calculated the same way as before using the wind direction coefficient of each section. On circuit 1 there are four different angles for the overhead lines relative to the north position. For each half hour, the thermal rating is obtained for every individual section and the lowest value is used. This discrepancy between thermal ratings in each section is only dependent on the overhead line orientation and wind direction, and consequently the angle of wind that hits the conductor. The section chosen for this example is the first one, between pole 1 and 9 with an angle of 10°.

7.1.1 Convection Heat Loss

The convection heat loss calculation is analogous to the one presented in Chapter 6. Dynamic viscosity of air, air density and thermal conductivity of air will need to be calculated using the ambient temperature of that specific time (12:00) and all convection losses will use the wind speed and direction (D_w) that occurred at that time as well. The wind speed is multiplied by a new factor that takes into account the roughness of the terrain and the decrease in wind speed that occurs naturally with decreased height. The roughness diminishes wind speed due to obstructions from buildings or high vegetation and their classes are shown in Table 7.1 [15].

$T_a = 2.5\ ℃$

$V_w = 8.6\ m/s$

$D_w = 0°$

The value in roughness was assumed to be of class 0.5 at the point of wind speed capture (60 m in height) and of class 1 at the height of the overhead line. To find the decrease in wind speed, a wind speed calculator [(1)] was used.

For a wind speed of 10 m/s at 60 m with a roughness class of 0.5 gives a wind speed of 6.79 m/s with a roughness class of 1 at 10 m.

This decrease in wind speed of 32.1 % was used and it accounts for the decrease in wind speed due to height and roughness of the terrain. Wind speed is thus multiplied by 0.679.

7.1.1.1 Dynamic Viscosity of Air

The dynamic viscosity of air is given by Equation 7.1.

$$\mu_f = \frac{1.458\times10^{-6}(T_m+273)^{1.5}}{T_m+383.4} \quad (7.1)$$

Where T_m is the average between the conductor and ambient temperatures. See Equation 7.2.

$$T_m = \frac{T_c+T_a}{2} \quad (7.2)$$

For an ambient temperature of 2.5 ℃:

$T_m = \frac{50+2.5}{2} = 26.25\ ℃$

[(1)] http://www.motiva.fi/myllarin_tuulivoima/windpower%20web/en/tour/wres/calculat.htm

And consequently,

$$\mu_f = \frac{1.458 \times 10^{-6} \times (26.25 + 273)^{1.5}}{26.25 + 383.4} = 1.842 \times 10^{-5}\ Pa$$

Table 7.1 - Roughness Classes [15].

Roughness Class	Landscape Type
0	Water surface
0.5	Completely open terrain with a smooth surface, e.g. concrete runways in airports, mowed grass, etc.
1	Open agricultural area without fences and hedgerows and very scattered buildings. Only softly rounded hills
1.5	Agricultural land with some houses and 8 meter tall sheltering hedgerows with a distance of approx. 1250 metres
2	Agricultural land with some houses and 8 meter tall sheltering hedgerows with a distance of approx. 500 metre
2.5	Agricultural land with many houses, shrubs and plants, or 8 meter tall sheltering hedgerows with a distance of approx. 250 metres
3	Villages, small towns, agricultural land with many or tall sheltering hedgerows, forests and very rough and uneven terrain
3.5	Larger cities with tall buildings
4	Very large cities with tall buildings and skyscrapers

7.1.1.2 Air Density

Air density is given by Equation 7.3.

$$\rho_f = \frac{1.293 - 1.525 \times 10^{-4} H_e + 6.379 \times 10^{-9} {H_e}^2}{1 + 0.00367 T_m} \quad (7.3)$$

Where H_e is the elevation in meters above sea level.

$$\rho_f = \frac{1.293 - 1.525 \times 10^{-4} \times 10 + 6.379 \times 10^{-9} \times 10^2}{1 + 0.00367 \times 26.25} = 1.178\ kg/m^3$$

7.1.1.3 Thermal Conductivity of Air

Thermal conductivity of air is given by Equation 7.4.

$$k_f = 2.424 \times 10^{-2} + 7.477 \times 10^{-5} \times T_m - 4.407 \times 10^{-9} \times {T_m}^2 \quad (7.4)$$

$$k_f = 2.424 \times 10^{-2} + 7.477 \times 10^{-5} \times 26.25 - 4.407 \times 10^{-9} \times 26.5^2 = 2.620 \times 10^{-2} \ \frac{W}{m}\text{°C}$$

7.1.1.4 Convection Heat Loss Calculation

Initial equations will be omitted as they were explained previously in Chapter 6.

$$q_{cn} = 0.0205 \ \times (1.178\ )^{0.5} \times (19.3)^{0.75} \times (50 - 2.5)^{1.25} = 25.5\ W/m$$

$K_{angle} = 1.194 - \cos(\emptyset) + 0.194\cos(2\emptyset) + 0.368\sin(2\emptyset)$ for $\emptyset = 10°$, $K_{angle} = 0.52$

$$q_{clow} = \left[1.01 + 0.0372 \times \left(\frac{19.3 \times 1.178 \times 8.6 \times 0.679}{1.842 \times 10^{-5}}\right)^{0.52}\right] \times 2.620 \times 10^{-2} \times 0.52 \times (50 - 2.5)$$

$$= 89\ W/m$$

$$q_{chigh} = \left[0.0119 \times \left(\frac{19.3 \times 1.178 \times 8.6 \times 0.679}{1.842 \times 10^{-5}}\right)^{0.6}\right] \times 2.620 \times 10^{-2} \times 0.52 \times (50 - 2.5)$$

$$= 100\ W/m$$

7.1.2 Radiated Heat Loss

Radiated heat loss calculation is similar to the one presented in Chapter 6.

$$q_r = 0.0178D\varepsilon\left[\left(\frac{T_c+273}{100}\right)^4 - \left(\frac{T_a+273}{100}\right)^4\right] = 0.0178 \times 19.3 \times 0.7 \times \left[\left(\frac{50+273}{100}\right)^4 - \left(\frac{2.5+273}{100}\right)^4\right] =$$

$12.32\ \text{W/m}$

7.1.3 Solar Heat Gain

In order to determine the solar heating (q_s) several components are needed (see Equation 6.9 in Chapter 6). Solar altitude(H_c), solar azimuth (Z_c) and heat flux (Q_s).

Solar altitude depends on the latitude of the overhead line, solar declination (δ) and hour angle (ω) (see Equation 7.5). The hour angle is the number of hours from noon times 15°. For example, 10 am is -30°, while 5 pm is 75°. For mid night, the hour angle is 180° while 1 am is -165°.

$$H_c = \arcsin\left[\cos(Latitude) \times \cos(\delta) \times \cos(\omega) + \sin(Latitude) \times \sin(\delta)\right] \quad (7.5)$$

Solar azimuth is given by the solar azimuth constant (C) and solar azimuth variable (χ) (see Equation 7.6).

$$Z_c = \ C + \arctan\left(\chi\right) \quad (7.6)$$

Where χ is given by Equation 7.7, while the solar azimuth constant depends on the solar azimuth variable and is shown on Appendix Table I.1.

$$\chi = \frac{\sin(\omega)}{\sin(Latitude)\times\cos(\omega)-\cos(\text{Latitude})\times\tan(\delta)} \quad (7.7)$$

Heat flux is given by Equation 7.8 and depends on certain coefficients on the atmosphere that are split between being a clear or industrial atmosphere and are given in Appendix Table I.1.

$$Q_s = A + BH_c + CH_c{}^2 + DH_c{}^3 + EH_c{}^4 + FH_c{}^5 + GH_c{}^6 \quad (7.8)$$

The first step is to calculate the solar declination (δ) given by Equation 7.9 and the hour angle.

$$\delta = 23.4583 \times \sin\left(\frac{284+N}{365} \times 360\right) \quad (7.9)$$

The argument of the sin is in degrees and N is the day of the year. The 1st of January has an N of 1, while the 30st of August has an N of 242.

The solar declination for the 2nd of January is thus: $\delta = 23.4583 \times (\sin\left(\frac{284+2}{365} \times 360\right) = -22.9\,°$

For mid-day, the hour angle is zero: $\omega = 0°$

It is now possible to obtain the solar altitude and solar azimuth:

$$H_c = \arcsin[\cos(radians(52.84)) \times \cos(radians(-22.9)) \times \cos(radians(0)) + \sin(radians(52.84)) \times \sin(\text{radians}(0))] \times \frac{180}{\pi} = 14.5°$$

$$\chi = \frac{\sin(radians(0))}{\sin(radians(52.84)) \times \cos(radians(0)) - \cos(\text{radians}(52.84)) \times \tan(radians(-22.9))} \times \frac{180}{\pi} = 0°$$

It was necessary to convert angles to radians and back to degrees due to the *arc* functions only accepting radians as argument.

The solar azimuth is calculated using Equation 7.6, where $C = 180°$ (See Appendix Table I.2).

$$Z_c = C + \arctan(\chi) = 180 + \arctan(0) = 180°$$

The only component missing in order to calculate the heat loss is the heat flux (Q_s).

The heat flux is given by Equation 7.8 and assuming a clear atmosphere:

$$Q_s = -42.2391 + 63.8044 \times 14.5 - 1.9220 \times 14.5^2 + 3.46921 \times 10^{-2} \times 14.5^3 - 3.61118 \times 10^{-4} \times 14.5^4 + 1.94318 \times 10^{-6} \times 14.5^5 - 4.07608 \times 10^{-9} \times 14.5^6 = 571\ W/m^2$$

A total heat flux elevation correction factor was considered but is only noticeable for high altitudes and since the conductor is considered to be 10 m in height, the new total heat flux corrected would be 1.001147 higher and is thus ignored as seen in Equation 7.10.

$K_{solar} = A + B \times H_e + C \times H_e{}^2$, where $A = 1; B = 1.148 \times 10^{-4}; C = -1.108 \times 10^{-8}$ (7.10)

For a height of 10 m, $K_{solar} = 1.001147$

The calculation of the solar heat gain is now possible and is given by Equation 6.9.

$$q_s = \alpha Q_s sin(\theta) A'$$

Where

$$Q_s = 571\ W/m^2$$

$$A' = \frac{D}{1000} = \frac{19.3}{1000} = 0.0193\ m$$

$$\theta = \arccos[\cos(H_c) \times \cos(Z_c - Z_1)] = \arccos\ [\cos\ (radians(14.5) \times \cos(radians(180 - 90)] = 165°$$

$$q_s = 0.9 \times 571 \times \sin(165) \times 0.0193 = 9.89\ W/m$$

7.1.4 Thermal Rating

The thermal rating is given by Equation 6.10.

$$I = \sqrt{\frac{q_c + q_r - q_s}{R(T_c)}} = \sqrt{\frac{100 + 12.32 - 9.89}{0.0001514}} = 822\ A$$

This process is then repeated for each half hour and then it is plotted against the current flowing on each circuit.

7.2 Scenario 1

Under normal operating conditions, the current on circuit 1 will only be generation in a given time as Bry is being totally fed by a different grid substation, thus, all generation flows to Frct T1 and Ptr Central Grid.

The current on circuit 2 is given by the difference between generation and Frct T1 load multiplied by a voltage factor (see Figure 7.2). When current is negative, it means that the generation export is not enough to feed Frct T1 load, therefore current starts to flow from Ptr Central Grid downstream to feed that load.

For example, on the 21st of August 2:30 pm there is:

$$Total\ generation\ (Glssmoor\ and\ RdT\ 1\ wind\ farms) = 458\ A$$

$$Frct\ T1\ and\ T2\ 33kV\ load = 149\ A$$

$$Frct\ T1\ load = 149\ A \times 62\ \% = 92\ A$$

$$Current\ on\ circuit\ 1 = 458\ A$$

$$Current\ on\ circuit\ 2 = 458 - 92 = 366\ A$$

When studying the increase in export, one needs to include limiting factors like overheating, sag, annealing or the disappearance of grease with temperature. Since all calculations of dynamic line ratings have the conductor´s operating temperature fixed at 50°C, all these factors are ignored, although there are other components that restrict overhead line capacity, for example, switchgear, isolators, disconnectors, etc. The following two figures show dynamic line ratings, static ratings and circuit current, colored in green, dark red and blue respectively on circuit 1 and 2. On the first circuit, there are a few occasions in which circuit current exceeds the P27 static rating, approximately 53.5 hours in a year (0.6 % of a full year – see Figure 7.7) while dynamic ratings are never exceeded, meaning that the present overhead line is already on its full capacity. On circuit 2, there are occurrences of current flowing to Ptr Central Grid, i.e. export, and times of import from Ptr Central Grid. When the circuit current is negative as seen in Figure 7.4 it means that Frct T1 load is being totally fed by Ptr Central Grid, while a positive value means that the generation output exceeds Frct T1 load and thus is flowing to Ptr Central Grid as export. Over a full year the current never exceeds overhead line static ratings. For full size pictures please refer to Appendix – Results: Theoretical Approach Scenario 1 and Appendix – Results: Theoretical Approach Scenario 3.

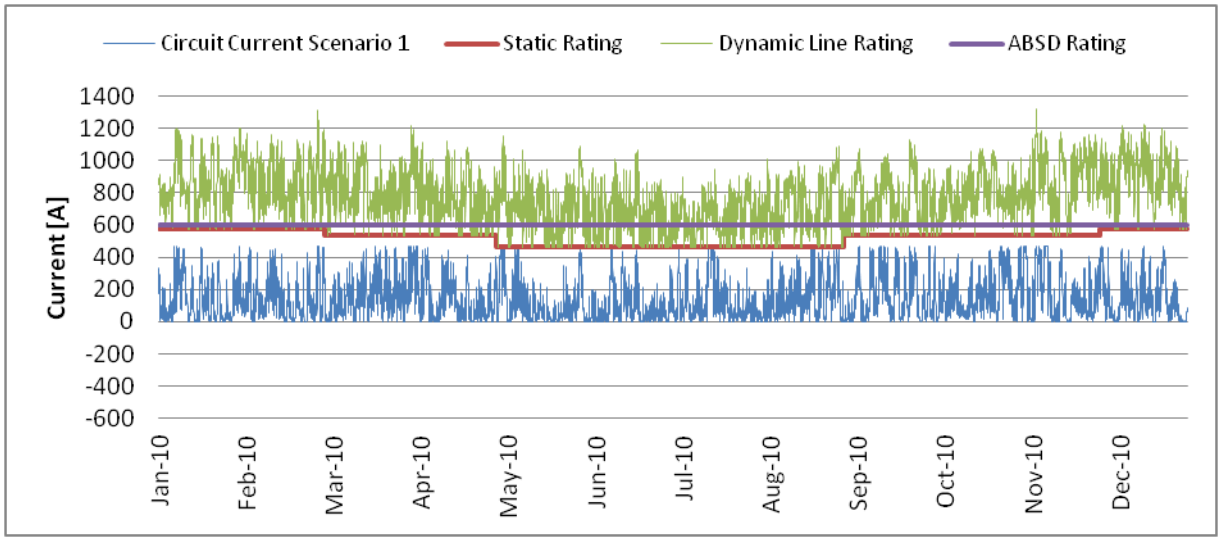

Figure 7.3 – **Circuit 1 Scenario 1** - Dynamic ratings vs. static ratings vs. circuit load vs. ABSD rating.

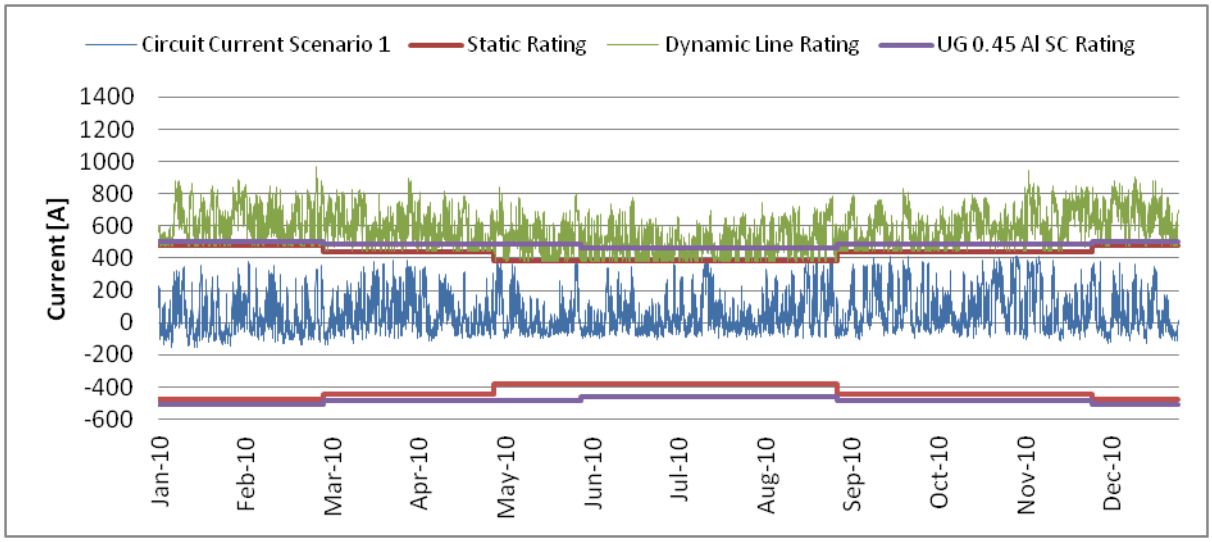

Figure 7.4 – **Circuit 2 Scenario 1**- Dynamic ratings vs. static ratings vs. theoretical export vs. ABSD rating.

The headroom is calculated for each half hour and is split into three headrooms:

- Static headroom: Given by the difference between the static rating of each season and the current flowing through the circuit;

- Dynamic headroom: Given by the difference between the new thermal rating using real time weather information and the current flowing through the circuit;

- Restricted dynamic headroom: Same as the dynamic headroom but restricted by the components on the circuit being studied. For circuit 1, the dynamic headroom is restricted by the ABSD rating. For circuit 2, the dynamic headroom is by the underground cable static rating of the corresponding season.

As seen in Figure 7.5 and Figure 7.6. Circuit 1 without being restricted has a minimum headroom of 5.5 MW and an average of 36.4 MW, while maintaining the same minimum value of 5.5 MW and a decreased average of 25.7 MW when being restricted by the ABSD. The second circuit admits less headroom, with a minimum of 3.4 MW and an average of 29.4 MW with no restrictions. If we apply the present restriction given by the 0.45 Al SC cable, the headroom falls to a minimum of 3.3 MW and an average of 23.8 MW. If that cable section is reinforced with 0.45 OF SC, the minimum headroom becomes 3.4 MW, the same as DLR with no restrictions, with an average of 26.2 MW. This reinforcement is not shown on Figure 7.6. The minimum headroom of 5.5 MW and 3.4 MW happens when there is maximum generation export from both Glssmoor and RdT 1 wind farms but the cooling on the conductor does not follow the increase of this generation because of the wind direction factor. Both dynamic headrooms are above the static headroom.

The minimum headroom occurrs in the 21st of August 2:30 pm. Calculations follow the same approach as before and are thus simplified here, i.e. only forced convection is calculated:

$Total\ generation\ on\ 21st\ of\ August\ 2{:}30\ pm = 458\ A$

$V_w = 13.3\ m/s$

$D_w = 41°$

$T_a = 24.4\ ℃$

$T_c = 50\ ℃$

$D = 19.3\ mm$

$\rho_f = 1.136\ kg/m^3$

$\mu_f = 1.894 \times 10^{-5}\ Pa$

$k_f = 2.702 \times 10^{-2}\ \frac{W}{m}℃$

$q_s = 13.7\ W/m$

$q_r = 7.4\ W/m$

There are six different sections in circuit 1 (see Table 6.6) with four different angles relative to the north as explained before. The wind direction factor for each section is:

$$K_{angle\ sect\ 1} = 1.194 - \cos(|41 - 10|) + 0.194 \times \cos\big(2 \times (|41 - 10|)\big) + 0.368 \times \sin\big(2 \times (|41 - 10|)\big) = 0.75$$

$$K_{angle\ sect\ 2,5} = 1.194 - \cos(|41 - 40|) + 0.194 \times \cos\big(2 \times (|41 - 40|)\big) + 0.368 \times \sin\big(2 \times (|41 - 40|)\big) = 0.39$$

$$K_{angle\ sect\ 3} = 1.194 - \cos(|41 - 50|) + 0.194 \times \cos\big(2 \times (|41 - 50|)\big) + 0.368 \times \sin\big(2 \times (|41 - 50|)\big) = 0.50$$

$$K_{angle\ sect\ 4,6} = 1.194 - \cos(|41 - 45|) + 0.194 \times \cos\big(2 \times (|41 - 45|)\big) + 0.368 \times \sin\big(2 \times (|41 - 45|)\big) = 0.44$$

The section less cooled is the one with the lowest wind direction factor, section two and five. Natural convection and forced convection for low wind speed is ignored as the largest is given by forced convection for high wind speed:

$$q_{chigh} = \left[0.0119 \times \left(\frac{19.3 \times 1.136 \times 13.3 \times 0.679}{1.894 \times 10^{-5}}\right)^{0.6}\right] \times 2.702 \times 10^{-2} \times \mathbf{0.39} \times (50 - 24.4) \cong 53\ W/m$$

Thermal rating is given by:

$$I = \sqrt{\frac{q_c + q_r - q_s}{R(T_c)}} = \sqrt{\frac{53 + 7.4 - 13.7}{0.0001514}} \cong 555\ A$$

The headroom is now calculated subtracting the new thermal rating achieved with the total current flowing in this circuit, given by the total generation export at that specific time.

$$Headroom = 555 - 458 = 97\ A \Leftrightarrow 97 \times 33 \times \sqrt{3} \sim 5.5\ MW$$

The headroom with the ABSD restriction is the same because the rating of the ABSD is 600 A, below the dynamic thermal rating achieved of 555 A.

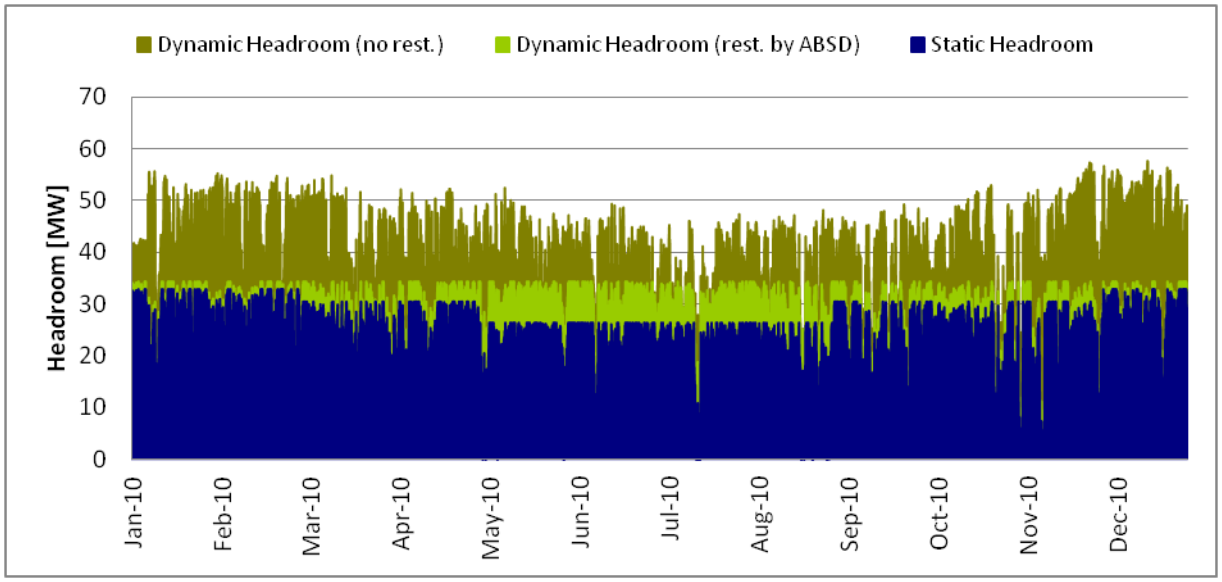

Figure 7.5 – **Circuit 1 scenario 1** - Headroom available under three pre-set conditions: Present conditions; dynamic ratings restricted by the air breaker switch disconnector and dynamic ratings with no restrictions.

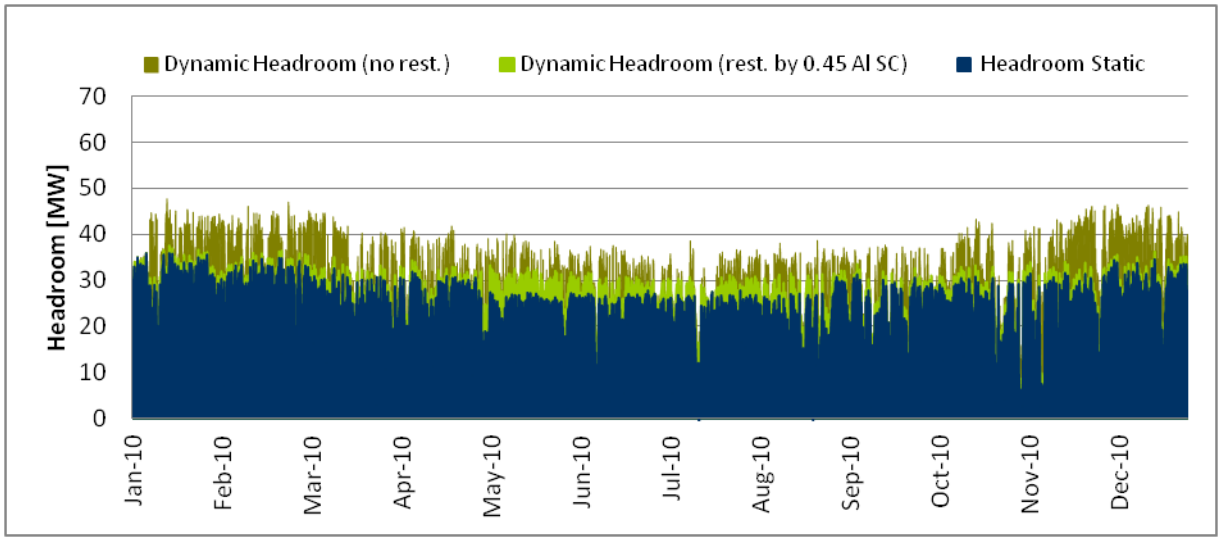

Figure 7.6 – **Circuit 2 scenario 1** - Headroom available under three pre-set conditions: Present conditions; dynamic ratings restricted by the 0.45 AL SC underground cable and dynamic ratings with no restrictions.

Figure 7.7 and Figure 7.8 give the percentage in a year in which the current exceeds the static rating (red line), dynamic rating (green line) and dynamic rating with the relevant restriction for an increase in MW installed. Each increase in MW is given by a factor applied to Glssmoor wind farm export, i.e. for an increase in each MW, a factor of 1.0625 is applied to Glssmoor export.

Glssmoor has a capacity of 16 MW. For each MW increase, a factor of 1.0625 is applied to its full capacity, in this way, the increase in MW follows the same profile as Glssmoor wind farm.

$$MW\ increase = 16 \times x = 17\ MW \Leftrightarrow x = 1.0625$$

The results are achieved through counting the number of occurrences, in hours, where the current exceeds each rating, converting afterwards to percentage in a year. For circuit 1 the restriction is the air breaker switch disconnector (green dashed line). For circuit 2 there are two restrictions: the present underground cable sections of 0.45 Al single circuit (green dashed line) and 0.45 oil filled single circuit (purple dashed line). The horizontal axis represents an increase in MW wind generation, ranging from the present situation, 0 MW to an increase of 16 MW. Circuit 1 is already in full capacity as for a null increase in MW generation it is already 0.6 % in a year with its current exceeding the static rating of the overhead line. There is headroom for approximately 7 MW (0.1 %) and 6 MW (0.1 %) for circuit 1 and 2 respectively by applying DLR until restrictions start to limit their dynamic ratings. This data is presented in Table 7.5.

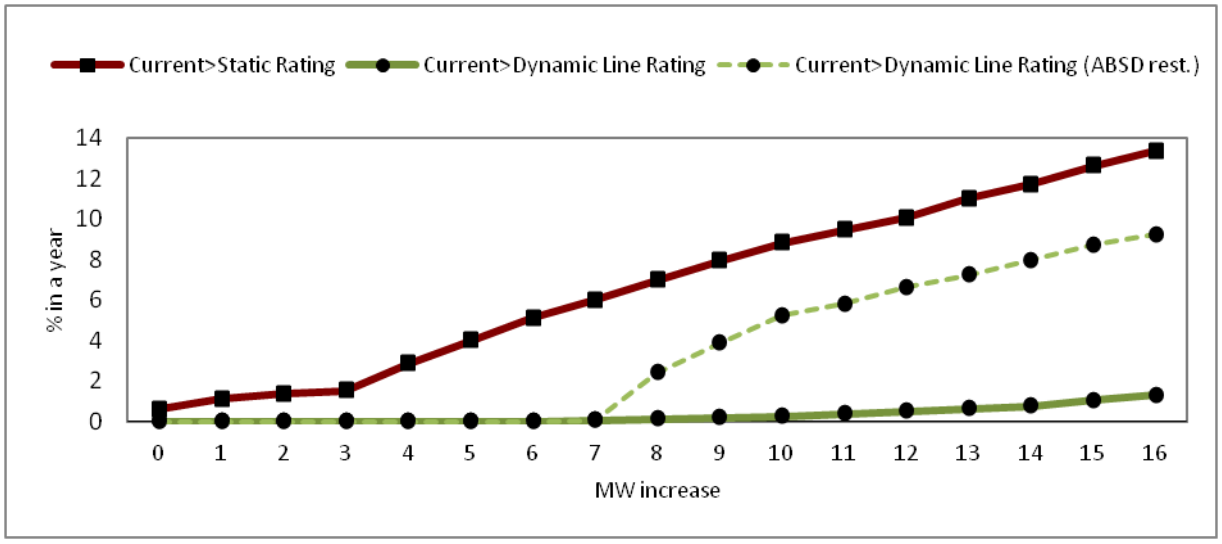

Figure 7.7 – **Circuit 1 scenario 1** - Percentage of year in which the corresponding current exceeds each rating for a MW generation increase (circuit overload).

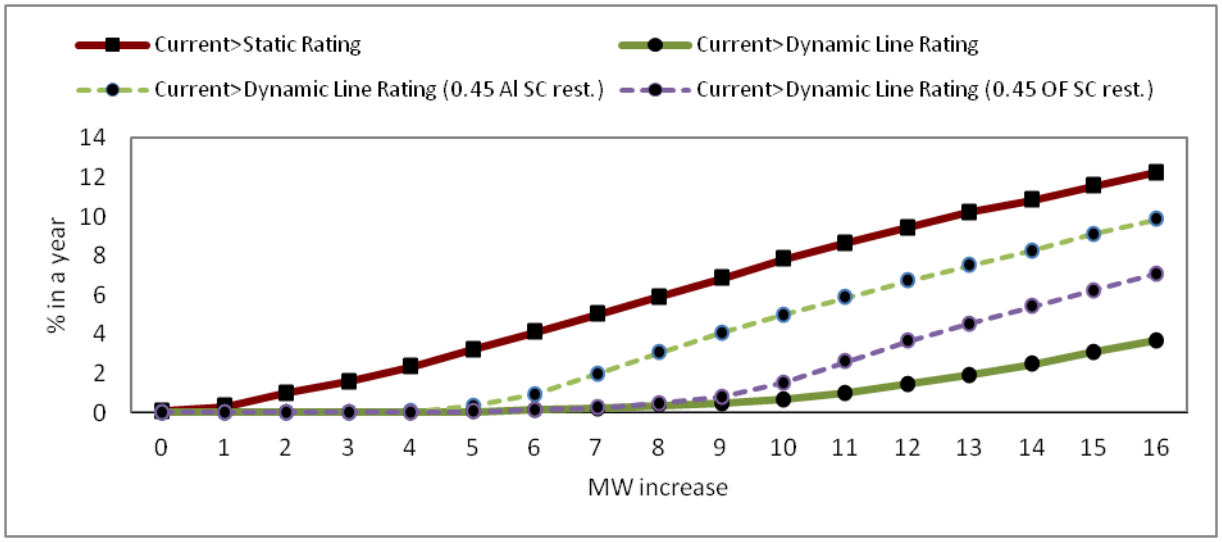

Figure 7.8 – **Circuit 2 scenario 1** - Percentage of year in which the corresponding current exceeds each rating for a MW generation increase (circuit overload).

7.3 SCENARIO 3

Scenario3I represents a different group operating arrangement with the normal open point at Bry Primary T1 closed, which decreases the amount of generation export on both circuit 1 and 2 as Bry T1 is fed by the generation from RdT 1 and Glssmoor wind farms. For example, on the 21st of August 2:30 pm there is:

$$Total\ generation\ (Glssmoor\ and\ RdT\ 1\ wind\ farms) = 458\ A$$

$$Frct\ T1\ and\ T2\ 33\ kV\ load = 149\ A \qquad Frct\ T1\ load = 149\ A \times 62\ \% = 92\ A$$

$$Bry\ T1\ 33\ kV\ load = 46\ A$$

$$Current\ on\ circuit\ 1 = 458 - 46 = 412\ A \qquad Current\ on\ circuit\ 2 = 458 - 92 - 46 = 320\ A$$

The results are obtained through similar processes described for scenario 1.

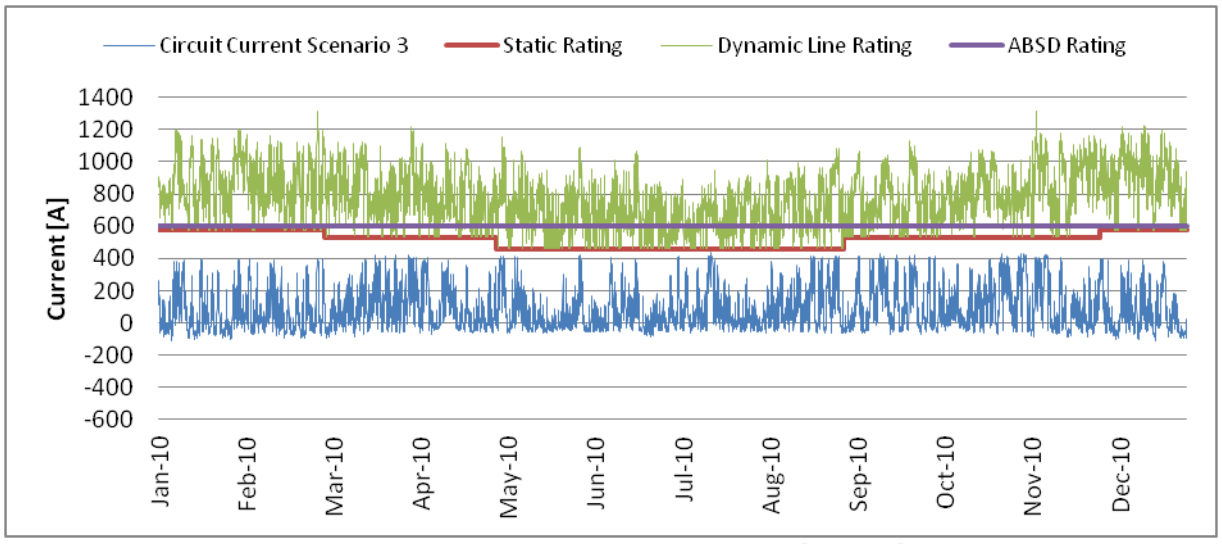

Figure 7.9 - **Circuit 1 scenario 3 -** Dynamic ratings vs. static ratings vs. theoretical export vs. ABSD rating.

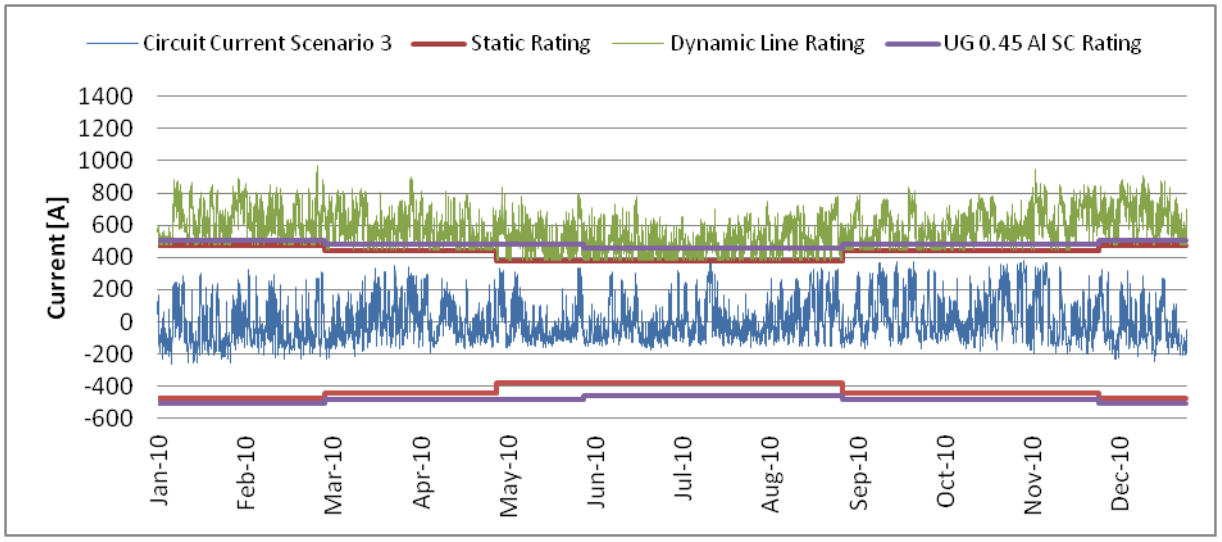

Figure 7.10 - **Circuit 2 scenario 3** - Dynamic ratings vs. static ratings vs. theoretical export vs. ABSD rating.

In this scenario, the headroom for circuit 1 reaches 8.2 MW and 38.2 MW average and by applying the restriction the minimum is still of 8 MW with a decreased average of 27.4 MW. Circuit 2´s minimum headroom is 6.0 MW with 32.6 MW as average. With the present restriction of 0.45 AL SC cable, it decreases to 5.0 MW and 27.0 MW. If that cable section is reinforced with 0.45 OF SC, the minimum headroom becomes 6 MW with an average of 29.4 MW. This reiforcement is not shown on Figure 7.12.

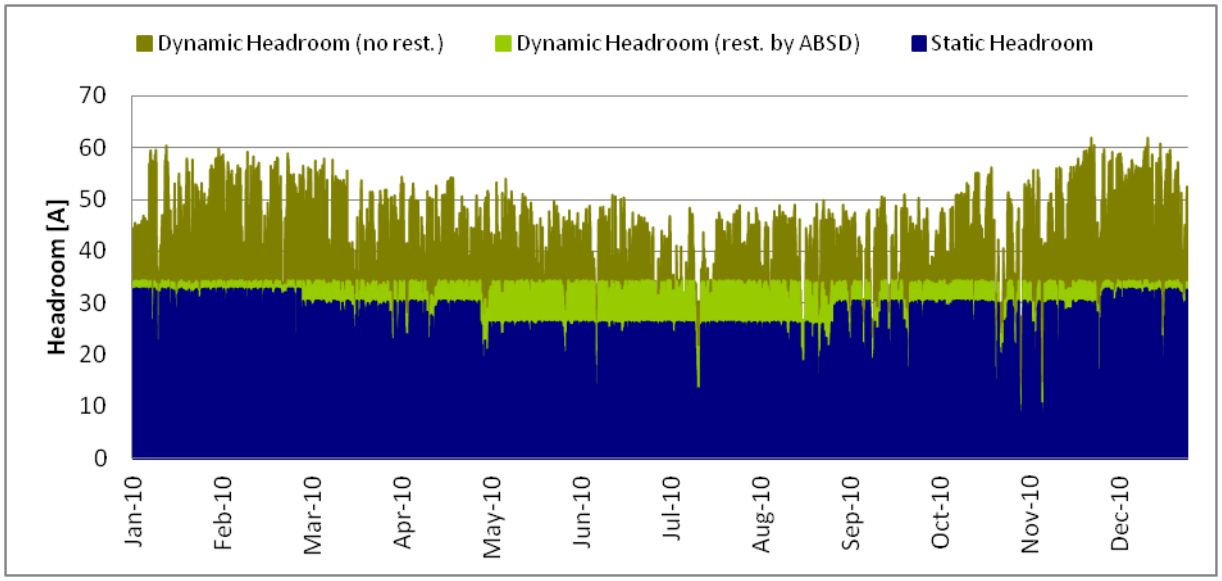

Figure 7.11 – **Circuit 1 scenario 3** - Headroom available under three pre-set conditions: Present conditions; dynamic ratings restricted by the air breaker switch disconnector and dynamic ratings with no restrictions.

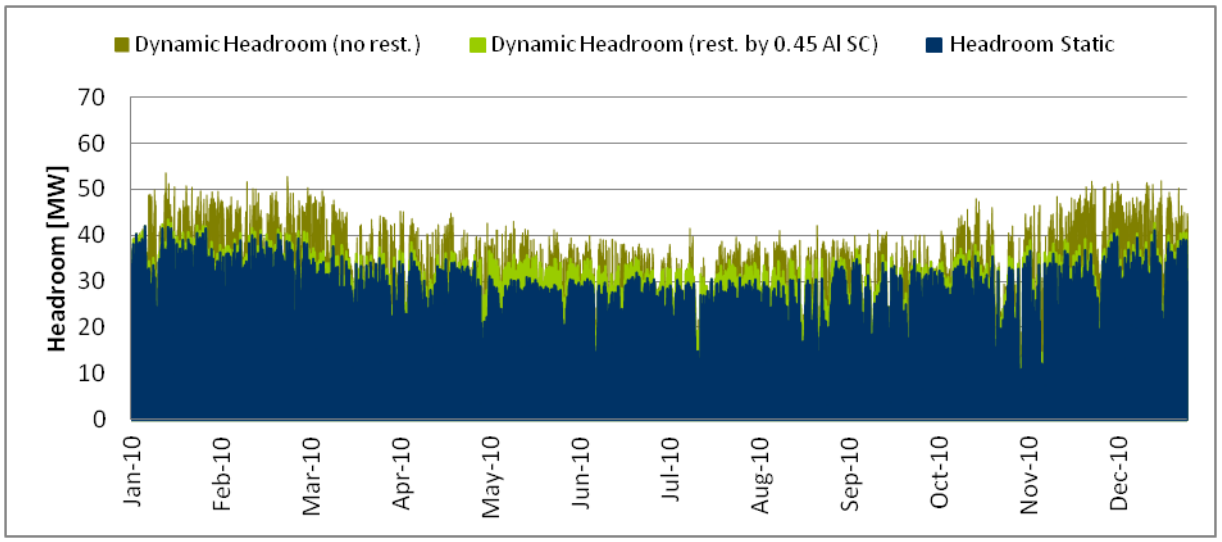

Figure 7.12 - Circuit 2 scenario 3 - Headroom available under three pre-set conditions: Present conditions; dynamic ratings restricted by the 0.45 Al SC underground cable and dynamic ratings with no restrictions.

By comparing scenarios 1 and 3, there is an evident gain in the amount of generation that can be installed on these circuits even without applying dynamic ratings. With DLR and no restrictions, circuit 1 has capacity for almost 10 MW of generation while circuit 2 starts to become overloaded for

an increase of 8 MW. The restrictions affect the overall headroom, with circuit 2 becoming overloaded for an increase of 7 MW. This data is presented in Table 7.7.

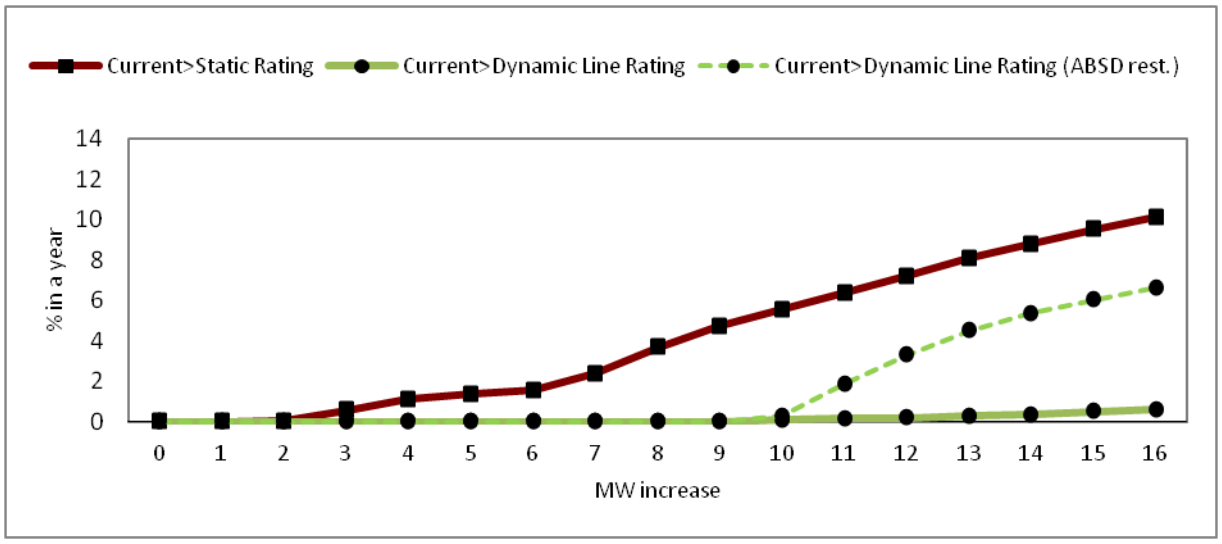

Figure 7.13 – **Circuit 1 scenario 3** - Percentage of year in which the corresponding current exceeds each rating for a MW generation increase (circuit overload).

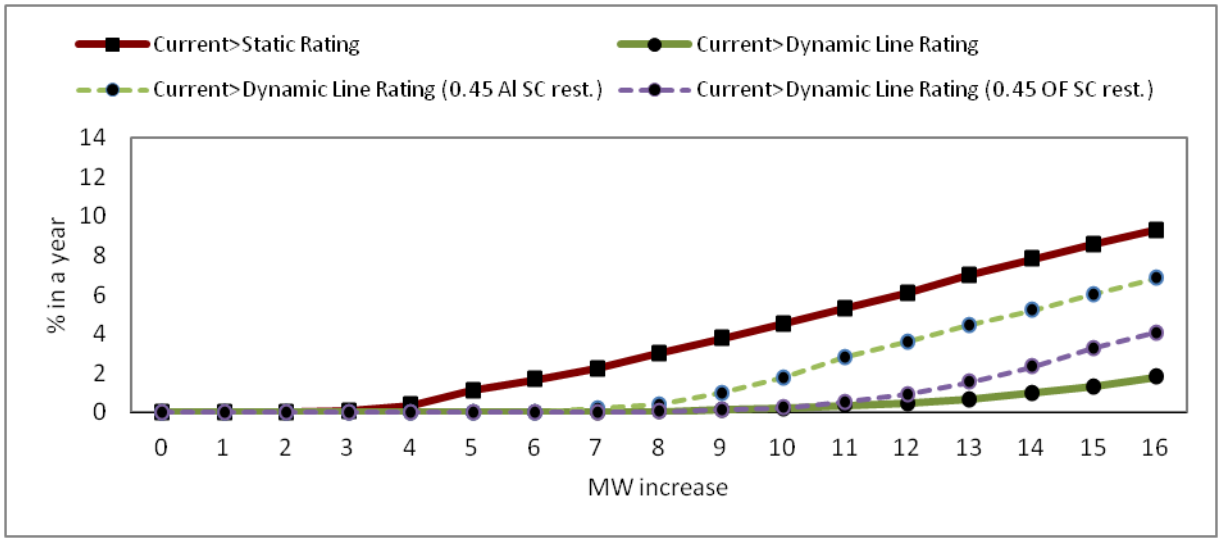

Figure 7.14 - Circuit 2 scenario 3 - Percentage of year in which the corresponding current exceeds each rating for a MW generation increase (circuit overload).

7.4 Real Export Approach vs. Theoretical Export Approach

The previous chapter used wind farm´s export data taken from the wind turbines power curve, thus producing a very linear and precise growth in production per wind speed. In this sub-chapter the export will be taken directly from Scada which makes it more realistic and the results achieved are far better than the previous approach. All the graphics will be presented in “Appendix – Results: Real Approach Scenario 1” and “Appendix – Results: Real Approach Scenario 3”, not being included here due to the similarity of the previous ones with analogous discussions and explanations.

The main difference between these set of results and the previous one is the decrease in generation export from the wind farms, especially for low wind speeds as it takes more time for a wind turbine to start generating. These results also account for maintenance interruptions on wind turbines, meaning that even if there are strong winds, the export may not be at its maximum due to maintenance on one or several turbines. The results will be presented in Table 7.2 for scenarios 1 and 3. The highlighted numbers represent the circuit that is limiting the overall circuit system, i.e. the minimum headroom for both circuit 1 and 2 for a given scenario.

Table 7.2 - Real export approach: Headroom for circuit 1 & 2 scenarios 1 & 3. 1st restriction is the ABSD for circuit 1 and 0.45 OF SC for circuit 2. 2nd restriction is the ABSD for circuit 1 and 0.45 Al SC for circuit 2.

Headroom [MW]	Scenario 1				Scenario 3			
	Circuit 1		Circuit 2		Circuit 1		Circuit 2	
	Min.	Avg.	Min.	Avg.	Min.	Avg.	Min.	Avg.
Static Rating	**0.4**	23.9	0.9	23.5	**3.1**	25.3	3.7	26.7
Dynamic Rating	10.5	38.7	**8.8**	31.6	13.2	40.1	**11.5**	34.8
Dynamic Rating 1st restriction	**7.8**	28.0	8.7	28.4	**10.3**	29.4	10.6	31.6
Dynamic Rating 2nd restriction	7.8	28.0	**5.1**	26.0	10.3	29.4	**7.0**	29.2

Table 7.3 - Theoretical export approach: Headroom for circuit 1 & 2 scenarios 1 & 3. 1st restriction is the ABSD for circuit 1 and 0.45 OF SC for circuit 2. 2nd restriction is the ABSD for circuit 1 and 0.45 Al SC for circuit 2.

Headroom [MW]	Scenario 1				Scenario 3			
	Circuit 1		Circuit 2		Circuit 1		Circuit 2	
	Min.	Avg.	Min.	Avg.	Min.	Avg.	Min.	Avg.
Static Rating	-0.2	21.6	**-1.2**	21.3	1.5	23.4	**0.5**	24.5
Dynamic Rating	5.5	36.4	**3.4**	29.4	8.2	38.2	**6.0**	32.6
Dynamic Rating 1st restriction	5.5	25.7	**3.4**	26.2	8.2	27.4	**6.0**	29.4
Dynamic Rating 2nd restriction	5.5	25.7	**3.3**	23.8	8.2	27.4	**5.0**	27.0

The following tables, from Table 7.4 to Table 7.7 show the percentage of overload in a year (2010), i.e. when the current on circuit one or two exceeds each specific rating. Results on both approaches (theoretical and real) are presented, the green cells representing a non overload circuit while red cells an overload circuit for more than 0 % in a year.

Table 7.4 - **Real export approach:** **Scenario 1** Percentage in a year of overload per MW generation increase. 1st restriction is the ABSD for circuit 1 (C1) and 0.45 OF SC for circuit 2 (C2). 2nd restriction is the ABSD for circuit 1 and 0.45 Al SC for circuit 2.

MW Increase	C1	C2	C1	C2	C1	C2	C1	C2
	Static Rating		Dynamic Rating		Dynamic Rating 1st restriction		Dynamic Rating 2nd restriction	
0	0,0	0,0	0,0	0,0	0,0	0,0	0,0	0,0
1	0,1	0,0	0,0	0,0	0,0	0,0	0,0	0,0
2	0,2	0,1	0,0	0,0	0,0	0,0	0,0	0,0
3	0,3	0,3	0,0	0,0	0,0	0,0	0,0	0,0
4	0,5	0,5	0,0	0,0	0,0	0,0	0,0	0,0
5	1,1	0,8	0,0	0,0	0,0	0,0	0,0	0,0
6	1,7	1,3	0,0	0,0	0,0	0,2	0,0	0,0
7	2,1	1,7	0,0	0,0	0,0	0,3	0,0	0,0
8	2,5	2,1	0,0	0,0	0,2	0,7	0,2	0,2
9	2,9	2,4	0,0	0,0	0,7	1,1	0,7	0,3
10	3,2	2,8	0,0	0,0	1,3	1,5	1,3	0,6
11	3,7	3,3	0,0	0,0	1,8	1,8	1,8	0,9
12	4,0	3,6	0,0	0,1	2,1	2,2	2,1	1,3
13	4,4	4,0	0,0	0,2	2,5	2,6	2,5	1,6
14	4,9	4,3	0,1	0,4	2,8	3,0	2,8	1,8
15	5,3	4,8	0,1	0,5	3,2	3,4	3,2	2,0
16	5,6	5,2	0,1	0,7	3,6	3,8	3,6	2,2

Table 7.5 - **Theoretical export approach:** **Scenario 1** Percentage in a year of overload per MW generation increase. 1st restriction is the ABSD for circuit 1 (C1) and 0.45 OF SC for circuit 2 (C2). 2nd restriction is the ABSD for circuit 1 and 0.45 Al SC for circuit 2.

MW Increase	C1	C2	C1	C2	C1	C2	C1	C2
	Static Rating		Dynamic Rating		Dynamic Rating 1st restriction		Dynamic Rating 2nd restriction	
0	0,6	0,1	0,0	0,0	0,0	0,0	0,0	0,0
1	1,1	0,3	0,0	0,0	0,0	0,0	0,0	0,0
2	1,4	1,0	0,0	0,0	0,0	0,0	0,0	0,0
3	1,5	1,6	0,0	0,0	0,0	0,0	0,0	0,0
4	2,9	2,3	0,0	0,0	0,0	0,0	0,0	0,0
5	4,0	3,2	0,0	0,0	0,0	0,3	0,0	0,0
6	5,1	4,1	0,0	0,1	0,0	0,9	0,0	0,1
7	6,0	5,0	0,1	0,2	0,1	2,0	0,1	0,2
8	7,0	5,9	0,1	0,4	2,4	3,1	2,4	0,5
9	7,9	6,9	0,2	0,5	3,9	4,1	3,9	0,8
10	8,8	7,8	0,3	0,7	5,2	5,0	5,2	1,5
11	9,5	8,6	0,4	1,0	5,8	5,9	5,8	2,6
12	10,1	9,4	0,5	1,5	6,6	6,7	6,6	3,6
13	11,0	10,2	0,6	1,9	7,2	7,5	7,2	4,5
14	11,7	10,8	0,8	2,5	8,0	8,3	8,0	5,4
15	12,6	11,5	1,0	3,1	8,7	9,1	8,7	6,2
16	13,4	12,2	1,3	3,7	9,2	9,8	9,2	7,1

Table 7.6 - **Real export approach:** **Scenario 3** Percentage in a year of overload per MW generation increase. 1st restriction is the ABSD for circuit 1 (C1) and 0.45 OF SC for circuit 2 (C2). 2nd restriction is the ABSD for circuit 1 and 0.45 Al SC for circuit 2.

MW Increase	C1	C2	C1	C2	C1	C2	C1	C2
	Static Rating		Dynamic Rating		Dynamic Rating 1st restriction		Dynamic Rating 2nd restriction	
0	0,0	0,0	0,0	0,0	0,0	0,0	0,0	0,0
1	0,0	0,0	0,0	0,0	0,0	0,0	0,0	0,0
2	0,0	0,0	0,0	0,0	0,0	0,0	0,0	0,0
3	0,0	0,0	0,0	0,0	0,0	0,0	0,0	0,0
4	0,1	0,0	0,0	0,0	0,0	0,0	0,0	0,0
5	0,2	0,1	0,0	0,0	0,0	0,0	0,0	0,0
6	0,3	0,3	0,0	0,0	0,0	0,0	0,0	0,0
7	0,5	0,5	0,0	0,0	0,0	0,0	0,0	0,0
8	1,0	0,7	0,0	0,0	0,0	0,1	0,0	0,0
9	1,5	1,0	0,0	0,0	0,0	0,2	0,0	0,0
10	1,9	1,5	0,0	0,0	0,0	0,3	0,0	0,0
11	2,3	1,9	0,0	0,0	0,2	0,5	0,2	0,0
12	2,6	2,2	0,0	0,0	0,6	0,9	0,6	0,1
13	3,0	2,5	0,0	0,0	1,1	1,3	1,1	0,2
14	3,3	2,9	0,0	0,0	1,5	1,6	1,5	0,4
15	3,7	3,2	0,0	0,1	1,9	2,0	1,9	0,7
16	4,0	3,6	0,0	0,2	2,2	2,3	2,2	1,1

Table 7.7 - **Theoretical export approach:** **Scenario 3** Percentage in a year of overload per MW generation increase. 1st restriction is the ABSD for circuit 1 (C1) and 0.45 OF SC for circuit 2 (C2). 2nd restriction is the ABSD for circuit 1 and 0.45 AL SC for circuit 2.

MW Increase	C1	C2	C1	C2	C1	C2	C1	C2
	Static Rating		Dynamic Rating		Dynamic Rating 1st restriction		Dynamic Rating 2nd restriction	
0	0,0	0,0	0,0	0,0	0,0	0,0	0,0	0,0
1	0,0	0,0	0,0	0,0	0,0	0,0	0,0	0,0
2	0,0	0,0	0,0	0,0	0,0	0,0	0,0	0,0
3	0,6	0,1	0,0	0,0	0,0	0,0	0,0	0,0
4	1,1	0,4	0,0	0,0	0,0	0,0	0,0	0,0
5	1,4	1,1	0,0	0,0	0,0	0,0	0,0	0,0
6	1,6	1,7	0,0	0,0	0,0	0,0	0,0	0,0
7	2,4	2,3	0,0	0,0	0,0	0,2	0,0	0,0
8	3,7	3,0	0,0	0,1	0,0	0,4	0,0	0,1
9	4,7	3,8	0,0	0,1	0,0	1,0	0,0	0,2
10	5,5	4,5	0,1	0,2	0,3	1,8	0,3	0,2
11	6,4	5,3	0,1	0,4	1,9	2,8	1,9	0,6
12	7,2	6,1	0,2	0,5	3,3	3,6	3,3	0,9
13	8,1	7,0	0,3	0,7	4,5	4,5	4,5	1,5
14	8,8	7,8	0,4	1,0	5,4	5,2	5,4	2,3
15	9,5	8,6	0,5	1,3	6,0	6,0	6,0	3,3
16	10,1	9,3	0,6	1,8	6,6	6,8	6,6	4,1

7.5 Energy, Emissions and Profit Analysis

By increasing overhead line capacity in areas where generation is already being curtailed there is an increase in export. Therefore, in a full year, there will be extra amount of energy, CO_2 emissions savings [1] and profit as well [2].

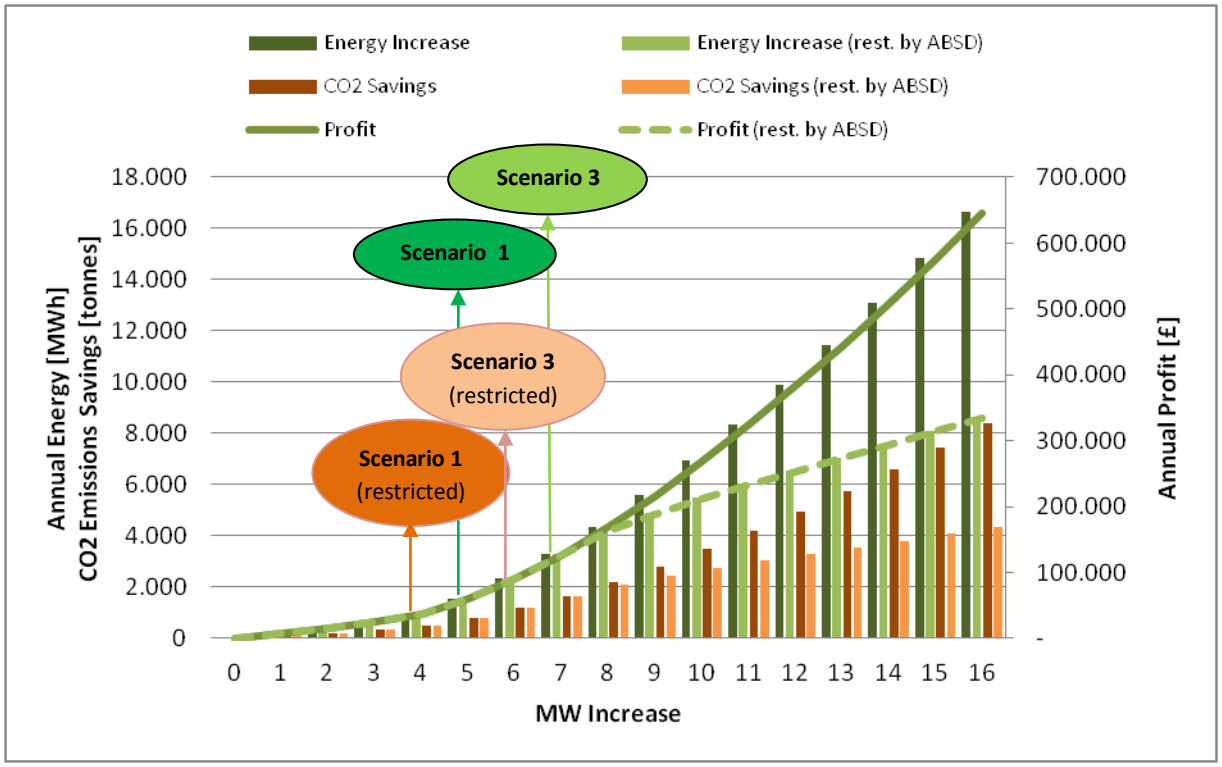

Figure 7.15 - Annual Energy, CO_2 emission savings and profit.

Figure 7.15 demonstrates the energy increase, CO_2 emission savings and profit for each MW installed. According to Figure 7.7 and Figure 7.8, there is headroom to install around 4 MW under scenario 1, restricted by circuit 2´s underground cables. For the non restricted scenario 1, i.e. 5 MW generation increase, the extra annual energy would be around 1500 MWh with savings of more than 700 tonnes in CO_2 emissions. An annual profit of approximately 60 k£ would be possible under the renewable obligation certificates of 2012 (38.69 £/MWh). Scenario 3, would have slightly better results as it would allow more generation to flow. There would be an increase of around 3200 MWh in energy production with more than 1500 tonnes of CO_2 emission savings. A total profit of 125 k£ would be possible as well.

[1] Conversion factor of 0.5 kg of CO_2 per kWh - 2010 Guidelines to DEFRA
[2] Renewables Obligation 2011/2012 Buyout price of 38.69 £ per MWh

8 Conclusions and Future Work

Throughout this dissertation a feasibility study on dynamic line ratings was presented, which gave a background on all different variables and components of applying this technology. It is an approach that exists for many years now, but due to lack of support in existing standards and policy, it´s not easy to implement dynamic thermal ratings without first changing those standards. It may have several advantages but the uncertainty and the non support in current policies makes it difficult to use as an option to business as usual approach of either re-conducturing or installing a new circuit.

8.1 Conclusions

This chapter will mainly focus on an overview of the advantages and limitations as a technology and as seen by infrastructure planning engineers. The implementation of dynamic ratings pushes forward a new way of planning which may be difficult to apprehend at first. Bear in mind that this thesis approach was for a weather data dependency.

8.1.1 Advantages

- With the continued effort on allowing more generation to be connected, dynamic line ratings are seen as a way to step into the future in a new and innovative way, deferring or greatly reducing reinforcement costs;

- By applying a dynamic thermal rating system, real time information on line capacity and overall conditions will be known, increasing its reliability and improving the response time against failures and possible outages;

- Increase in energy yields by allowing more renewable generation to be connected, thus help achieving the low carbon vision;

- Simplified integration of renewable generators, which in turn reduces connection costs and associated issues. Less reinforcement schemes means less interaction with landowners. By reducing connection costs there will be a beneficial impact in the long term on electricity prices from renewable sources.

8.1.2 Uncertainties and Disadvantages

- The reliability on weather information allows for a certain degree of inaccuracy and the outcome of the analysis must be dealt with caution;

- In following this approach there will be an urgent need to update all standards and policies in order to include it as a viable and reliable option in the long term for overhead line capacity enhancement projects;

- Dynamic ratings, due to their high dependency on real time weather data, specifically wind speed may limit its application to either higher elevation overhead lines or areas close to wind generation;

- The use of dynamic ratings will introduce a degree of variance in overhead line capacity. Planning 5 or 10 years ahead may prove more difficult as the rating of the overhead line isn´t static.

8.2 Future Work

The development of a link between dynamic line ratings assessment and modeling software would be important to achieve. Real time weather data, i.e. wind speed and direction, ambient temperature, overhead line profile and geographic position would feed the modeling tool as input (see Figure 8.1). Several load flows would be carried to then evaluate the gain in overhead line capacity in a full year by applying dynamic ratings. Each circuit group would have a capacity or load profile associated to that year as demonstrated in Figure 8.2.

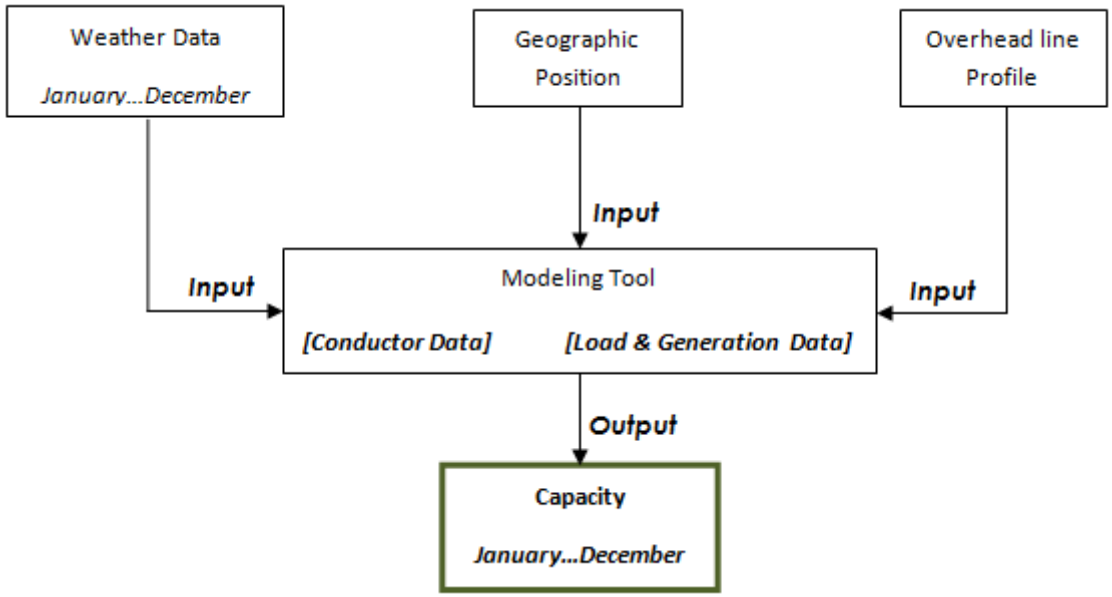

Figure 8.1 - Future work flow chart.

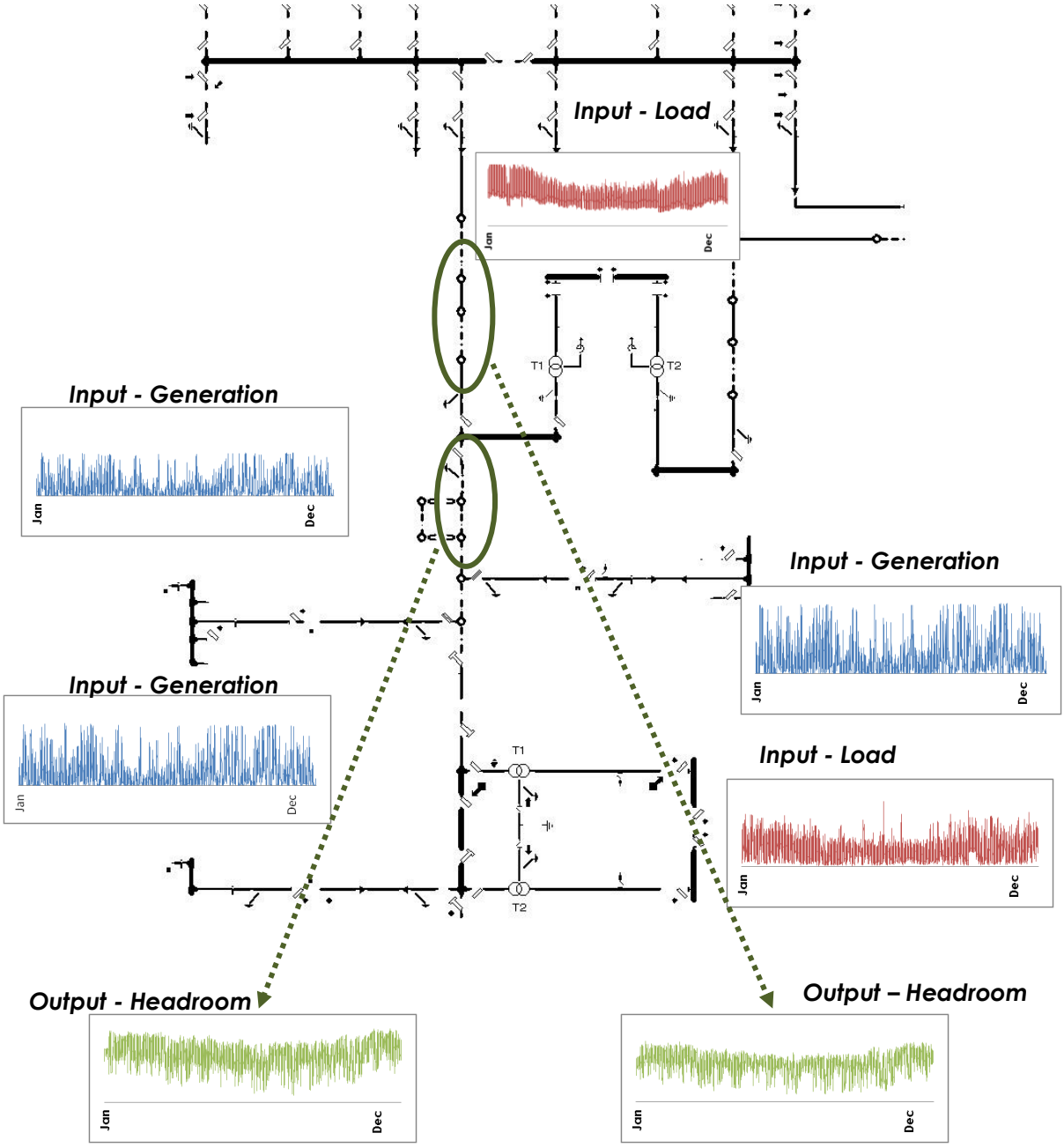

Figure 8.2 - Future work graphic.

9 References

[1] OFGEM, (31st March 2011). “Electricity Distribution Annual Report for 2008-09 and 2009-10”.

[2] IEEE Power Engineering Society, (30th January 2007). “IEEE Standard for Calculating the Current-Temperature of Bare Overhead Conductors”.

[3] D.A. Douglass, Abdel-Aty Edris, (1996). “Real-Time Monitoring and Dynamic Thermal Rating of Power Transmission Circuits”, IEEE Transactions on Power Delivery, vol. 11 (3), p. 1407-1418.

[4] Engineering Recommendation P27, (1986). “Current Rating Guide for High Voltage Overhead Lines Operating in the UK Distribution System”.

[5] Bryan W. Brennan, Mike P. Diedesch, Jared R. Johnson, Wei Zhang, (2008). “Dynamic Line Ratings for the Cowlitz-LaGrande Transmission Lines”, Washington State University, EE416 Electrical Engineering Design Final Report.

[6] The Institution of Engineering and Technology, (2006). “Distributed Generation”.

[7] Energy Networks Association, (June 2010). “Distributed Generation Connection Guide”.

[8] UK Power Networks Intranet, (2011). “Low Carbon London”.

[9] AREVA, (2010). “MiCOM P341 Dynamic Line Rating Protection Relay – Application Guide P341/EN AG/G64”.

[10] ALSTOM Grid, (May 2011). “Network Protection & Automation Guide – Protective Relays, Measurement & Control”.

[11] Colin Bayliss, Brian Hardy, (2007). “Transmission and Distribution Electrical Engineering”, 3rd edition.

[12] CIGRE JWG B2/C1.19, (2010). “Increasing Line Capacity of Overhead Transmission Lines – Needs and Solutions”.

[13] UK Power Networks, (October 2011). “UK Power Networks Renewables Distribution (2011-0419), Questionnaire to the Promoter”.

[14] Central Networks, (July 2008). “Innovation in Central Networks Registered Power Zone”.

[15] Danish Wind Industry Association, http://www.motiva.fi/myllarin_tuulivoima/windpower%20web/core.htm.

[16] Mathias Noe, Michael Steurer, (2007). “High-temperature superconductor fault current limiters: concepts, applications, and development status”, Supercond. Sci. Technol. 20 (2007) R15–R29.

[17] Murray W. Davis, (1977). “A New Thermal Rating Approach: The Real Time Thermal Rating System for Strategic Overhead Conductor Transmission Lines Part I – General Description and

Justification of the Real Time Thermal Rating System", IEEE Transactions on Power Apparatus and Systems, Vol. PAS-96, No. 3.

[18] Murray W. Davis, (1977). "A New Thermal Rating Approach: The Real Time Thermal Rating System for Strategic Overhead Conductor Transmission Lines Part II – Steady State Thermal Rating Program", IEEE Transactions on Power Apparatus and Systems, Vol. PAS-96, No. 3.

[19] Murray W. Davis, (1977). "A New Thermal Rating Approach: The Real Time Thermal Rating System for Strategic Overhead Conductor Transmission Lines Part IV – Daily Comparisons of Real-Time and Conventional Thermal Ratings and Establishment of Typical Annual Weather Models", IEEE Transactions on Power Apparatus and Systems, Vol. PAS-96, No. 3.

[20] K. Kazerooni, J. Mutale, M. Perry; S. Venkatesan; D. Morrice, (June 2011). "Dynamic thermal rating application to facilitate wind energy integration", Issue Date 19-23 June 2011, p. 1-7.

[21] Dave Roberts, Philip Taylor, Andrea Michiorri, (2008). "Dynamic Thermal Rating for Increasing Network Capacity and Delaying Network Reinforcements", CIRED Seminar 2008: SmartGrids for Distribution Paper No. 3.

[22] Konstantinos Kopsidas, Simon M. Rowland, Boud Boumecid, (October 2009). "A Holistic Method for Conductor Ampacity and Sag Computation on an OHL Structure", IEEE Transactions on Power Delivery, Vol. 24, No. 4.

10 Appendixes

I. Appendix – IEEE Standard for Calculating the Current-Temperature of Bare Overhead Conductors

All equations for the steady state thermal rating calculation will be presented on this appendix. According to the simplified steady state heat balance equation:

$$I = \sqrt{\frac{q_c + q_r - q_s}{R(T_c)}} \tag{I.1}$$

it is necessary to determine the amount of cooling from convection, the radiated heat loss, the solar heat gain and the resistance at the conductor´s operating temperature.

Dynamic Viscosity of Air

$$\mu_f = \frac{1.458\times10^{-6}(T_m+273)^{1.5}}{T_m+383.4} \tag{I.2}$$

Where T_m is the average between the conductor´s and ambient temperature and given by the following equation:

$$T_m = \frac{T_c+T_a}{2} \tag{I.3}$$

Air Density

$$\rho_f = \frac{1.293-1.525\times10^{-4}H_e+6.379\times10^{-9}{H_e}^2}{1+0.00367T_m} \tag{I.4}$$

Where H_e is the elevation in meters above sea level.

Thermal Conductivity of Air

$$k_f = 2.424\times10^{-2} + 7.477\times10^{-5}T_m - 4.407\times10^{-9}{T_m}^2 \tag{I.5}$$

Natural Convection

$$q_{cn} = 0.0205{\rho_f}^{0.5}D^{0.75}(T_c - T_a)^{1.25} \tag{I.6}$$

Forced Convection

$$q_{clow} = \left[1.01 + 0.0372\left(\frac{D\rho_f V_w}{\mu_f}\right)^{0.52}\right] k_f K_{angle}(T_c - T_a) \quad \text{(I.7)}$$

$$q_{chigh} = \left[0.0119\left(\frac{D\rho_f V_w}{\mu_f}\right)^{0.6}\right] k_f K_{angle}(T_c - T_a) \quad \text{(I.8)}$$

The factor K_{angle} represents the wind direction factor and varies from 0.38 when the wind is parallel to the conductor and 1 when it is perpendicular and it is given by the following equation.

$$K_{angle} = 1.194 - \cos(\emptyset) + 0.194\cos(2\emptyset) + 0.368\sin(2\emptyset) \quad \text{(I.9)}$$

Radiated Heat Loss

$$q_r = 0.0178D\varepsilon\left[\left(\frac{T_c+273}{100}\right)^4 - \left(\frac{T_a+273}{100}\right)^4\right] \quad \text{(I.10)}$$

Solar Heat Gain

$$q_s = \alpha Q_s sin(\theta) A' \quad \text{(I.11)}$$

Where

$$Q_s = A + BH_c + CH_c{}^2 + DH_c{}^3 + EH_c{}^4 + FH_c{}^5 + GH_c{}^6 \quad \text{(I.12)}$$

And, $\theta = \arccos\left[\cos(H_c)\cos(Z_c - Z_1)\right]$ (I.13)

Each coefficient from equation (II.11) varies between the types of atmosphere that exist.

Appendix Table I.1 - Solar heat gain coefficients.

	Clear Atmosphere	Industrial Atmosphere
A	-42.2391	53.1821
B	63.8044	14.2110
C	-1.9220	6.6138×10^{-1}
D	3.46921×10^{-2}	-3.1658×10^{-2}
E	-3.61118×10^{-4}	5.4654×10^{-4}
F	1.94318×10^{-6}	-4.3446×10^{-6}
G	-4.07608×10^{-9}	1.3236×10^{-8}

The term H_c and Z_c are the altitude and azimuth of the sun and are given by the following equations:

Altitude of the sun (H_c)

$$H_c = arcsin[\cos(Latitude)\cos(\delta)\cos(\omega) + \sin(Latitude)\sin(\delta)] \quad \text{(I.14)}$$

Where δ is the solar declination and ω the hour angle. The solar declination is the angle between the sun rays and the Earth´s equator and the hour angle represents the displacement of the sun from the solar noon measured in degrees. They are given by equation II.14 and II.15 respectively.

$$\delta = 23.4583sin\left[\frac{284+N}{365}360\right] \quad \text{(I.15)}$$

$$Z_c = C + \arctan(\chi) \quad \text{(I.16)}$$

Where C is the solar azimuth constant given by table II.b and χ the solar azimuth variable given by the following equation:

$$\chi = \frac{\sin(\omega)}{\sin(Latitude)\cos(\omega) - \cos(Latitude)\tan(\delta)} \quad \text{(I.17)}$$

Appendix Table I.2 - Solar azimuth C.

Hour angle ω [degrees]	C if $\chi \geq 0$ [degrees]	C if $\chi < 0$ [degrees]
$-180 \leq \omega < 0$	0	180
$0 \leq \omega \leq 180$	180	360

The resistance of the line at a given temperature can be interpolated using known values, i.e. having the temperature for 20°C and 75°C it is possible to obtain the resistance at 50°C.

$$R(T_c) = \left[\frac{R(T_{high}) - R(T_{low})}{T_{high} - T_{low}}\right](T_c - T_{low}) + R(T_{low}) \quad \text{(I.18)}$$

II. Appendix – IEEE & CIGRE Standards

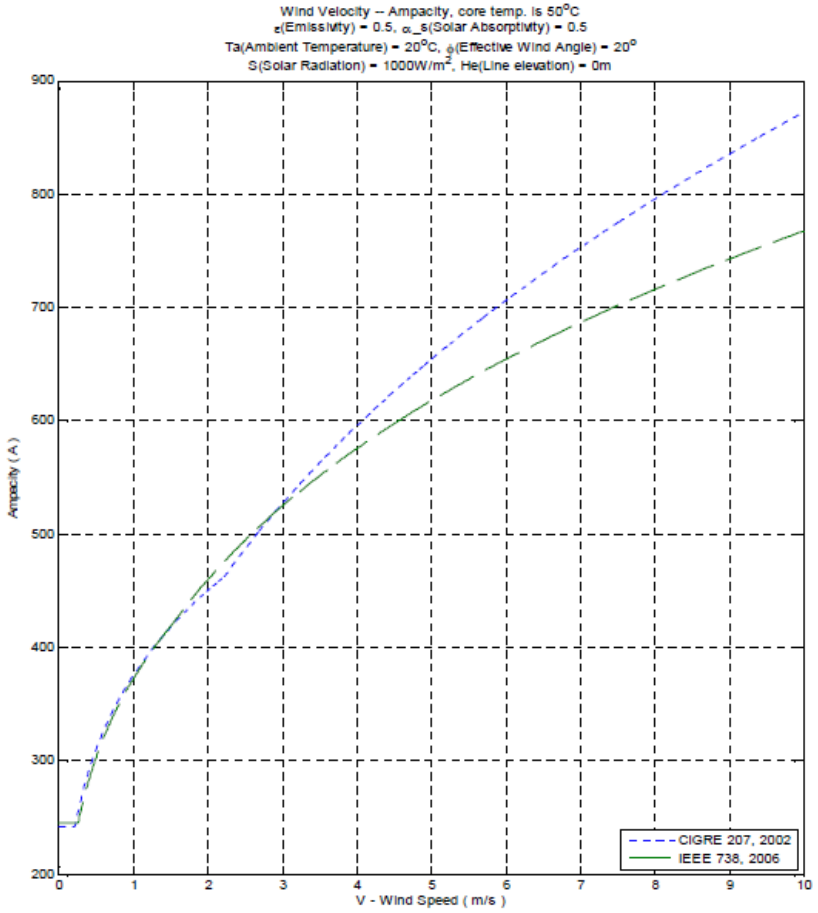

Appendix Figure II.1 - Ampacity vs wind speed for IEEE & CIGRE standards.

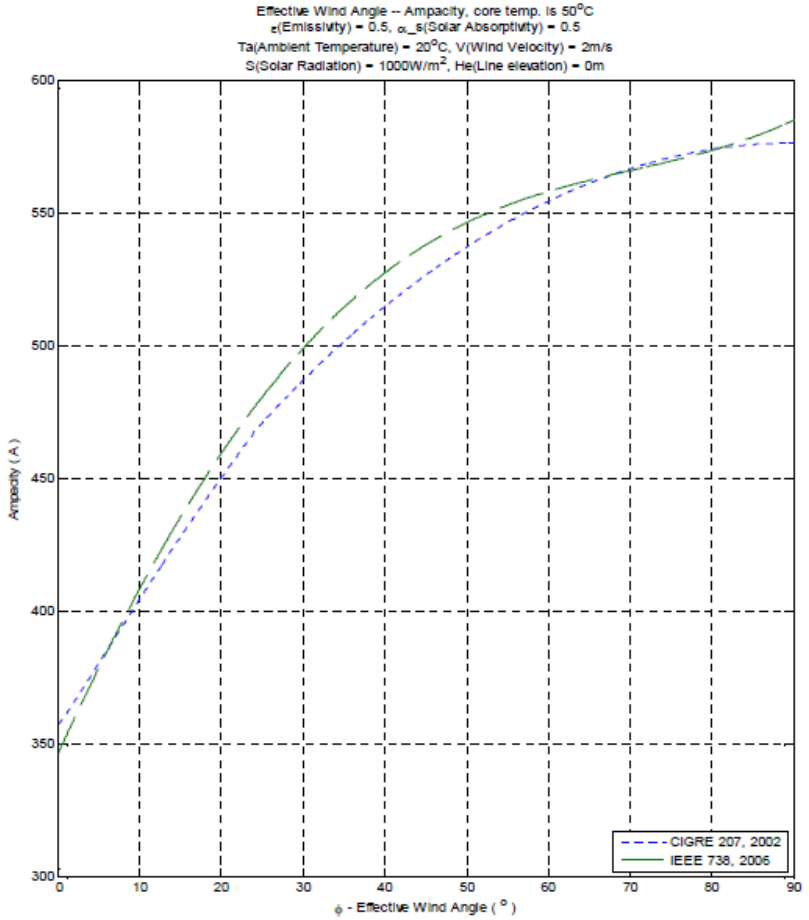

Appendix Figure II.2 - Ampacity vs effective wind angle for IEEE & CIGRE standards.

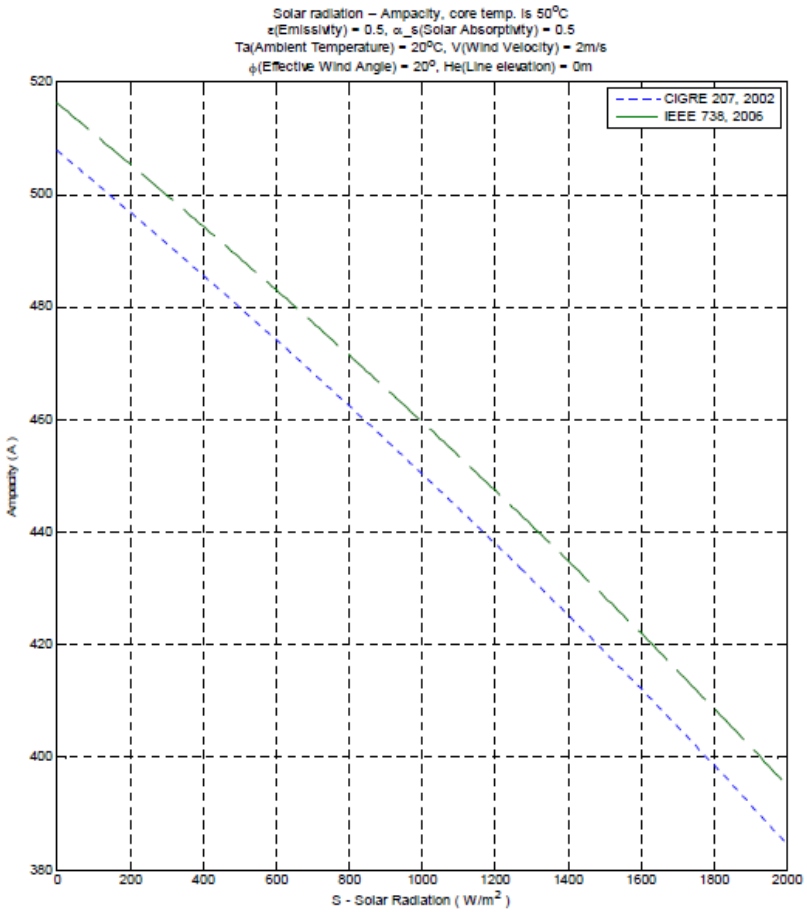

Appendix Figure II.3 - Ampacity vs solar radiation for IEEE & CIGRE standards

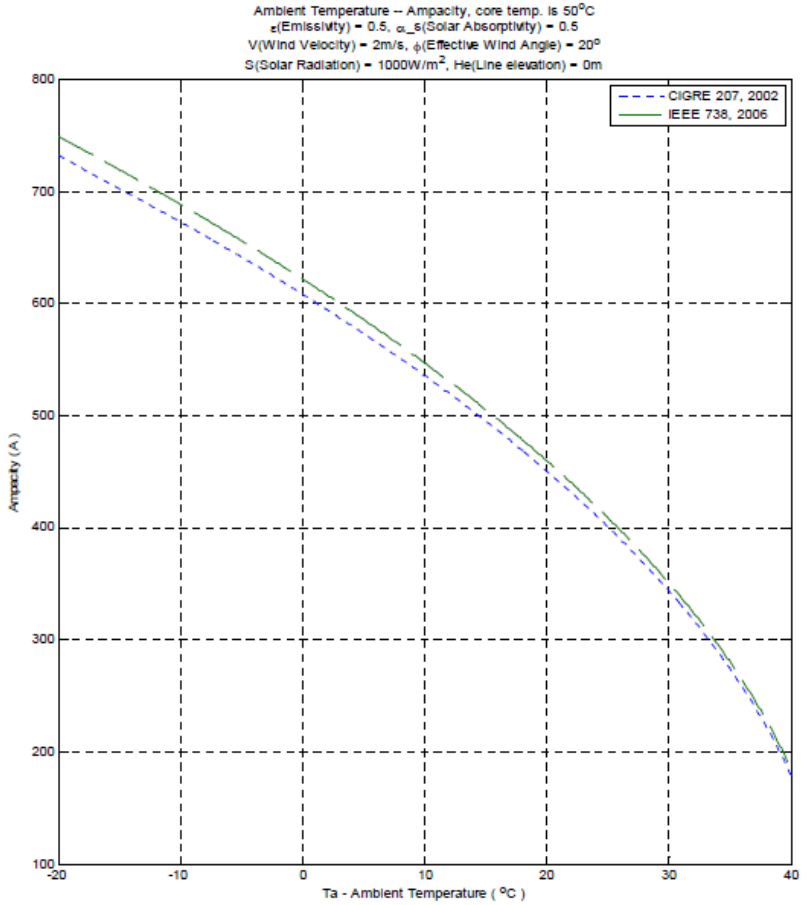

Appendix Figure II.4 - Ampacity vs ambient temperature for IEEE & CIGRE standards

III. Appendix – Route Map Circuit 1

Appendix Figure III.1 - 200 ACSR OHL with pole 5 on the right and 6 on the left.

Appendix Figure III.2 - 200 ACSR OHL with pole 6 and onwards.

Appendix Figure III.3 - 200 ACSR OHL in the distance.

Appendix Figure III.4 - 200 ACSR OHL with pole 73 on the right and pole 74 on the left.

IV. Appendix – Route Map Circuit 2

Appendix Figure IV.1 - 150 ACSR OHL coming out of Frct Primary Substation.

Appendix Figure IV.2 - 150 ACSR OHL crossing a field with pole number 24 in sight. No visual obstruction of notice.

Appendix Figure IV.3 - 150 ACSR OHL crossing the first highway through an underground section with pole 17 on the right and pole 16 on the left.

Appendix Figure IV.4 - 200 ACSR OHL after first underground section with pole 16 on sight.

Appendix Figure IV.5 - 200 ACSR OHL crossing the second highway with pole 11 on the right and pole 10 on the left.

Appendix Figure IV.6 - 150 ACSR OHL in the distance.

V. Appendix – Results: Theoretical Approach Scenario 1

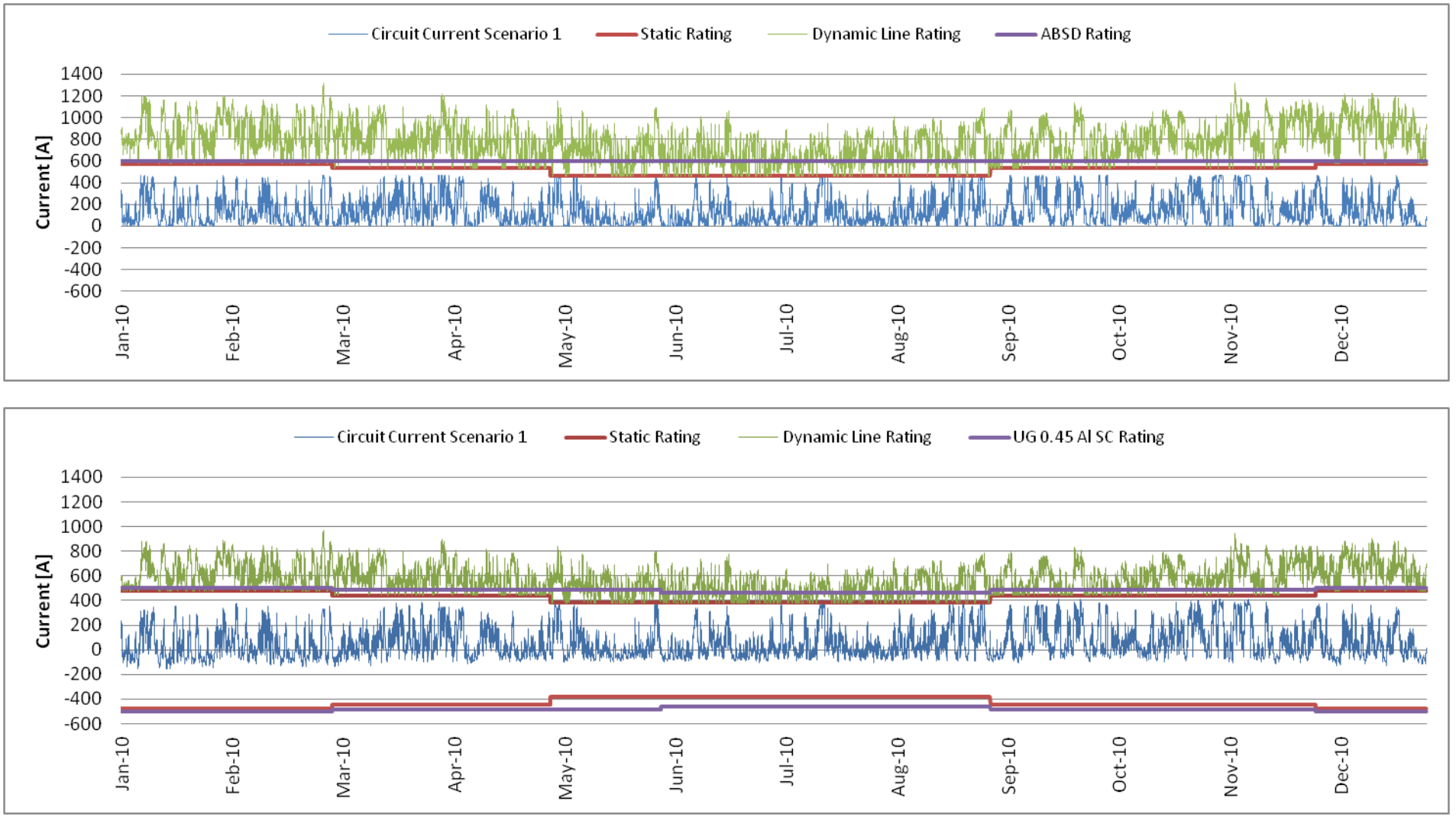

Appendix Figure V.1 - Circuit 1 (top) & 2 (bottom) theoretical approach scenario 1 - Dynamic ratings vs. static ratings vs. circuit load vs. ABSD rating.

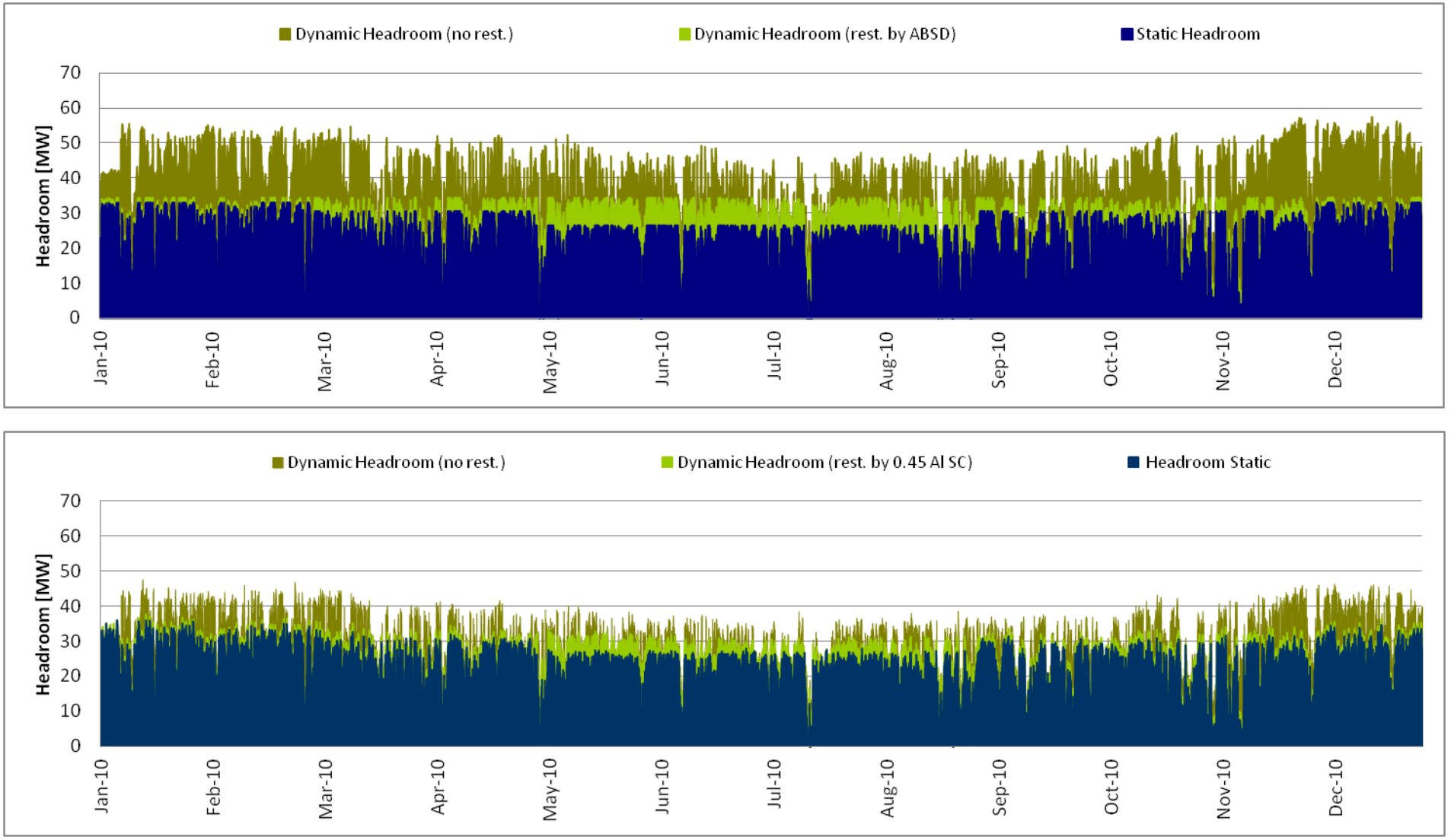

Appendix Figure V.2 - Circuit 1 (top) & 2 (bottom) theoretical approach scenario 1 - Headroom available under three pre-set conditions: Present conditions; dynamic ratings restricted by the air breaker switch disconnector (circuit 1) or underground section 0.45 Al SC (circuit 2) and dynamic ratings with no restrictions.

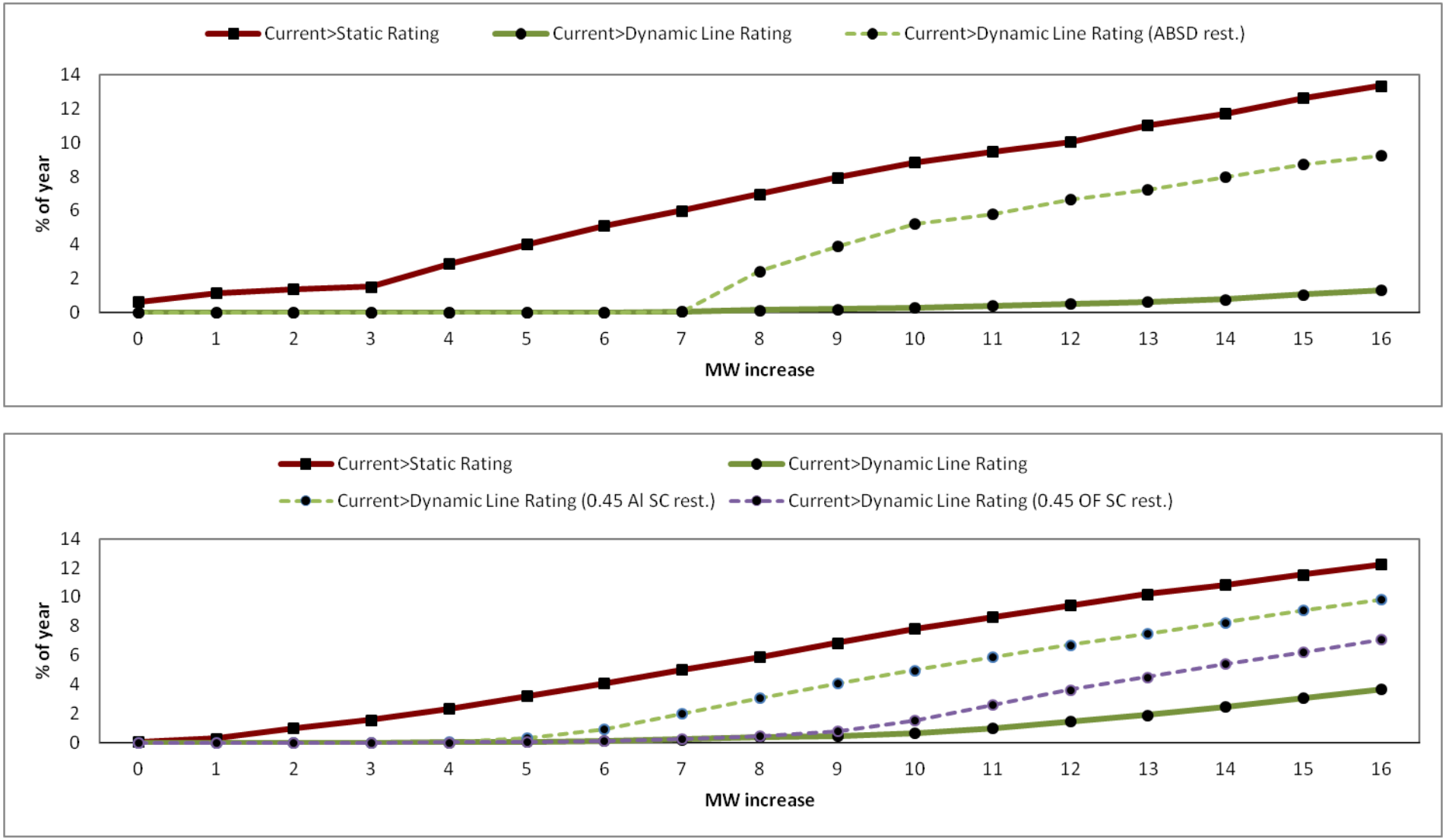

Appendix Figure V.3 - Circuit 1 (top) & 2 (bottom) theoretical approach scenario 1 - Percentage of year in which the corresponding current exceeds each rating for a MW generation increase (circuit overload).

VI. Appendix – Results: Theoretical Approach Scenario 3

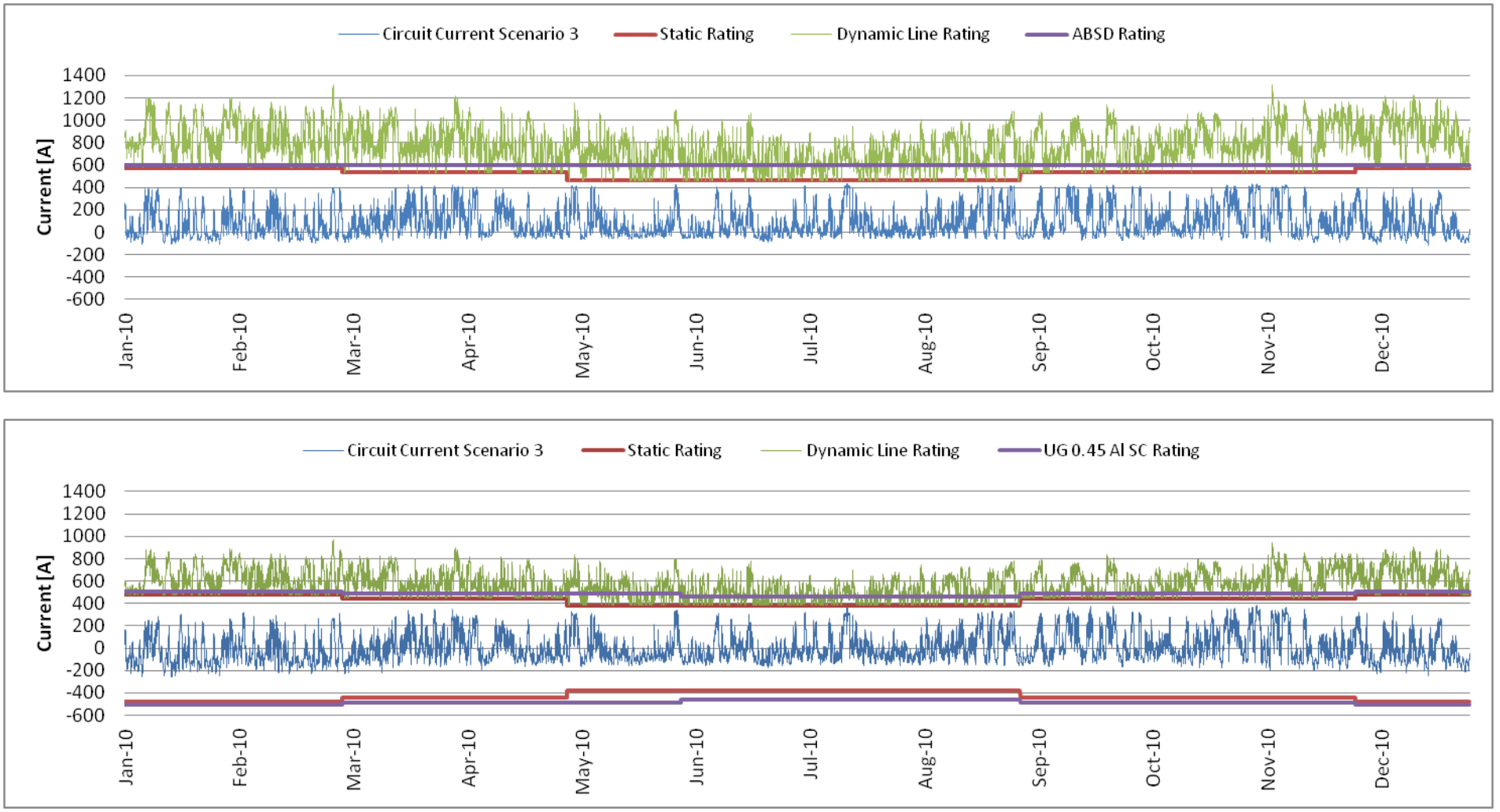

Appendix Figure VI.1 - Circuit 1 (top) & 2 (bottom) theoretical approach scenario 3 - Dynamic ratings vs. static ratings vs. circuit load vs. ABSD rating.

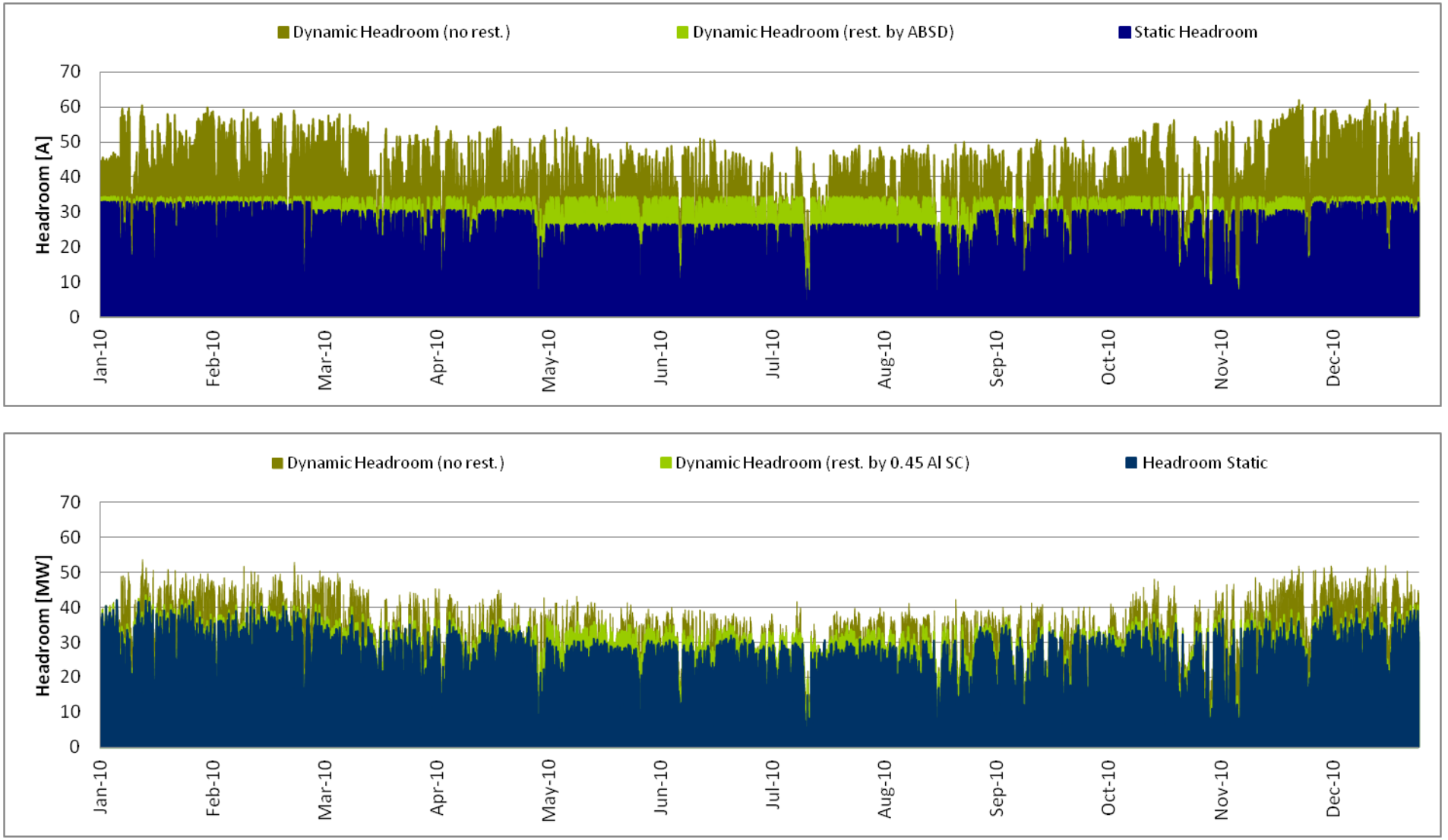

Appendix Figure VI.2 - Circuit 1 (top) & 2 (bottom) theoretical approach scenario 3 - Headroom available under three pre-set conditions: Present conditions; dynamic ratings restricted by the air breaker switch disconnector (circuit 1) or underground section 0.45 Al SC (circuit 2) and dynamic ratings with no restrictions.

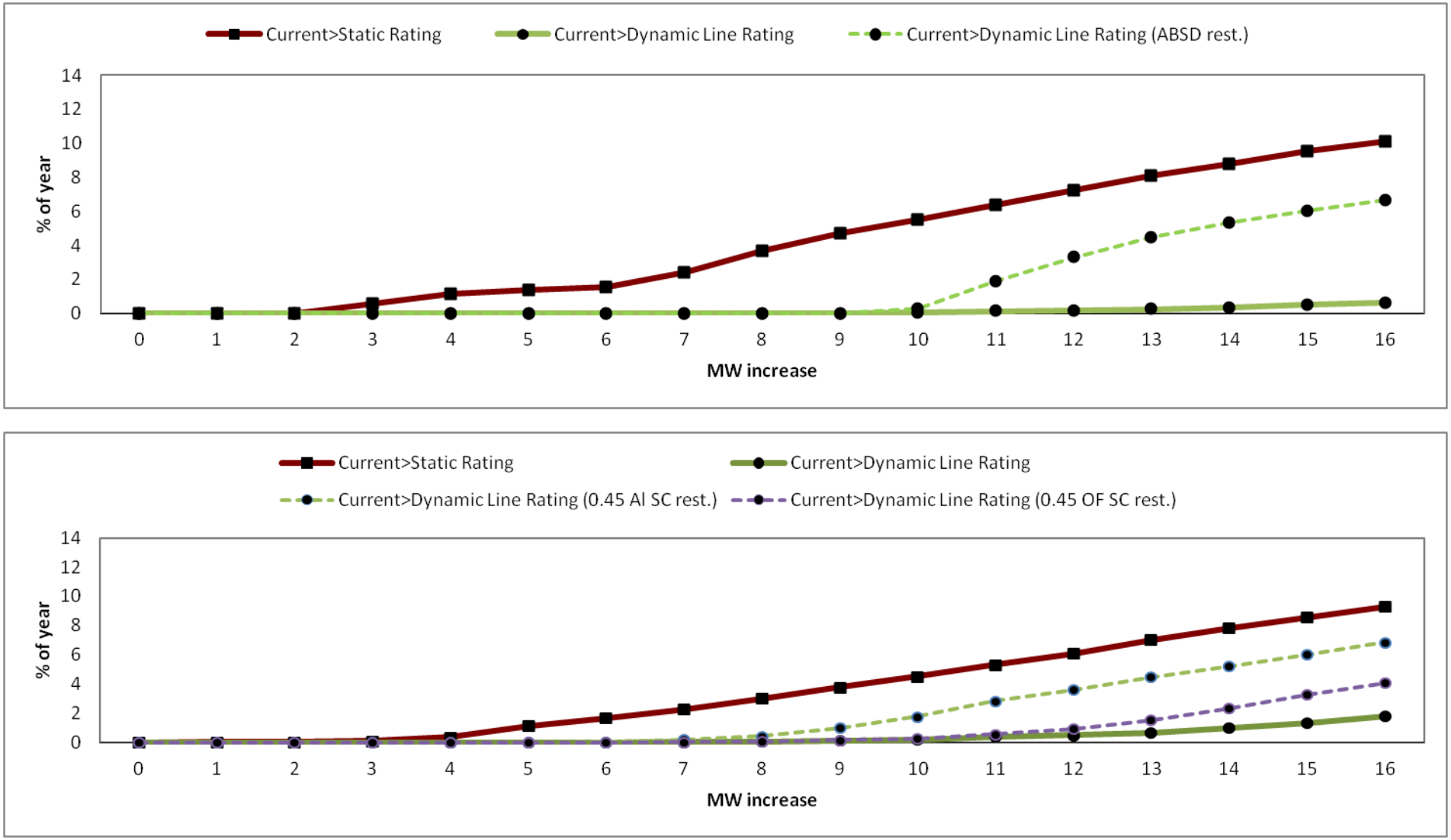

Appendix Figure VI.3 - Circuit 1 (top) & 2 (bottom) theoretical approach scenario 3 - Percentage of year in which the corresponding current exceeds each rating for a MW generation increase (circuit overload).

VII. Appendix – Results: Real Approach Scenario 1

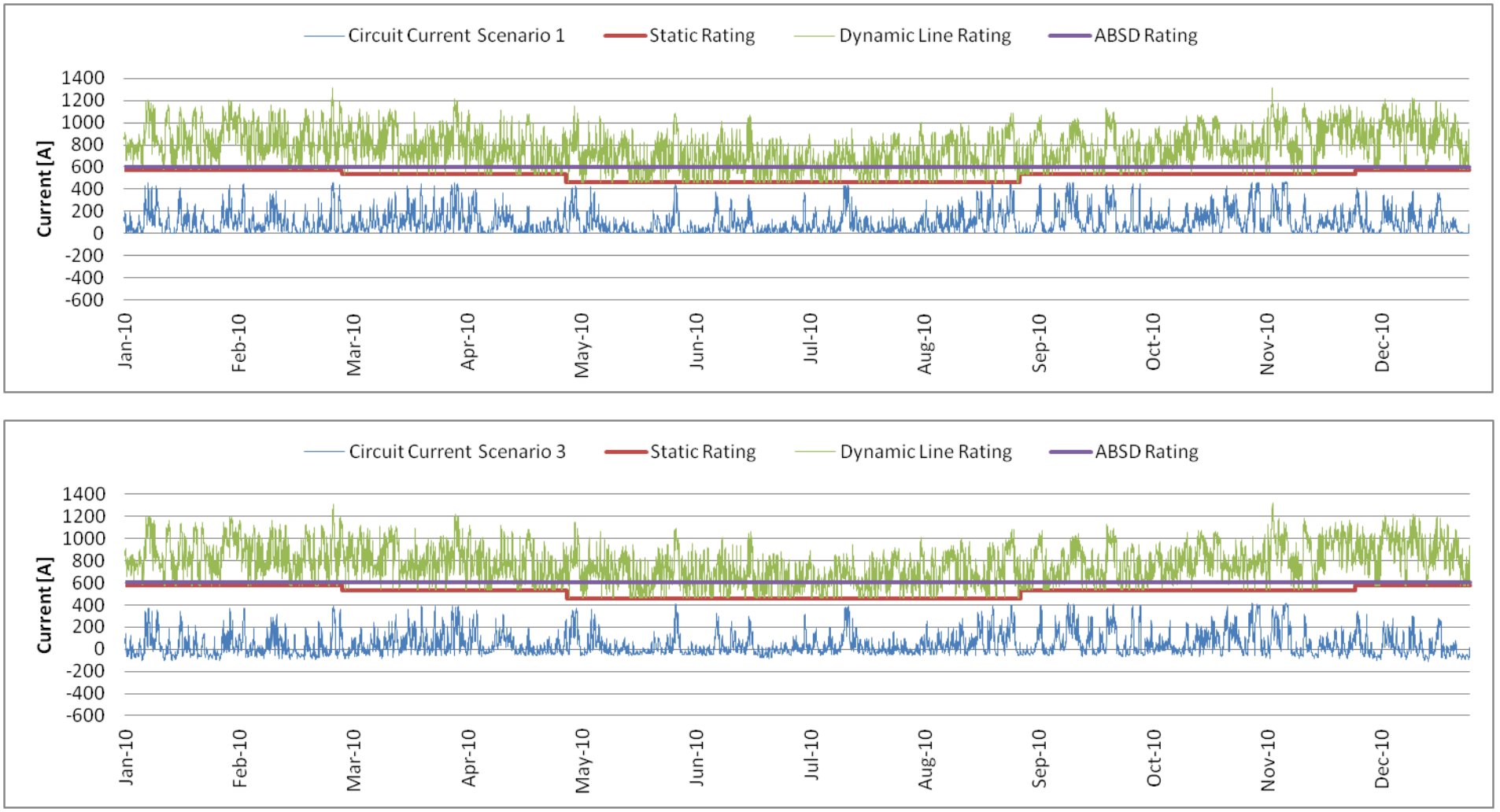

Appendix Figure VII.1 - Circuit 1 (top) & 2 (bottom) real approach scenario 3 – Dynamic ratings vs. static ratings vs. circuit load vs. ABSD rating.

Appendix Figure VII.2 - Circuit 1 (top) & 2 (bottom) real approach scenario 3 - Headroom available under three pre-set conditions: Present conditions; dynamic ratings restricted by the air breaker switch disconnector (circuit 1) or underground section 0.45 Al SC (circuit 2) and dynamic ratings with no restrictions.

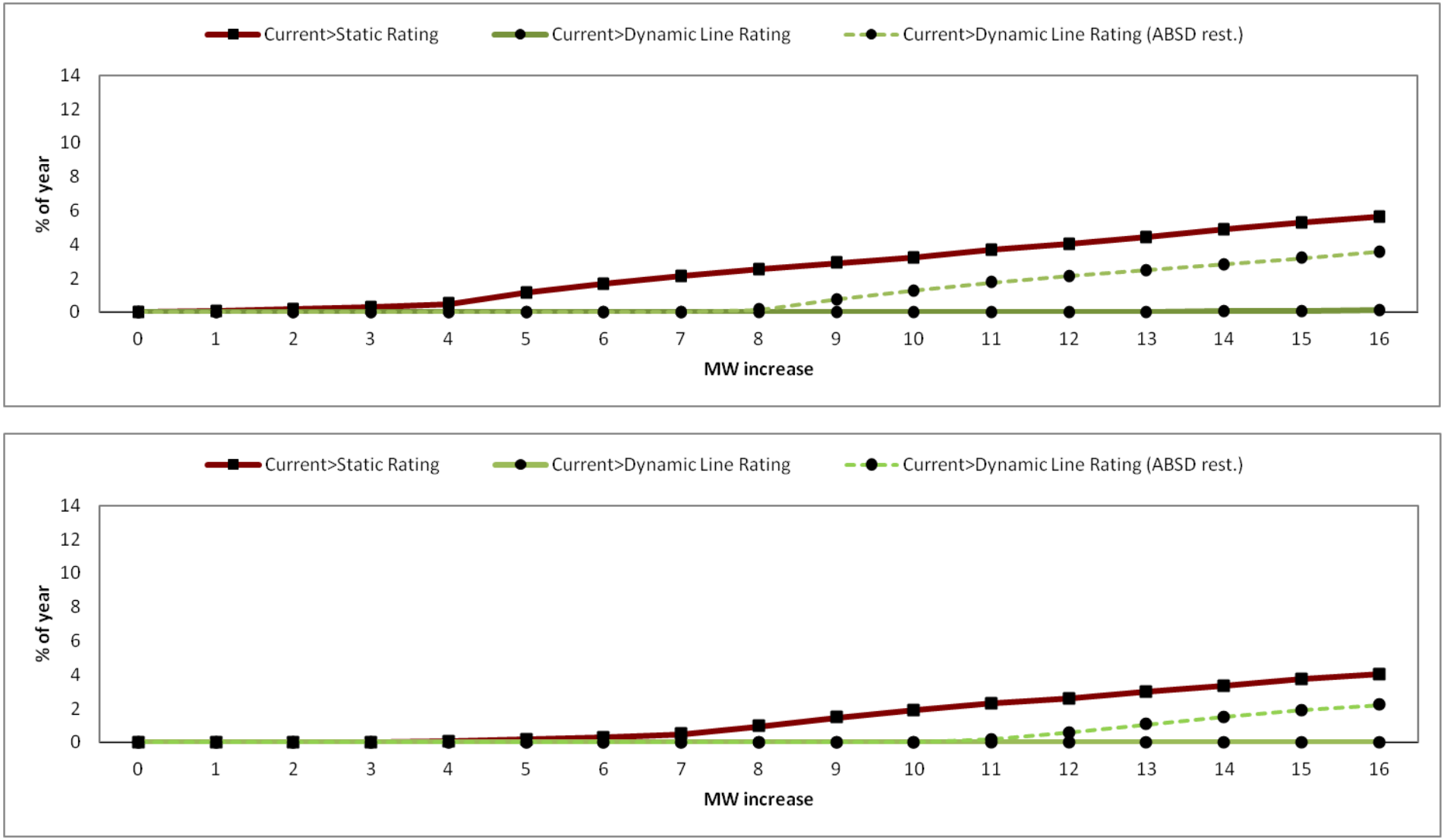

Appendix Figure VII.3 - Circuit 1 (top) & 2 (bottom) real approach scenario 3 - Percentage of year in which the corresponding current exceeds each rating for a MW generation increase (circuit overload).

VIII. Appendix – Results: Real Approach Scenario 3

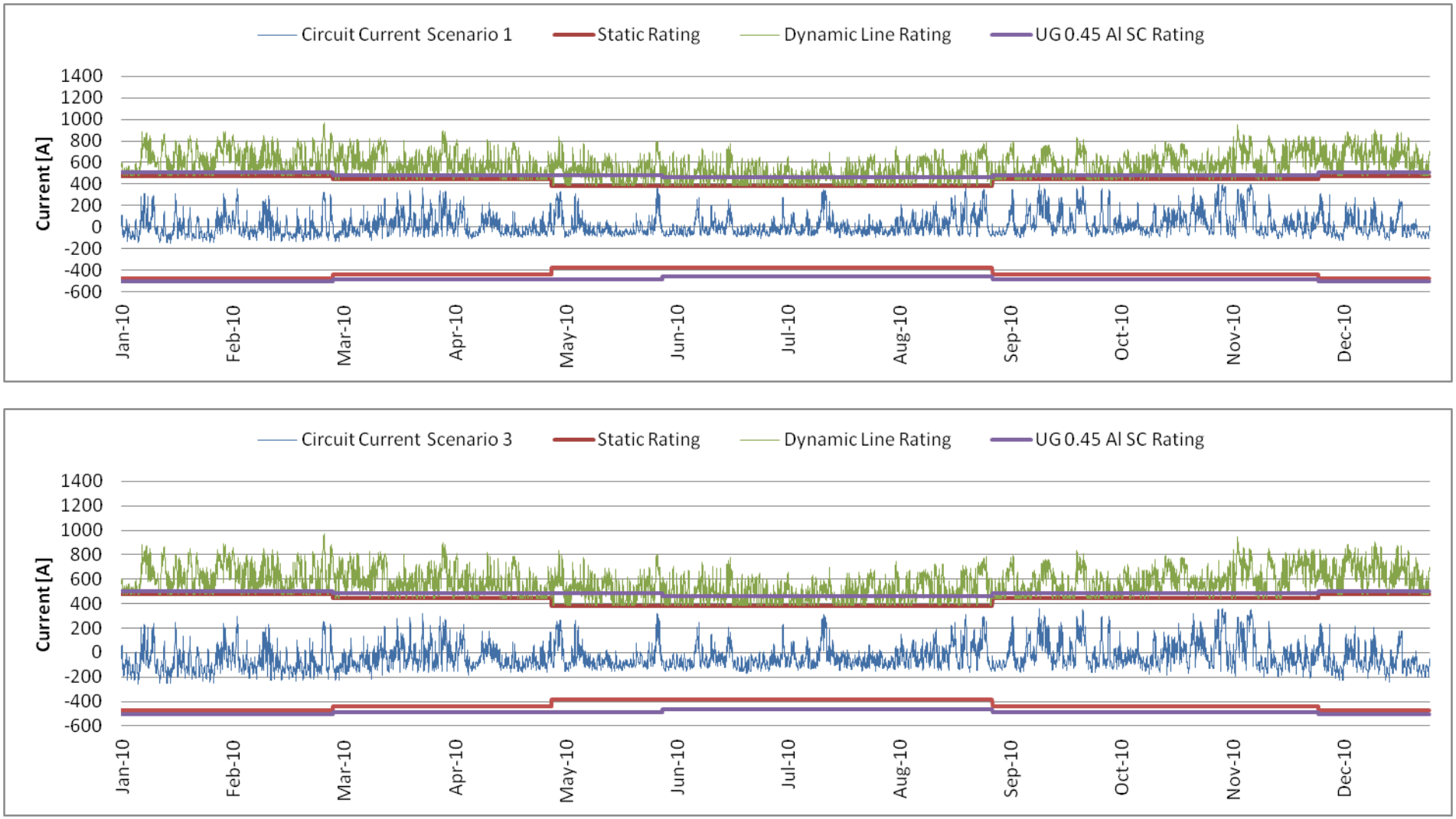

Appendix Figure VIII.1 - Circuit 1 (top) & 2 (bottom) real approach scenario 3 – Dynamic ratings vs. static ratings vs. circuit load vs. ABSD rating.

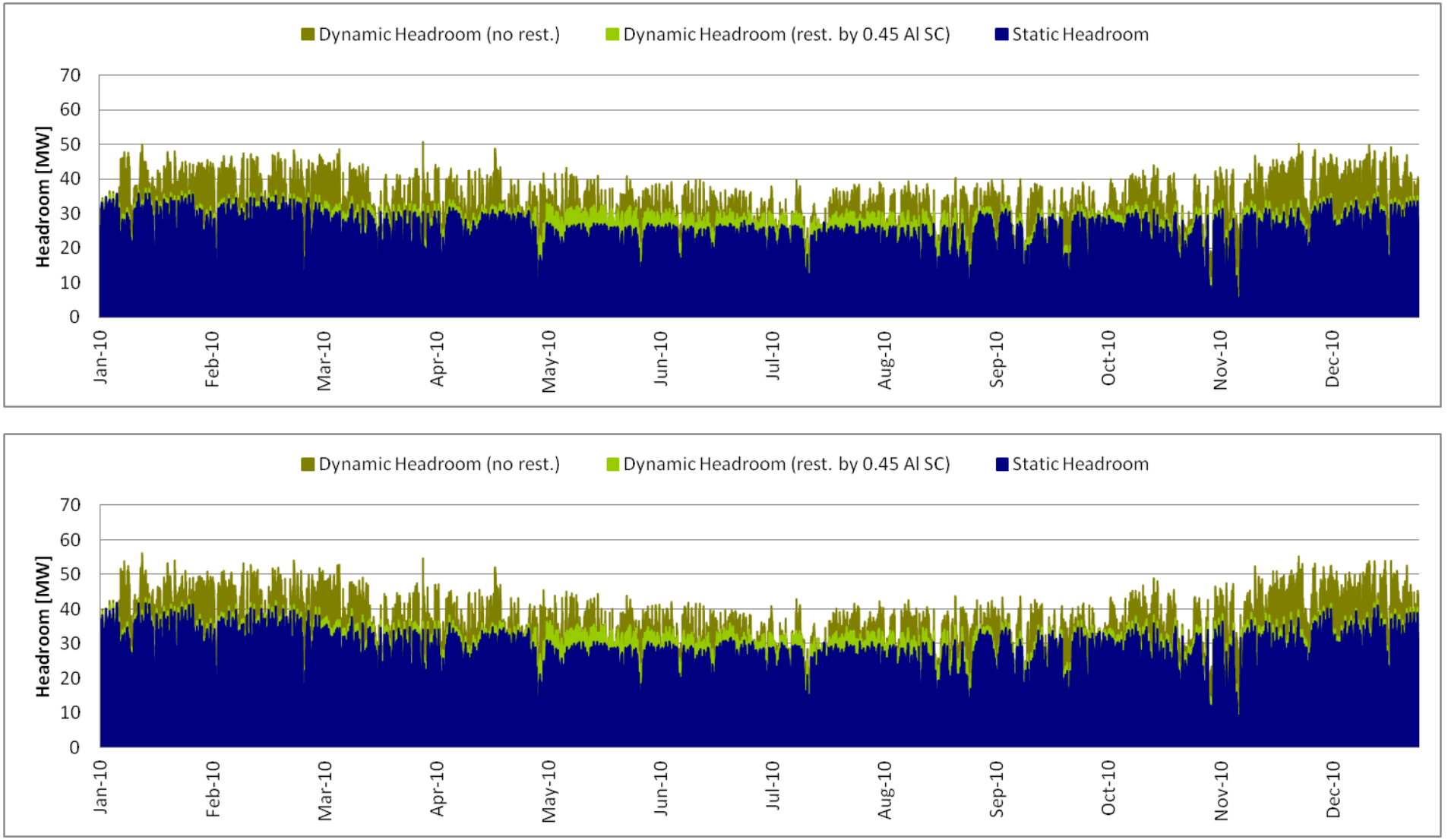

Appendix Figure VIII.2 - Circuit 1 (top) & 2 (bottom) real approach scenario 3 - Headroom available under three pre-set conditions: Present conditions; dynamic ratings restricted by the air breaker switch disconnector (circuit 1) or underground section 0.45 Al SC (circuit 2) and dynamic ratings with no restrictions.

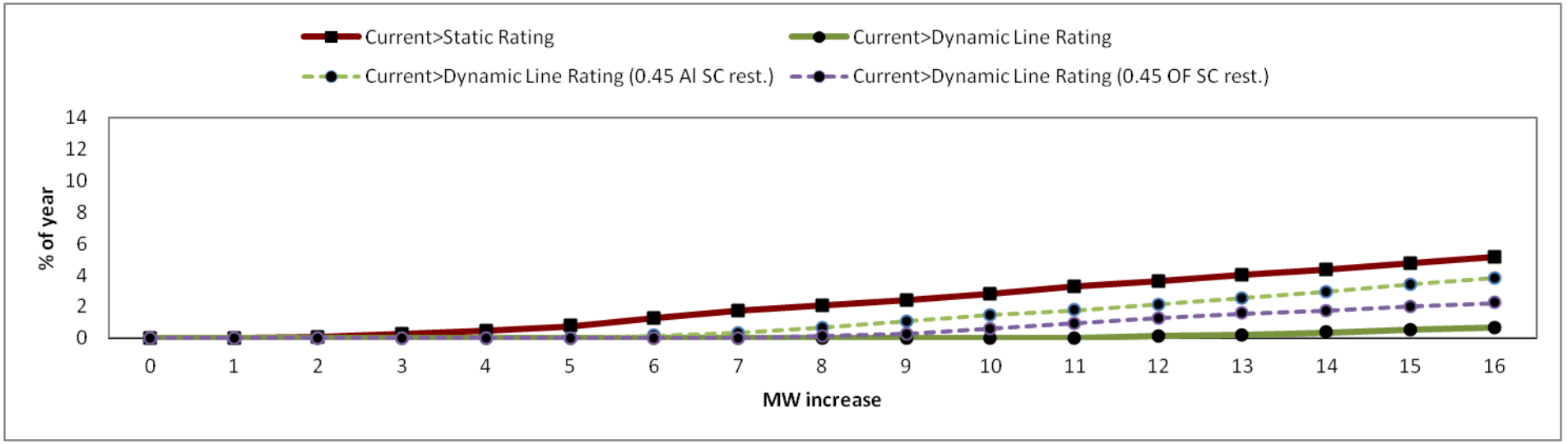

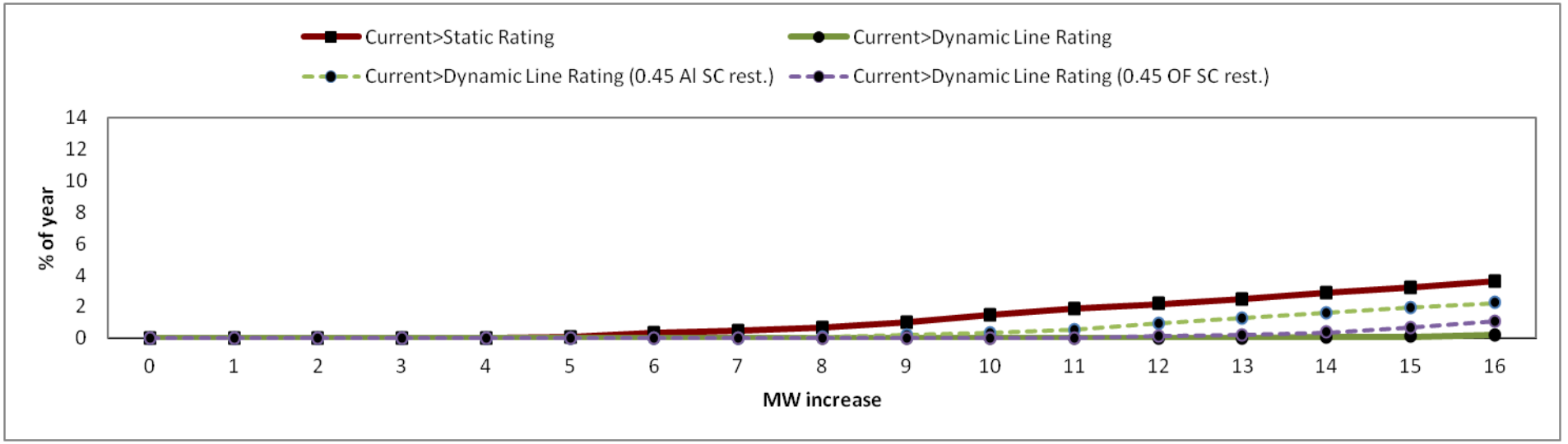

Appendix Figure VIII.3 - Circuit 1 (top) & 2 (bottom) real approach scenario 3 - Percentage of year in which the corresponding current exceeds each rating for a MW generation increase (circuit overload)